8-2012

PHENOTHIAZINES INDUCE ABORTIVE AUTOPHAGY LEADING TO CANCER CELL DEATH

Catherine T. Charles

PHENOTHIAZINES INDUCE ABORTIVE AUTOPHAGY LEADING TO CANCER CELL DEATH

by

Catherine Nguyen Charles, B.A., B.S.

APPROVED:

_____

Gordon B. Mills, M.D., Ph.D.
Supervisory Professor

_____

Peter J. Davies, M.D., Ph.D.

_____

Honami Naora, Ph.D.

_____

David McConkey, Ph.D.

_____

Huang Peng, M.D., Ph.D.

_____

Dean, Graduate School of Biomedical Sciences
The University of Texas Health Science Center at Houston

PHENOTHIAZINES INDUCE ABORTIVE AUTOPHAGY LEADING TO CANCER CELL DEATH

A

DISSERTATION

Presented to the Faculty of

The University of Texas

Health Science Center at Houston

and

The University of Texas

M. D. Anderson Cancer Center

Graduate School of Biomedical Sciences

in Partial Fulfillment

of the Requirements

for the Degree of

DOCTOR OF PHILOSOPHY

by

Catherine Nguyen Charles, B.A., B.S.

Houston, Texas

August, 2012

ACKNOWLEDGMENTS

I am grateful for the privilege and opportunity to train in Dr. Gordon Mills' laboratory. I thank Dr. Mills for the countless hours of discussion, guidance, and for providing me with amazing opportunities to collaborate with experts in various aspects of cancer cell signaling. My experiences have built my knowledge of systems biology and prepared me for my future endeavors. I am also thankful for the support and efforts of my current committee members: Drs. Peter Davies, Honami Naora, David McConkey, Huang Peng, and past committee members Drs. Joseph Alcorn, Garth Powis, Jeffrey Myers, and Wei Zhang. I am especially grateful for Drs. Davies and Naora, who have been guiding me from the beginning of my PhD studies. I would like to also thank the current and former members of Dr. Mills' lab for their instructions on various techniques and their guidance throughout my studies: Yiling Lu, Qinghua Yu, Shuangxing Yu and Nancy Shih. I'd like to thank Zhang Dong for teaching me mouse study techniques and helping me in my xenograft models. I'd like to thank Jane Li for her help in preparing my lysates from my animal studies for RPPA and Nancy for pushing hard to get the sample processed in the core on time to complete my studies. I'm grateful to Jae-Ho Cheong, Jiyong Liang and Sofie Claerhout their discussions of various experimental designs for my studies. I've greatly benefited from Sofie's expertise and willingness to discuss and share with me the key aspects of autophagy signaling studies and for the countless hours of image collections on the confocal microscopy. I am indebted to Sofie for in her valuable inputs throughout my project.

I've received countless input and support from the amazing post-docs in the Mills' research group: Sofie Claerhout, Shreya Mitra, and Jennifer Molina. Doris Siwak worked with me for months in the data analysis and the generation of heatmaps for my RPPA studies and for cheering me on in the end. I thank Zhenlin Ju, Wenbin Lu and Fan Zhang for their help in the statistical analysis of my data. I would like to thank everyone in the Department of Systems Biology for being such a wonderful group of people to work with. I've had the opportunity to interact with several faculties who've given me great help with input on my project. I'd like to thank the students in Dr. Mills' lab and in the Department of Systems Biology for their companionship. I also would like to thank the administrative team of the Department of Systems Biology for their support throughout my studies.

Additionally, I would like to thank Drs. William Bornmann and David Maxwell, who were my co-mentors in my pharmacoinformatics training. I have benefited from the generosity of the Dunn family through their foundation, and I had the privilege of meeting them and thank them for the Prestwick Compound Library which I used at the earlier stage of my project. Finally, I would like to acknowledge the Keck Center Pharmacoinformatics Training Program of the Gulf Coast Consortia for providing partial funding of my studies through the Pharmacoinformatics Predoctoral Fellowship.

DEDICATION

This dissertation is dedicated to my family whose love and support helped me through my long journey of my Ph.D. education.

PHENOTHIAZINES INDUCE ABORTIVE AUTOPHAGY

LEADING TO CANCER CELL DEATH

Publication No._____

Catherine Nguyen Charles, B.A, B.S

Supervisory Professor: Gordon B. Mills, M.D., Ph.D.

Autophagy is an evolutionarily conserved process that functions to maintain homeostasis and provides energy during nutrient deprivation and environmental stresses for the survival of cells by delivering cytoplasmic contents to the lysosomes for recycling and energy generation. Dysregulation of this process has been linked to human diseases including immune disorders, neurodegenerative muscular diseases and cancer.

Autophagy is a double edged sword in that it has both pro-survival and pro-death roles in cancer cells. Its cancer suppressive roles include the clearance of damaged organelles, which could otherwise lead to inflammation and therefore promote tumorigenesis. In its pro-survival role, autophagy allows cancer cells to overcome cytotoxic stresses generated the cancer environment or cancer treatments such as chemotherapy and evade cell death. A better understanding of how drugs that perturb autophagy affect cancer cell signaling is of critical importance to improve the cancer treatment arsenal.

In order to gain insights in the relationship between autophagy and drug treatments, we conducted a high-throughput drug screen to identify autophagy modulators. Our high-throughput screen utilized image based fluorescent microscopy for single cell analysis to identify chemical perturbants of the autophagic process. Phenothiazines emerged as the largest family of drugs that alter the autophagic process by increasing LC3-II punctae levels in different cancer cell lines. In addition, we observed multiple biological effects in cancer cells treated with phenothiazines. Those antitumorigenic effects include decreased cell migration, cell viability, and ATP production along with abortive autophagy. Our studies highlight the potential role of phenothiazines as agents for combinational therapy with other chemotherapeutic agents in the treatment of different cancers.

TABLE OF CONTENTS

ACKNOWLEDGMENTS…… iii

DEDICATION……v

ABSTRACT……vi

TABLE OF CONTENTS……viii

LIST OF FIGURES……..xii

LIST OF TABLES……xv

LIST OF ABBREVIATIONS……...xvi

CHAPTER 1: INTRODUCTION

Autophagy…….. 2

Physiological functions of autophagy…… 2

Autophagy functions as quality control of proteins and organelles……3

Autophagy is a multi-step process……..5

The core regulators of the autophagosome machinery…….. 6

Monitoring autophagy……7

Autophagy and cancer……11

Targeting autophagy differences in cancer versus normal cells…….13

Phenothiazines……16

Expression of dopamine receptors outside of central nervous system……..18

Phenothiazines and cancer……..20

Dissertation Overview……22

CHAPTER 2: MATERIALS AND METHODS

Compounds and reagents……..24

Cell lines……...24

Fluorescent image based high-throughput drug screen for autophagy……..26

Modulators

siRNA transfection……..27

SDS-PAGE and western blot analysis ……27

Antibodies…….28

Transmission electron microscopy (TEM)……...29

Crystal violet cell viability assay……30

Cell viability and proliferation assay ……30

Caspase-7 activity assay……30

ATP assay……31

$DiOC_6$ apoptosis Assay…… ……..31

Clonogenic viability assay……..32

Matrigel invasion assay……..32

Confocal microscopy……..33

Mice studies……34

Tumor implantation and treatment……34

Reverse phase protein array (RPPA)……..35

CHAPTER 3: Development of a High-throughput and High-content Image Based Screen for the Identification of Modulators of Autophagy in Cancer Cells

Experimental rationale and goals……37

Result……45

Discussion……57

CHAPTER 4**:** Comparative Studies of Phenothiazines' Effects on Cell Viability and Tumorigenic Potentials of Cancer Cells

Experimental rationale and goals……59

Results……..60

Discussion……79

CHAPTER 5**:** Identification of Perphenazine's Target on the Autophagy Signaling Network.

Experimental rationale and goals……83

Results……..84

Discussion……..102

CHAPTER 6: Determination of the Effects of Perphenazine on Cancer Cell Signaling Pathways *in vivo* and in Other Cancer Cell Lines

Experimental rationale and goals……...110

Results…… 111

Discussion……..120

CHAPTER 7: Overview, Future Directions……125

APPENDIX 1: Active autophagy modulators identified by HTS……134

APPENDIX 2: Protein expression profiles of human cells treated……...139
with perphenazine at different time points

REFERENCES……..157

VITA……187

LIST OF FIGURES

FIGURE 1: The multi-steps of autophagy……9

FIGURE 2: Ubiquitin-like regulation of autophagosomal pathway……10

FIGURE 3: Structure of phenothiazine……..19

FIGURE 4: GFP-LC3 fluorescent reporter for autophagosomes in cells…….40

FIGURE 5: Automated image capture of each well in a 96-well microplate……42

FIGURE 6: Automated segmentation of different cellular components……..43

FIGURE 7: Identification of positive controls for a high-throughput ……44
cell based image screen for modulators of autophagy

FIGURE 8: Phenothiazines identified as modulators of autophagy in HTS…….46
screen

FIGURE 9: Phenothiazines identified as active modulators of……..47
autophagy by HTS screen

FIGURE 10: Validation of up-regulation of LC3- II by compound identified……49
as positive hits in drug screen

FIGURE 11: MCF-7/ GFP-LC3 Cells treated with chlorpromazine……50

FIGURE 12: Western blot analysis for the formation of endogenous LC3-II……51

FIGURE 13: Cytoxicity of chlorpromazine in normal and breast cancer cells……..54

FIGURE 14: Treatment with chlorpromazine increased caspase-7……...56
activation in cancer cells

FIGURE 15: Relative potencies of different phenothiazines in modulating……..61
autophagy and inducing apoptosis

FIGURE 16: Comparative analysis of phenothiazines in decreasing……63
cell viability
FIGURE 17: Perphenazine treated cells have increased PARP……65
cleavage and LC3-II in a time dependent manner
FIGURE 18: Perphenazine mediated decreased cell viability is contributed……67
by apoptosis
FIGURE 19: Measure of loss of mitochondrial potential in PPZ treated cells……..69
FIGURE 20: Ultrastructural analysis of autolysosomes by EM……..71
FIGURE 21: Perphenazine decreases cellular ATP……74
FIGURE 22: Effects of perphenazine on invasive potential of cancer cells……..76
FIGURE 23: Effects of different phenothiazines on clonogenic potentials……78
of cancer cells.
FIGURE 24: Substitution on phenothiazines affects lipophilic activity……..82
FIGURE 25: Effects of perphenazine treatment on the autophagy signaling…… 85
pathway
FIGURE 26: Pharmacologic inhibition of core regulators of the……88
autophagosomal pathway
FIGURE 27: Inhibition of autophagy signaling network fails to inhibit……...91
accumulation of LC3
FIGURE 28: Perphenazine mediated decrease in cell viability is independent…...94
of Atg5 activity.
FIGURE 29: tf-LC3 showing perphenazine treatment blocks LC3……97
degradation

FIGURE 30: Perphenazine treatment causes lysosomal volume……..99
expansion (immunofluorescence)

FIGURE 31: Perphenazine treatment causes autophagosomal vacuole……..101
and lysosomal expansion (EM)

FIGURE 32: Phenothiazines contain weak amine base groups and…….....109
undergo protonation in acidic environments

FIGURE 33: *In vivo* study of signaling events altered with perphenazine……..113
treatment

FIGURE 34: Protein expression profiles of cancer cells treated with……..118
perphenazine

FIGURE 35: Waterfall graphs showing proteins with the strongest level of……...119
upregulation or downregulation due to perphenazine treatment

FIGURE 36: Model of proposed mechanism of perphenazine mediated……124
cancer cell death

LIST OF TABLES

Table 1: Mutational status and clinical classification of cell lines used in our……..25
studies

Table 2: Mutational status and clinical classification of breast lines……..……54
used and response to current therapies

ABBREVIATIONS

2-DG	2-deoxyglucose
3-MA	3-methyl adenine
ACC	acetyl-CoA carboxylase
AICAR	amino imidazole carboxamide ribonucleotide
AMPK	adenosine monophosphate protein kinase
ATF6	activating transcription factor 6
Atg	autophagy-related gene
ATP	adenosine triphosphate
Baf A1	Bafilomycin A1
BiP	immunoglobulin heavy chain binding protein
BSA	bovine serum albumin
CQ	Chloroquine
DAPI	4’-6-diamidino-2-phenylindole
DMEM	Dulbecco’s modified Eagle medium
$DIOC_6$	3,3′-dihexyloxacarbocyanine iodide
EBSS	Earle’s buffered salt solution
ER	endoplasmic reticulum
FBS	fetal bovine serum
GAPDH	glyceraldehyde 3-phosphate dehydrogenase
HCQ	hydroxychloroquine
hr	hour

HRP	horseradish peroxidase
HTS	high-throughput screen
IGF	insulin-like growth factor
IGF1R	insulin-like growth factor 1 receptor
kDa	kilodalton
LC3	microtubule-associated protein 1 light chain 3
MAPK	mitogen-activated protein kinases
MEFs	mouse embryonic fibroblasts
mTOR	mammalian target of rapamycin
mTORC1	mammalian target of rapamycin complex 1
mTORC2	mammalian target of rapamycin complex 2
MTT	3-(4, 5-dimethylthiazol-2-yl)-2,5-diphenyl tetrazolium bromide
PARP	poly (ADP-ribose) polymerase
PBS	phosphate buffered saline
PCD	programmed cell death
PDGF	platelet-derived growth factor
PDK1	protein-dependent kinase 1
PDK2	protein-dependent kinase 2
PE	phosphatidylethanolamine
PH	pleckstrin homology
PI	propidium iodide
PI3K	phosphatidylinositide 3 kinase
PI(3)P	phosphatidylinositol 3-phosphate

PI(4)P	phosphatidylinositol 4-phosphate
PIP2	phosphatidylinositol bisphosphate
PI(4,5)P2	phosphatidylinositol 4,5-bisphosphate
PIP3	phosphatidylinositol trisphosphate
PI(3,4,5)P3	phosphatidylinositol (3,4,5)-trisphosphate
PMSF	phenylmethylsulfonyl fluoride
PtdIns	phosphatidylinositol
PVDF	polyvinylidene fluoride
RNA	ribonucleic acid
RNase	ribonuclease
RPMI	Roswell Park Memorial Institute medium
RPPA	reverse phase protein array
SDS-PAGE	sodium dodecyl sulfate-polyacrylamide gel electrophoresis
siRNA	short interference RNA
TSC2	tuberous sclerosis protein 2
ULK	Unc-51 like kinase
UPR	unfolded protein response
UVRAG	ultraviolet irradiation resistance associated gene

CHAPTER 1

INTRODUCTION

The American Cancer Society estimates 226,870 new cases of breast cancers in women and 2,190 new cases in men the United States in 2012. Although breast cancer cases have declined since 1990, it remains the second leading cause in cancer related deaths in women in the United States. The ACS estimates it will claim the lives of 39,510 women and 410 men this year (2). These statistics provide a strong impetus for studying novel pathways that could help develop better therapeutics for the treatment of breast cancer.

Chemotherapy is an important tool for the treatment of breast cancers. It can increase the survival of patients in the adjuvant as well as in the metastatic setting. However, there are several different mechanisms by which cancer cells have inherent or acquired resistance to the variety of chemotherapeutic agents used. Since autophagy is also known as programmed cell death type II, an alternative form of cell death to apoptosis, it has attracted a lot of interest as a potential target for cancer therapeutics (3). Indeed, our laboratory has shown that targeting autophagy can enhance therapeutic effectiveness of some cancer treatments (4).

AUTOPHAGY

Autophagy is derived from Greek, “auto” meaning self and “phagia” meaning eating and describes a catabolic process involving a double membraned phagophore (which forms the autophagosome) and which following fusion with the lysosome leads to degradation of cytoplasmic contents. It is a highly conserved mechanism, found in yeasts to mammals (5). There are three major types of autophagy: microautophagy, chaperone-mediated autophagy (6), and macroautophagy (7). These are defined by the method by which they deliver their cytoplasmic cargo to the lysosomes. The focus of this study is macroautophagy, hereafter referred to as autophagy. Autophagy is an important evolutionarily conserved process of cellular maintenance, differentiation, development of mammals, and cell survival. Autophagy is also known as a cell death mechanism; programmed cell death type II (PCD II), a cell death distinct from apoptosis which is known as programmed cell death type I (PCD I) (8). Disruption or dysregulation of autophagy is implicated in many diseases including microbial infection, heart disease, neurodegenerative diseases, and cancer (9).

Physiological functions of autophagy

Autophagy is constitutively activated and occurs at a basal level in cells and functions as a homeostasis mechanism. It serves as a quality control in cells, limiting the accumulation of aggregated proteins, damaged organelles and macromolecules by sequestering them for degradation through the lysosomal system. By catabolic degradation of cellular components, autophagy also serves as

a cellular recycling system for the generation of energy and macromolecules for biosynthesis in cells (10). This function is especially important in ensuring cell survival by maintaining cellular energy level during limited glucose, oxygen, and amino acid conditions (11). Additionally, by clearing cells of damaged organelles and aggregated proteins, autophagy prevents them from building up and reaching toxic levels which could result in tissue damage, inflammation, and cancer development (12), (13),(14), (15), (16), (17).

Autophagy functions as quality control of proteins and organelles

Autophagy functions as quality control of organelles, aggregated proteins and ubiquitinated protein. Other systems of protein quality controls in the cells are mediated through the endoplasmic reticulum (ER) and the proteasomal degradation pathway.

The ER is a cytosolic compartment which functions in folding and modification of newly synthesized secretory, cell surface or organelle proteins and also functions as one of the cell's calcium reservoirs (18). Soluble proteins which are misfolded are transported out of the ER to be targeted for ubiquitination and proteasomal degradation in the cytosol by ER-associated degradation (ERAD) I pathway (19). Insoluble, misfolded or aggregated proteins are processed through activation of autophagy, also known as the ERAD II pathway (20). During adverse conditions such as impaired glycosylation, oxidative stress, hypoxia, nutrient deprivation, bacteria or viral infection, ER function is perturbed and has exceeded its capacity to fold proteins, ER stress ensues (21), (22). Accumulation of unfolded

proteins in the ER lumen can cause ER stress which activates the Unfolded Protein Response (UPR), a group of pathways which function to restore ER homeostasis (23). There are three known transducers of ER stress which sense ER lumen unfolded protein levels to activate the UPR. These include the RNA-dependent protein kinase like ER kinase (PERK), activating transcription factor 6 (ATF6) and inositol-requiring enzyme 1 (IRE1). The UPR is an adaptive signaling pathway that shifts protein synthesis from global proteins to the synthesis of chaperones and other proteins involved in the restoration of the function of the ER. The outcome of the activation of UPR is context dependent which could result in reduction of proteins entering the ER, increased protein clearance from the ER, or increased protein folding capacity of the ER. During sustained or irreversible ER stress, the UPR changes from a cytoprotective function and initiates apoptotic cell death (24), (25). ER stress is also an activator of autophagy (26), (27, 28), (28), whereby the ER is a major cargo of the autophagosome. Here, autophagy functions as a pro-survival process to remove ER that contains unfolded proteins (27). ER stress, like autophagy functions as a pro-survival or pro-death mechanism which is cell and context dependent (29). ER stress can induce autophagy (24); on the other hand, we have previously shown that abortive autophagy is an inducer of ER stress (30). Although ER stress and autophagy are distinct homeostatic cellular pathways, they are interlinked and share common regulatory proteins. The connection between autophagy and ER is through Beclin 1 through its regulation at the ER membrane (31). Interestingly, several stimuli which activate autophagy also activate ER stress. Such stimuli include nutrient deprivation, energy perturbation, DNA damage, and

oxidative stress. The UPR is upregulated in many tumor cells, whereas it is quiescent in normal cells (32).

The ER, ubiquitin-proteasomal degradation pathway, and autophagy are three mechanisms that function in cellular protein quality control. These three protein quality control mechanisms are compensatory to each other; when cells are unable to recover stresses through the activation of either one of them alone, activation of the other pathways occur (12), (33).

Autophagy is a multi-step process

Autophagy begins with a nucleation step for the formation of a phagophore, or isolation membrane in the cytosol. The phagophore undergoes elongation and forms a cup-like structure that encloses cytosolic components which include organelles and aggregated proteins for the delivery to the lysosome. The double-membrane vacuole forms the autophagosome. During maturation, the autophagosome expands and fuses with a late endosome (11). It subsequently fuses with a lysosome to form an autophagolysosome (or autolysosome). At the final stage of the autophagosome process, the enzymes of the lysosome degrade the autolysosome's contents and provide metabolic substrates as energy source or as building blocks in the cell (34) (FIGURE 1). This process occurs at a basal level in all cells, but can rapidly be upregulated by adverse conditions such as nutrient deprivation, growth factor withdrawal, cytotoxic stress, hypoxia, protein aggregates and metabolic stress (35),(10),(36).

The core regulators of the autophagosome machinery

The regulation of the autophagosomal process is coordinated by autophagy related proteins (Atg) originally discovered and studied in yeast systems (37) (38) (39), (39, 40), (38). Over 30 mammalian homologues of the yeast autophagy related genes have been identified (41). Core Atg genes regulate the autophagic process through the formation four complexes. The first complex is the Atg1/Unc-51 like kinase (ULK) complex which is controlled by mTOR phosphorylation. The second complex consists of Vps34, a class-III phosphatidylinositol 3-kinase (PI3K), and Vps15 form a complex with Beclin 1, the homolog of yeast Atg6 (42), Bif-1 (Bax-interacting factor -1), and UVRAG (ultraviolet irradiation resistance associated gene) (43) which is involved in the nucleation of the phagophore. The elongation of the membranes is mediated through two complexes, which coordinate ubiquitination-like modifications of target proteins: the Atg12-conjugation and the LC3-modification system (44), (45), (41)(FIGURE 2). The Atg12 complex is necessary for the formation of the pre-autophagosomal structures and the modification of LC3 is required for the elongation and formation of autophagosomes (46). The first ubiquitination-like steps involve conjugation to covalently link Atg12 to Atg5. This occurs through the activation of Atg12 by Atg7 followed by Atg10 mediated transfer to Atg5 (47). Atg12-Atg5 then complexes with Atg16, subsequently associating with the phagophore (48).

LC3, the mammalian ortholog of the yeast Atg8 protein, was originally isolated as a microtubule-associated protein and named microtubule-associated protein 1 light chain 3 (LC3) (49). It exists as a soluble pro-LC3 form which

undergoes several ubiquitination-like modifications upon autophagy induction to eventually associate with the precursors of the autophagosomal structures and the autophagosomes (50). Pro-LC3 undergoes cleavage leading to exposure of a carboxyl terminal glycine to form LC3-I (46). LC3-I is activated by Atg7 (E1-like protein) and is subsequently transferred to Atg3 (E2-like protein) for modification to LC3-II (51). Prior to autophagy induction, LC3 is soluble and is distributed throughout the cytosol. Upon autophagy induction, LC3 is modified to LC3-I and becomes lipidated with phosphoethanolamine (PE), forming LC3-II. LC3-II then associates with the inner and outer membrane of the autophagosomes. Once the autophagosomes fuses with the lysosomes, the outer membrane associated LC3- II is removed from PE by Atg4 for recycling (52), (53),(51) and the LC3-II on the inner the membrane is degraded by lysosomal enzymes. Upon autophagy completion, the Atg proteins are recycled (54).

Monitoring autophagy

Autophagosomes can be monitored in live or fixed cells using fluorescent microscopy with the use of a green fluorescent protein linked to LC3 (GFP-LC3) to track its localization changes (55). Since autophagy is a dynamic process, blocking autophagic signaling network or flux can result in a build-up of the LC3-II marker. The LC3 reporter for autophagy therefore must be used in conjunction with other assays such Western blot analysis and ultrastructural studies by electron microscopy (EM) to confirm the increase in autophagosomes (56). The activity of autophagy is measured by determining autophagic flux by measuring the

degradation of one of its substrate, p62. p62 protein, also known as SQSTM1, is a protein involved in diverse cellular signaling pathways, having roles in transcription factor activation, inflammation, cell survival and cellular stress functions (57). In addition to associating with ubiquitin, p62 also interacts with LC3 and localizes to autophagosomes where it is a substrate of autolysosomal degradation (58), (59). Increased p62 levels in the cells, is consistent with autophagic flux being blocked (60), (12).

The completion of the autophagy process involves the delivery of autophagosomal contents to lysosomes for degradation. Monitoring the autophagosomal to lysosomal fusion step of the autophagy pathway can be accomplished by use of a green fluorescent protein, linked to a red fluorescent protein (GFP-RFP) and fused to LC3. With this reporter, LC3 bound on autophagosomes fluoresces red and green, but upon fusion with the lysosome, it loses the green fluorescence of GFP because GFP is more sensitive to lysosomal pH (61). In certain experimental conditions, the lysosomal function is impaired and both GFP and RFP signals persist. Thus, when GFP and RFP persist, this indicates the autophagosome did not fuse with the lysosome. Vesicles which only show RFP are fused autolysosomes (61).

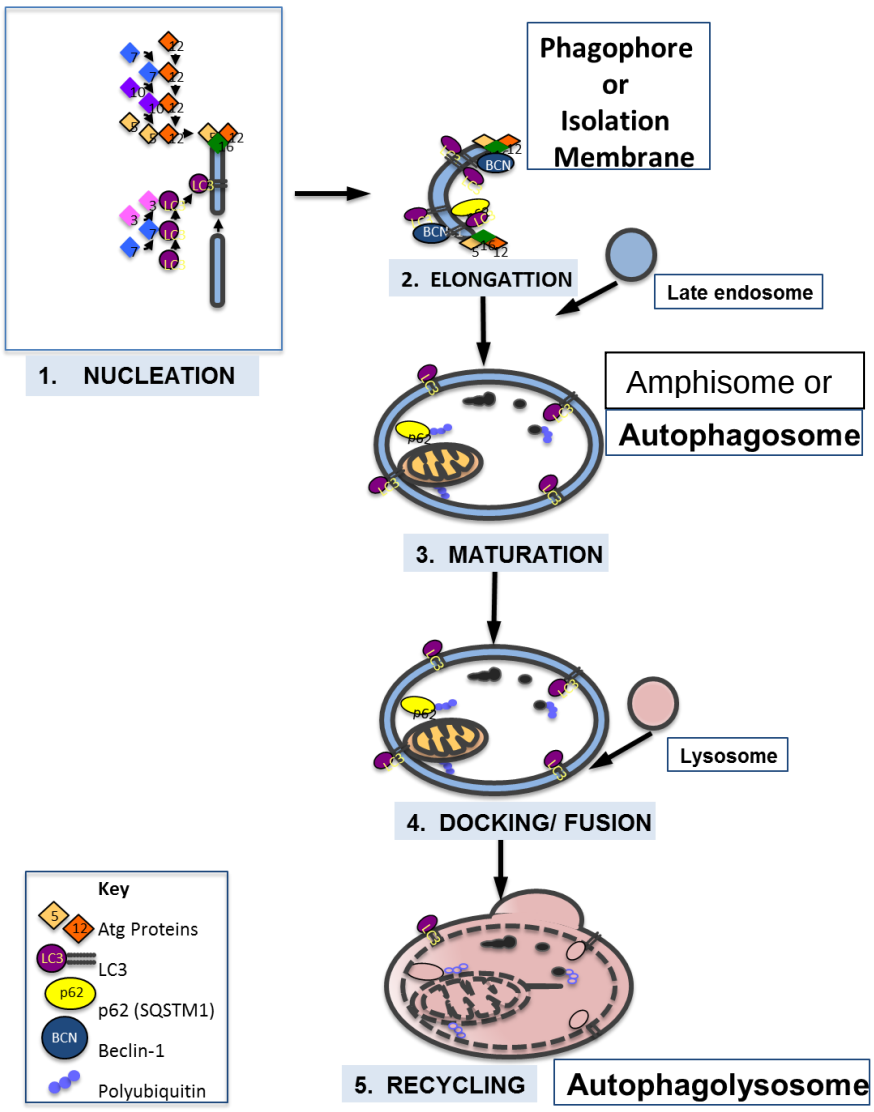

Adapted from *Trends in Cell Biology*. 21:387-92 (2011)

FIGURE 1: Multi-steps of autophagy. Autophagy is a multi-step process beginning with (1) vesicle nucleation to form a phagophore, which (2) elongates to form a C- cup which encloses to form a double-membrane vesicle (the autophagosome) engulfing cytoplasmic materials (organelles, and polyubiquitinated and aggregated proteins). The autophagosome (3) matures and can either fuse with late endosomes to form an amphisome or (4) fuse directly with the lysosome to form the autophagolysosome or autolysosome.

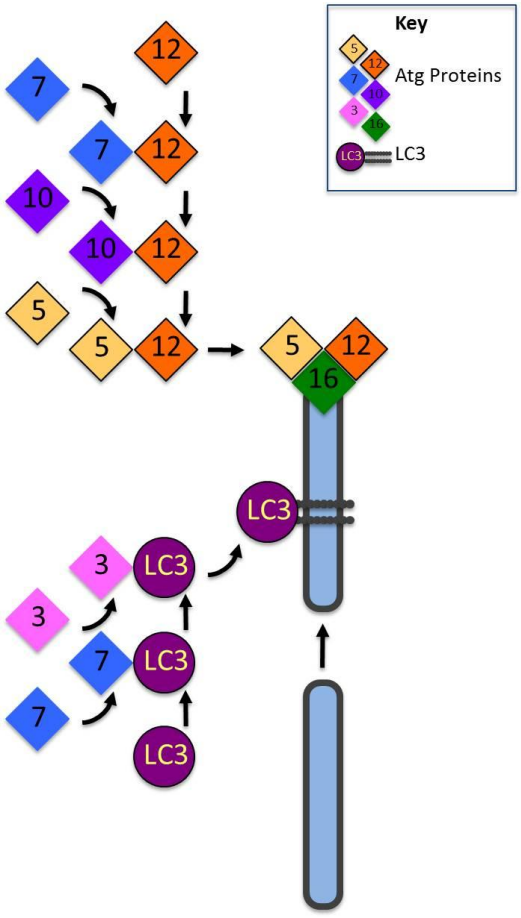

FIGURE 2: Ubiquitin-like regulation of autophagosomal pathway.

Key regulatory proteins of the autophagy pathways undergo conjugation and modification by two ubiquitin-like modifications. Atg12- conjugation is required for formation of the pre-autophagosomal structures and LC3- modification is necessary for the formation of autophagosomes. Adapted from *Trends in Cell Biology*. 21:387-92 (2011).

AUTOPHAGY AND CANCER

The importance of autophagy in cancer has clearly been recognized by the scientific research community as seen in the numerous clinical trials involving manipulation of autophagy for cancer treatment (http://www.clinicaltrials.gov) (62). Although autophagy is an attractive target for cancer therapy development, there is much ongoing discussion as to whether it should be stimulated or inhibited for anticancer strategy. Due to its contradictory roles in cell survival, it is often referred to as a double- edged sword. Autophagy's dual roles as a cell death and cell survival mechanism must be understood based on cellular context. Currently, the evidence largely supports the role of autophagy as tumor suppression in the earlier stage of transformation but changes to supporting tumor survival in advanced cancers (62). Autophagy's pro-tumorigenic or tumor suppressive role is dynamic and is determined by several factors which include the tumor stage, cellular status, and tissue of origin (63).

The link between autophagy and cancer was through the discovery of the tumor suppressor Beclin 1(64). Beclin 1 expression level is lower in certain cancer lineages as compared to normal cells. When Beclin 1 was re-introduced into the cancer cell lines with low Beclin 1 levels, *in vivo* tumorigenesis of xenografts was suppressed. Beclin 1 is monoallelically deleted in many human cancers including breast, ovarian, prostate, and brain tumors (65), (66). Beclin 1's role as a tumor suppressor is further supported by findings that the domain required for Vps34 binding for autophagy induction, is the domain which confers its tumor suppressive function (67), (64). It has also been observed that deficiency in other autophagy

genes such as Atg genes increased cells' susceptibility to tumorigenesis (68), (69). The Mizushima laboratory generated mouse models with deletion in Atg5 in various tissues. They showed that conditional deletion of Atg5 in liver led to development of benign liver tumors (68); Inami *et al.* found similar results with conditional deletion of Atg7 (70). Both groups showed that although benign tumors developed, they were not able to progress to invasive tumors.

Accumulating evidence suggests that autophagy plays a protective role in advanced tumors, permitting the cells to survive the cytotoxic and metabolic stress of chemotherapeutics (71), (62), (72). Activation of autophagy in response to cancer therapies including radiation and chemotherapy has been attributed to the development to drug resistance. Therapy induces cellular stresses such as elevated ROS production, accumulation of ER chaperones and p62, activation of DNA damage responses, genomic damage, chromosomal instability, and cytokine production which could lead to inflammation and cell death. Autophagy mitigates these stresses by sequestering the damaged organelles and toxic byproducts for degradation to re-establish homeostasis.

There is a large body of pre-clinical data showing that blocking autophagy enhances therapeutic efficacy of different chemoagents. Following inhibition of autophagy activation as a pro-survival mechanism in response to the insult of the treatments, the cells succumb to the stress mediated by the therapy (73). Autophagy in its cytoprotective role has been attributed to cancer cell resistance to therapy in MCF-7 cells (74). Cancer cells treated with cytotoxic agents which results in DNA damage upregulate autophagy to delay cell death by sequestering

damaged mitochondria to the autophagosomes for degradation and delaying apoptosis (74). Activation of autophagy in response to perifosine treatment resulted in decreased cytoxicity in chronic myeloid leukemia cells (CML); when autophagy was inhibited, cell killing by perifosine was enhanced (75). Inhibition of autophagy by desmethylclomipramine enhanced the cytotoxic potential of doxorubicin in breast cancer cells (76). Together, these evidence support autophagy inhibition as a therapeutic strategy.

Targeting differences in autophagy in cancer versus normal cells

Since autophagy impacts many cellular functions there are significant challenges in developing targeted therapy with low toxicity to normal cells. Targeting differences between cancer and normal cells such as autophagy activation levels or metabolic differences could offer therapeutic opportunities with decreased toxicity to normal cells.

Several studies demonstrate that cancers driven by the K- Ras oncogene have elevated autophagy. It is proposed that Ras activation reprograms metabolic pathways, making the cells dependent on autophagy to survive these metabolic stresses. These cancers are addicted to autophagy for survival and are especially sensitive to autophagy inhibition (63). Mancias *et al.* compared of autophagy levels in high and low grade pancreatic cancer cells with K-Ras mutations against normal pancreatic ductal epithelium and showed that K-Ras mutated cells had elevated basal autophagy. Genetic and pharmacological inhibition of autophagy in the K-Ras mutated cells blocked their tumorigenic potential *in vitro* as well as *in vivo*. The K-

Ras mutated cells' metabolism was dependent on autophagy and inhibition of autophagy caused decreased oxidative phosphorylation. Eileen White's laboratory also reported that cancers driven by the K-Ras oncogene were dependent on autophagy for survival and tumor transformation. They reported that when high levels of H-Ras or K-Ras; often found in human tumor cells, were introduced into non-tumorigenic mouse kidney epithelial cells, these cells had elevated autophagy levels. This was observed in several human cancer cell lines which included bladder, lung and pancreatic cancer cell lines (77). The authors proposed that activated Ras mutations placed high metabolic demands on the cells, thus forcing them to rely on autophagy to provide catabolic substrates to meet the energy demands for survival, growth and proliferation. When the K-Ras oncogene was expressed in the MCF10-A non-tumorigenic human breast cells, they required high basal autophagy in order to undergo tumor transformation which was abrogated when autophagy was inhibited genetically or pharmacologically (78). These findings showed a synthetic lethal interaction between Ras activation and autophagy deficiency (77), (79). Additionally, Ras driven cancers are also dependent on autophagy for glucose uptake and glycolytic flux as MEFs cells deficient in autophagy showed decreases in both glucose flux and uptake (80). Because the Ras mutated cells already have high levels of autophagy, they are not able to upregulate autophagy any further when faced with additional stressors in order to adapt and survive. The mechanism by which Ras driven cancers become addicted to autophagy is largely due to impairment of acetyl-CoA production which is important to maintain the tricarboxylic acid (TCA) cycle. Ras impairs acetyl-CoA

production through three mechanisms: activation of lactate dehydrogenase (LDH) causing pyruvate depletion; activation of pyruvate dehydrogenase kinase 1(PDK1) leading to pyruvate dehydrogenase (PDH) inhibition; and by inhibiting the AMP-activated protein kinase (AMPK) which results in blocked mobilization of lipid stores and β-oxidation. In doing so, the cells must rely on autophagy for fatty acids, and amino acids for acetyl-CoA synthesis as the supply normally obtained through pyruvate and β-oxidation is no longer available (72). One of the consequences of Ras' effects on acetyl-CoA production is decreased mitochondrial life span. Ras causes depletion of mitochondrial TCA cycle substrates and impairs biogenesis of new mitochondria due activation of HIF1 (81). Without functional autophagy to provide the TCA cycle substrates for mitochondrial respiration, the mitochondria become ineffective in providing the energy required to support tumorigenesis (82).

In developing cancer therapies, the goal is to target cancer cells while limiting toxicities to normal cells. As such, we are essentially searching for the cancer's Achilles' heel (83). Since solid tumors undergo rapid cell proliferation, they have high metabolic demands and often have outgrown the vascular supplies that sustain them, and undergo nutrient deprivation, hypoxia and are more dependent on autophagy than normal cells. Thus autophagy is a potential target for the development of therapeutic strategies. For certain cancers driven by the Ras oncogene, autophagy addiction also offers opportunities for targeting differences between the tumors and the normal surrounding cells.

PHENOTHIAZINES

Phenothiazines are in important family of drugs which are mostly known for their antipsychotic properties. Chlorpromazine was the first antipsychotic developed and holds an important place in the history of psychiatry. Phenothiazines were the mainstay of treatment for psychotic ailments for the 1950s to the 1990s, but have been replaced by second generation antipsychotics with decreased side effects. However, they remain in use today; phenothiazines such as chlorpromazine and fluphenazine continue to be on the World Health Organization's List of Essential Medicines (84).

Phenothiazines are tricyclic compounds containing a sulfur and a nitrogen with the structural formula $S(C_6H_4)_2NH$ (FIGURE 3). Subgroups of phenothiazines are divided based on the substitution on the nitrogen residue: the aliphatic, piperidine, and piperazine groups. Different substitutions on the core ring confer specificity to different cellular targets. The aliphatic side chains confer the least hydrophobicity, and therefore are not as effective in crossing cellular membranes.

Phenothiazines mediate their antipsychotic effects by inhibiting the interaction of dopamine and its dopamine receptor type 2 (D_2) (85), (86), (87). Phenothiazines also function as antagonists against other neurological transmitter receptors such as the serotonin ($5HT_{2A}$), muscarinic (M_1), adrenergic (α_1) and histamine (H_1) receptors, but their interactions are not as strong as dopamine receptor interaction (88), (89). Common side effects of the original phenothiazines include drowsiness and sedation. New generations of phenothiazines have curbed these side effects, but development of tolerance over time remains a problem.

Phenothiazines are also alpha-adrenergic blockers and not indicated for treatment of patients with cardiovascular diseases due to increased pulse rate and hypotension. All antipsychotic drugs including phenothiazines have potential of causing tardative dyskinesia syndrome after long-term and at high dose usage. This is manifested as involuntary rhythmic facial muscular movements.

Phenothiazines and their derivatives have an approximate half-life of 30 hr in patients. They are metabolized by the liver into at least 12 different metabolites which are generally excreted in the urine. In the blood, phenothiazines are heavily bound to plasma proteins, especially albumin.

The parental phenothiazine core ring structure itself has many diverse pharmacologic activities including antioxidant, antihelminthic, and antiseptic activities (90). Chlorpromazine is the proto-type antipsychotic, but many other phenothiazines are also important and used in the clinical setting for different treatments. Examples of other phenothiazines are promethazine which has antihistamine activity and thioridazine which is indicated for antipsychotic treatments (84). Phenothiazines have a long established history in the clinics and are well tolerated, therefore continue to be used for development of new therapeutic applications. The most interesting activities of phenothiazines as pertaining to our study are phenothiazines antitumor activities (91), (92), (93).

Expression of dopamine receptors outside of central nervous system

Dopamine receptors are predominantly expressed in the central nervous system (94), but they have also been reported to be found in other tissues (95). Dopamine receptor expression has been reported in the pituitary gland, in the peripheral nervous system along with some tissues such as the kidney, adrenal gland, and cardiovascular system (94), (95). Studies have shown that various types of tumors which included pancreatic, non-small cell lung cancer, prostate, colon expressed dopamine receptors (96), (97).

Sokoloff *et al.* conducted a study of 7 human tumor cell lines; pertinent to our studies, were the SKBR-3 and MCF-7 breast cancer lines. They reported that the breast cancer cell lines MCF-7 had no dopamine D2 receptors, and SKBR-3 cells had 38± 6 dopamine D2 receptors per cell (98).

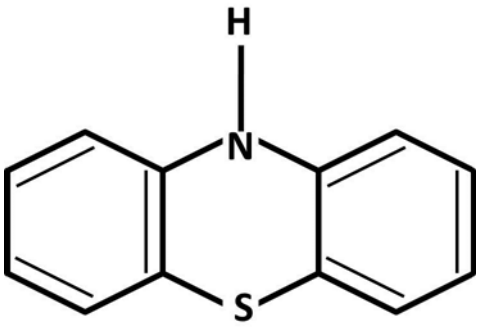

FIGURE 3: Structure of phenothiazine $S(C_6H_4)_2NH$. The parental phenothiazine ring is a sulfur and nitrogen tricyclic ring. It has been used extensively for the development of drugs through backbone modifications and substitutions. Substitutions at different positions on the parental ring changes the specificity of phenothiazines to different cellular targets.

Phenothiazines and cancer

Phenothiazines already play an important role in the cancer setting where they are prescribed for management of nausea and emesis which are often associated with advanced stages of cancers and chemotherapy (99). Their inclusion in cancer treatment helps improve the quality of life of patients undergoing chemotherapy and ensures completion of the treatment by alleviating discomforts of nausea and vomiting (100). Additionally, as antiemetics, phenothiazines prevent the reflexive regurgitation of oral medications and ensure patients receive full dose benefits. As sedative antipsychotics, they are prescribed to alleviate anxiety experienced by cancer patients (101). While the antiemetic and sedative role of phenothiazines are important to cancer patients, many studies have shown that phenothiazines also possess anti-proliferative potential against cancer cells.

Pre-clinical and clinical studies have shown that several drugs of the phenothiazine family have anti-proliferative and anti-neoplastic properties in diverse human cancer cell lines; these include non-small cell lung, breast, melanoma, lymphoblastoma and many other types of cancers (102), (103), (104). Chlorpromazine was shown to enhance the efficacy of the antineoplastic agent mitomycin C in mice models; inhibition of tumor formation was also accompanied by prolonged survival (105). CPZ was also shown to synergize with pentamidine to inhibit antiproliferation of cancer cells *in vivo* (106). *In vitro* studies show that phenothiazines can reverse multidrug resistance in human breast carcinomas (107). For instance, CPZ potentiates efficacy of tamoxifen and doxorubicin in breast cancer cells, the proposed mechanism by which CPZ enhances the toxicity of these

drugs was through its inhibition of drug efflux from the cells (108). Phenothiazines have been shown to inhibit the membrane efflux pump P-glycoprotein, which mediates drug multidrug resistance (MDR) (109). Phenothiazines have also been reported to downregulate the epidermal growth factor receptors (110), making them potential agents for the treatment of cancers with upregulated EGFR activation (111), (112), (113). The anti-proliferative properties of phenothiazines in different types of cancers have also been proposed to be due to their action as calmodulin regulators (114), (115), (116). Other reported anti-tumor activities of CPZ included enhancing sensitivity of cancer cells to radiation (117), and inhibition of energy metabolism of hypoxic cells (118). Together, these properties make CPZ and its derivatives attractive agents for development as anti-tumor therapy towards solid tumors which have hypoxic centers and which are resistant to therapy. Additionally, recently phenothiazines have been proposed to modulate autophagy, however mechanistic underpinnings have not been explored and these studies have not been followed-up (119) ,(120).

Dissertation Overview

The overall aim of this dissertation is to understand how modulation of autophagy in cancer cells affects cell viability and to determine whether autophagy could be targeted for cancer therapy.

Currently, there is limited availability of pharmacological modulators of autophagy with limited toxicities to normal cells. We therefore sought to identify novel modulators of autophagy. To accomplish this aim, we developed and implemented a cellular image-based high-throughput screen (HTS) to identify perturbants of autophagy in cancer cells. We used a compound library of off-patent FDA approved drugs and biologically active compounds to increase the likelihood that our findings would be clinically relevant and eventually be brought to the clinic. The highest ranking perturbants in our screen were identified as positive “hits” and were validated in secondary assays. The largest group of compounds identified in our screen as modulators of autophagy belonged to the phenothiazine family, and therefore became the focus of our studies. We sought to understand how modulation of autophagy by phenothiazines affects tumorigenic potential such as cell viability, invasion and clonogenic potential. Because autophagy is closely linked to cell energy metabolism, we wanted to understand whether phenothiazines affect cellular ATP levels. We also sought to determine if antitumorigenic effects mediated by the phenothiazines were inherent to the parental phenothiazine ring structure. We therefore conducted comparative structural functional studies of various representative phenothiazines. In general, all of the actions of the

phenothiazines in cancer cells paralleled their known structural functional activities as antipsychotics. This raised the possibility that the anti-tumorigenic potentials of different phenothiazines are mediated through their properties as dopamine receptor antagonists. We researched the literature for the status of dopamine receptor expression in the cancer cells that were in our study and determined that the breast cancer cell lines we used either had no dopamine receptors or low expression of dopamine receptors; yet autophagy modulation and cell death was observed. Therefore the antitumorigenic effects of phenothiazines were unlikely to be mediated through binding with dopamine receptors. Since breast cancer is the most common malignancy in women and the second leading cancer related death in women worldwide, we decided to focus on breast cancer as our model to study phenothiazines' modulation of autophagy in cancer cells *in vitro* as well as *in vivo*.

Additionally, we conducted a human xenografted mice study to determine if the findings our *in vitro* studies were replicated *in vivo*. We conducted a protein array analysis of the expression levels of proteins involved in cancer cell signaling pathways to determine if there were differences in signaling in tumors that showed response to our drug treatment as compared to tumors that did not show response. We analyzed protein expression profiles of tumors of different lineages treated with perphenazine to determine if our findings are generalized to different tumors, and if certain mutational backgrounds, or tissue of origin rendered them more sensitive to our drug. Findings in this study indicate that phenothiazines (combined with other agents) are viable candidates for development for antitumor strategy and warrant further investigation.

Compounds and reagents

Rapamycin was purchased from Cell Signaling Technology (Danvers, MA). Gleevec (Imatinib) was a kind gift from Dr. Seiji Kondo at MD Anderson Cancer Center. The Prestwick compound library (Prestwick Chemicals, Washington, DC) was a generous gift from the John S. Dunn Foundation through the Gulf Coast Consortia for Chemical Genomics. Phenothiazine compounds: Chlorpromazine, Chlorpyramine, Perphenazine, Promethazine, Promazine, Temozolomide, 2-deoxyglucose and Bafilomycin A1 were all from Sigma-Aldrich (St. Louis, MO). Z-VAD was from R&D systems (Minneapolis, MN). All compounds were dissolved in DMSO unless indicated otherwise. Control experiments showed that DMSO had no effect on any of the parameters measured. Earle's Balanced Salt Solution (EBSS) was from Hyclone, Thermo Scientific.

Cell lines

Human breast cancer cell lines were obtained from the American Type Culture Collection (ATCC) (Manassas, VA). MDA-MB-231, MDA-MB-468, MCF-7, BT-549, SKBR-3, ovarian cell lines SKOV-3, OVCAR-3, prostate cell lines LNCaP, PC-3 and melanoma cell lines SKMEL-5, MEWO, and WM-35 were maintained in RPMI 1640 medium supplemented with heat-inactivated 5% fetal bovine serum (FBS). Mouse embryonic fibroblasts (MEFs) and U2-OS cells were cultured in DMEM medium supplemented with heat-inactivated 5% FBS. MCF-10A non-malignant human mammary epithelial was maintained in DMEM/F12 with 5% horse serum, 10 μg/ml

insulin, 0.5mg/ml hydrocortisone, 20 ng/ml EGF and 100 ng/ml cholera toxin. All cells were maintained at 37 °C at 5% CO_2 at sub-confluent density to prevent induction of autophagy. All cell lines were validated by STR DNA fingerprinting using the AmpFℓSTR Identifier kit according to manufacturer' instructions (Applied Biosystems, Carlsbad, CA). The STR profiles were compared to known ATCC fingerprints (www.ATCC.org), Cell Line Integrated Molecular Authentication database (CLIMA) version 0.1.200808, and to the MD Anderson fingerprint database.

TISSUE	CELL LINE	MUTATIONAL STATUS	CLINICAL SUB-TYPE	ER Status
Breast	BT-549	RB1, TP53, PTEN	Basal-like	ER-
Breast	MCF-10A	None detected	Triple negative Basal	ER-
Breast	MCF-7	CDKN2A, PIK3CA	HR+, luminal	ER+
Breast	MDA-MB-231	BRAF, CDKN2A, KRAS, TP53	Triple negative	ER-
Breast	MDA-MB-468	PTEN, RB1, TP53, SMAD4	Triple negative	ER-
Breast	SKBR-3	None detected	HR+,	ER-
Breast	T47D	PIK3CA, TP53	HR+, Luminal	ER+
Breast	ZR75-1	KRAS, PTEN	HR+, Luminal	ER+
Melanoma	MEWO	CDKN2A, TP53, NF1		
Melanoma	SKMEL-5	BRAF, CDKN2A, STK11		
Melanoma	WM 35	BRAF		
Ovarian	OVCAR-3	TP53		
Ovarian	SKOV-3	CDKN2A, PIK3CA, TP53		
Prostate	PC-3	PTEN, TP53		
Prostate	LNCaP	PTEN		
Bone	U2-OS	None detected		

Table 1. Mutational status and clinical classification of cell lines used in our studies.

Fluorescent image based high-throughput drug screen for autophagy modulators

The GFP-LC3 construct was a kind gift from Dr. Noboru Mizushima; Tokyo Medical and Dental University, Japan). U2-OS osteosarcoma cells stably expressing the GFP-LC3 construct were seeded at a density of 5,000 cells/ 100 µl media in black-walled clear bottom 96-well tissue culture plates. Cells were allowed to attach overnight. The following day, compounds were added to each well and incubated for 48 hr at 37° C with 5% CO_2. Cells were post-fixed with 4% paraformaldehyde in PBS for 15 min in the dark at room temperature. Cell nuclei were stained with Hoechst 33342 (1:1,000 dilution) for 5 min, washed with PBS, and maintained in 200 µl PBS for fluorescent microscopy imaging at 20X magnification on an IN Cell Analyzer 1000 Cellular Imaging and Analysis system which is equipped with a Nikon fluorescent microscope with an automated stage (GE Healthcare, Piscataway, NJ). 5 fields were captured per well for each 96-well plate. The nuclear regions were segmented using the Hoechst 3334 dye, and cytoplasmic regions were identified using the GFP signal. Only GFP positive cells were quantified for autophagy analysis. Autophagosome formation was determined for each cell using the multi-target analysis algorithm provided with the IN Cell Analyzer. Results were shown as percent autophagy.

siRNA transfection

Non-targeted RISC-Free control (D-001220-01-05), Beclin-1, Atg5 (L-004374-00), and Atg12 (L-010212-00) siRNAs (Dharmacon, Lafayette, CO) were diluted in molecular grade RNase-free water. Cells were plated in 6 cm tissue culture dish 24 hr prior to transfection at 40%-50% confluency. The media was replaced with fresh media prior to siRNA transfection by reverse transfection at 10 nM final concentration in 2 ml OPTIMEM I using RNAi Max transfection reagent (Invitrogen, Carlsbad, CA) and prepared according to the manufacturer's instructions. 24 hr after transfection, fresh media was added and the cells were transfected again with siRNA. 48 hr from the 1st transfection, the cells were treated with perphenazine at the indicated concentration. The cells were collected at the 72 hr after the 1st siRNA transfection (24 hr post drug treatment) for analysis by Western blot analysis.

SDS-PAGE and western blot analysis

At the endpoint of each experiment, cell culture dishes were placed on ice; both floating cells and adherent cells were collected and lysed in ice-cold lysis buffer (1% Triton X-100, 50 mM Hepes, pH 7.4, 150 mM NaCl, 1.5 mM $MgCl_2$, 1 mM EGTA, 100 mM NaF, 10 mM sodium pyrophosphate, 1 mM Na_3VO_4, 10% glycerol, 1 mM phenylmethylsulfonyl fluoride (PMSF), and 10 μg/ml aprotinin). Whole cell lysates were centrifugated at 13,000 rpm for 10 min at 4°C. The supernatants were collected for subsequent analysis. Cellular protein concentration in the supernatant was determined by BCA reaction (Pierce, Rockford, IL). The proteins were prepared in denaturing sample buffer adding 1 part 4x SDS sample buffer (40% Glycerol, 8%

SDS, 0.25M Tris-HCl, pH 6.8, 10% (2-mercaptoethanol) to 3 parts lysate. The sampled were heated to 95° F for 15 minutes. The proteins were separated by SDS-PAGE and transferred to PVDF membranes. The membranes were blocked with 5% (w/v) BSA in TBS-T (10 mM Tris-HCl, pH 7.4, 150 mM NaCl, 0.1% Tween 20) for 1 hr at room temperature. Membranes were incubated overnight at 4°C with antibodies in 5% (w/v) BSA in TBS-T. The membranes were briefly washed in TBS-T and incubated with the appropriate HRP-conjugated secondary antibody for one hr at room temperature. The membranes were washed extensively with TBS-T and the proteins were visualized by enhanced chemiluminescence (ECL) (Amersham Biosciences, Piscataway, NJ). Films were scanned using a Canoscan 600 LiDe scanner (Cannon USA Inc., Lake Success, NY).

Antibodies

The following antibodies were used: anti-p62 (BD Biosciences, Franklin Lakes, NJ), anti-LC3 (Novus Biologicals, Littleton, CO), anti-cleaved caspase 3, anti-cleaved PARP, anti-Atg5, anti-Atg12, anti-beclin-1 (Cell Signaling Technology, Beverly, MA), anti-β-actin (Sigma-Aldrich, St. Louis, MO), and mouse monoclonal antibody to GAPDH (Ambion, Austin, TX) and were used at the dilutions recommended by the manufacturers. HRP-conjugated goat anti-rabbit secondary antibody and HRP-conjugated goat anti-mouse secondary antibody (Bio-Rad, Hercules, CA) were used at a 1:2,500 dilutions in 5% (w/v) milk in TBS-T.

Transmission electron microscopy (TEM)

Cells were seeded in 6-well tissue culture plates and treated with DMSO, chlorpromazine, perphenazine, phenothiazine at the indicated doses. After treatment, cells were fixed with a solution containing 3% glutaraldehyde plus 2% paraformaldehyde in 0.1 M cacodylate buffer, pH 7.3, for 1 hr at room temperature before storage at 4°C. The samples were submitted to the electron microscopy core facility for further processing for imaging. Briefly, at the core facility, the samples were washed and treated with 0.1% Millipore-filtered cacodylate buffered tannic acid, postfixed with 1% buffered osmium tetroxide for 30 minutes, and stained *en bloc* with 1% Millipore-filtered uranyl acetate. The samples were dehydrated in increasing concentrations of ethanol, infiltrated, and embedded in LX-112 medium. The samples were polymerized for 2 days in a 70°C oven. Ultrathin sections were cut in a Leica Ultracut microtome (Leica, Deerfield, IL). The sections were subsequently stained with uranyl acetate and lead citrate using a Leica EM stainer. The samples were examined using the JEM 1010 (JEOL Inc., Peabody, MA) transmission electron microscope at an accelerating voltage setting of 80 kV. The digital images were acquired using an AMT Imaging System (Advanced Microscopy Techniques Corp., Danvers, MA).

TEM studies were conducted at the MD Anderson Cancer Center High Resolution Electron Microscopy Facility supported by Grant CA16672 by Kenneth Dunner Jr.

Crystal violet cell viability assay

Viability assay (crystal violet) was performed using standard procedures. Briefly, 5,000 MDA-MB-231 cells were seeded in 100 µl growth media in 96-well tissue culture plates. They were allowed to attach overnight and subsequently treated with the indicated doses of drugs for the indicated time points. Growth media was removed and 50 µl of the cells were fixed and stained in 20% methanol, 0.5% (w/v) crystal violet and washed extensively. The plates were inverted to dry out excess water. 100 µl of Sorenson's buffer (0.1M sodium citrate, pH 4.2 in 50% (v/v ethanol) was added to extract the crystal violet and incubated for 1 hr and subsequently read in a microplate reader at 570 nm absorbance.

Cell viability and proliferation assay

Cell viability was determined using the CellTiter- Blue (Promega Corp., Madison, WI) assay. Viable cells are able to convert resazurin to resorufin which fluoresces and can be quantified. MDA-MB-231 cells were seeded in 96-well tissue culture plates and treated as indicated for various time points. 5 µl CellTiter Blue (Promega Corp., Madison, WI), reagent was added and incubated at 37° C with 5% CO_2 for 2 hr and read on a luminescent plate reader.

Caspase-7 activity assay

The activation of caspase 7 in MCF-7 cells was assayed using the ApoOne Kit (Promega, Madison, WI) according to manufacturer's recommendations.

ATP assay

Cellular ATP was monitored using the ATPlite 1step luminescence assay (PerkinElmer, Boston, MA) which is a luciferase based assay whereby ATP reacts with D-luciferin and luciferase to emit light, proportional to the amount of ATP in the cells. Briefly, cells were seeded at 5,000 cells per well in 100 µl in 96-well black walled tissue culture plate. After overnight attachment, cells were treated as indicated. At the experimental endpoint, the microplates were equilibrated to room temperature and 100 µl ATPlite 1step reagent was added and placed on an orbital shaker for 2 minutes. The plates were read in a luminescent plate reader.

$DiOC_6$ apoptosis assay

Cells which are undergoing apoptosis have loss in the mitochondrial potential from mitochondrial transmembrane potential, which is the due to the difference in distribution of ions between the inner and outer membrane. This occurs early on in apoptosis and is accompanied by the opening of the mitochondrial permeability transition pores and release of cytochrome c. To measure changes in mitochondrial transmembrane potential during treatment with phenothiazines, MDA-MB-231 cells were quantified by flow cytometry using the 3,3'-Dihexyloxacarbocyanine Iodide ($DiOC_6$) (Invitrogen, Carlsbad, CA). Cells were seeded at 20,000 density in 3 ml media per well in 6-well tissue culture plates. The cells were allowed to attach overnight and treated with various concentrations of phenothiazines the following day and incubated for the indicated time. At the experimental endpoint, both floating and adherent cells were collected. Attached cells were collected by

trypsinization. FBS was added subsequently to inactivate the trypsin. The cells were washed with PBS and resuspended in fresh media. 50 nM $DiOC_6$ and propidium iodide (20 µg/ml in PBS with 0.1% Triton X-100, and 0.2 mg/ml RNase A) was added and incubated for 15 minutes before analysis using the FACScan cytofluorometer (Becton Dickinson, San Jose, CA).

Clonogenic viability assay

Colony formation assay was performed by plating MDA-MB-231 cells in 6-well tissue culture plates at a density of 100 cells per well and allowed to attach overnight. The following day the cells were treated with phenothiazines and DMSO as indicated. Fresh medium was replaced every 3 days. After a 14 day treatment period, the media was removed and the cells were fixed and stained in 20% methanol, 0.5% (w/v) crystal violet and washed extensively. The colonies were photographed and analyzed using the FluorChemE imaging system using the AlphaVIEW SA version 3.2.3.0 software (Cell Biosciences Inc., San Jose, CA). The experiment was done in triplicate and repeated three times.

Matrigel invasion assay

MDA-MB-231 cell invasion was assayed in 24-well (8 µm) Biocoat Matrigel invasion chambers (BD Biosciences, Franklin Lakes, NJ) according to the manufacturer's protocol. Briefly, 2.5 $x10^5$ cells were plated in triplicate in 200 µl of RPMI in the insert compartments. The reservoir compartments of the 24 well plate contained 5% FBS as a chemo-attractant in RPMI. Both the insert and the reservoir

contained the drug for the treatment condition. After incubation for 16 hr, adherent cells on the lower surface of the inserts were fixed with 0.5% (w/v) crystal violet in 20% methanol solution for 30 minutes. The inserts were washed extensively. The non-migrated and non-invasive cells in the upper chambers were carefully removed with cotton tipped applicators. The migrated and invaded cells were imaged by light microscopy. The experiments were conducted in duplicates and repeated at least twice.

Confocal microscopy

Immunofluorescent localization and co-localization studies of MDA-MB-231 cells were carried out an Olympus FV1000 microscope at a 100X. Images were acquired using the Fluoview software and processed using ImageJ (http://rsbweb.nih.gov/ij/). Briefly, MDA-MB-231 cells either transiently expressing tf-LC3 or stably expressing GFP-LC3, were seeded in eight well chamber slides (BD Biosciences, Franklin Lakes, NJ) at a cell density of 50,000 cells per well. Cells were allowed to attach overnight and treated the following day as indicated. MDA-MB-231 stably expressing GFP-LC3 were immunostained for LAMP2 (BD Biosciences, Franklin Lakes, NJ) followed by staining with 568 nm (red) fluorescent linked secondary antibody according to manufacturer's instructions. Cells were fixed with 4% paraformaldehyde and counter-stained with 4'-6-diamidino-2-phenylindole (DAPI) and stored in the dark at 4°C.

Mice studies

Athymic nude female mice 20-25 g were used for *in vivo* tumor growth. The mice were obtained from the National Cancer Institute (NCI, Rockville, MD) and given food and water *ad libitum* under specific pathogen-free conditions in accordance to the guidelines of the Association for the Assessment and Accreditation for Laboratory Animal Care accredited facilities and the National Institute of Health guidelines. All the in vivo studies protocols were carried out as approved by the MD Anderson Animal Care and Use Committee.

Tumor implantation and treatment. For the breast tumor orthotopic model, MDA-MB-231 cells were aseptically resuspended at 1×10^7 cells per 200 µl of conditioned media and injected into the mammary fat pad of 5 week old athymic nude female mice. The tumors were allowed to establish to approximately $100mm^3$. Tumor volume was obtained using the formula: Tumor Volume = $L \times S^2/2$ (where L is the longest diameter, and S is the shortest diameter obtained using calipers). Once the tumor reached the target volume, they were randomly allocated to 3 groups, the DMSO, phenothiazine ring, and perphenazine treatment group. The mice were injected with 25 mg/kg phenothiazine, perphenazine, or DMSO in 100 µl volume by intraperitoneal administration (IP) every other day for a 2 ½ and to 3 ½ weeks period when the tumor exceeded 1.5 cm (approved tumor size at the time of the studies). At sacrifice, the mice were weighed, and tumors were excised for immunohistological and reverse phase protein array (RPPA) studies.

Reverse phase protein array (RPPA)

RPPA procedures for antibody staining, slide scanning, and data processing were performed as previously described with minor modifications (121), (122). Cellular proteins were prepared as described for western blotting prepared in denaturing sample buffer by adding 1 part 4X SDS sample buffer (40% glycerol, 8% SDS, 0.25M Tris-HCl, pH 6.8, 10% β-mercaptoethanol) to 3 parts protein lysates prior to heating to 95 °F for 15 minutes. Serially diluted lysates were arrayed on nitrocellulose-coated slides (Grace Biolab) using an Aushon 2470 Arrayer (Aushon BioSystems Inc., Billerica, MA). Each sample was robotically printed in 5 fold serial dilutions on multiple slides including positive and negative controls prepared from mixed cell lysates or dilution buffer, respectively, as well as multiple cell lines incubated with and without growth factors to provide dynamic range. Each slide was probed with a validated primary antibody followed by conjugated secondary antibody. The signal was obtained by amplification a Dako Cytomation–catalyzed system (123) and visualized by DAB colorimetric reaction. The slides were scanned, analyzed, and quantified using a customized-software MicroVigene (VigeneTech Inc.) to generate spot intensity. Each dilution curve was fitted with a logistic model "Supercurve Fitting" developed by the Department of Bioinformatics and Computational Biology in MD Anderson Cancer Center (http://bioinformatics.mdanderson.org/OOMPA). This fits a single curve using all the samples (i.e., dilution series) on a slide with the signal intensity as the response variable and the dilution steps are independent variable. The fitted curve is plotted with the signal intensities – both observed and fitted - on the y-axis and the log2-

concentration of proteins on the x-axis for diagnostic purposes. The protein concentrations of each set of slides were then normalized by median polish, which was corrected across samples by the linear expression values using the median expression levels of all antibody experiments to calculate a loading correction factor for each sample.

CHAPTER 3

Development of a High-throughput and High-content Image Based Screen for the Identification of Modulators of Autophagy in Cancer Cells

EXPERIMENTAL RATIONALE AND GOALS

Current chemotherapeutic drugs often target rapidly dividing cells, and consequently have toxicities against normal cells that have high proliferation rates such as hair follicles, bone marrow, and gastrointestinal tracts.

Autophagy is an attractive mechanism to study for the development of novel drug treatments for many reasons which include findings that some cancer cells are dependent on autophagy for survival and proliferation. There is much interest on how autophagy can be converted from a pro-survival mechanism to a pro-death mechanism but the molecular mechanism by which this conversion occurs is still poorly understood. To this end, the identification of modulators of autophagy will allow us to study perturbations of autophagy in cancer cells and contribute to a better understanding of potential mechanism of how autophagy modulation can lead to cancer cell death. One important aspect in the development of therapies is the ability to gain approval through the various stages of the clinical trials to be brought to the clinics. Many drugs fail to pass the rigorous process due to suboptimal pharmacokinetics and bioavailability. In order to ensure better outcome, it is common to begin studies with screens of compound libraries of drugs and small

chemical molecules where the bioavailability and pharmacokinetics are already known. This increases the likelihood that findings in the lab could eventually be brought to the clinics.

Since autophagy is a tightly regulated homeostatic mechanism which maintains energy and protein quality in the cells, we hypothesized that compounds which perturb the autophagy signaling network would affect cancer cell viability. In order to test our hypothesis, we attempted to identify modulators of autophagy using high-throughput screen that will allow us to study perturbations of autophagy in cancer cells. We selected drugs identified by our screen to identify where in the autophagy signaling network these drugs target to gain insights into potential mechanisms by which perturbations of autophagy signaling mediates cancer cell death.

Development of a high-throughput assay to screen autophagy modulators

A common starting point for identifying small molecule inhibitors of cancer molecular targets is by high-throughput screening of diverse compound libraries. To this end, we developed a high-throughput, high content, image based screen for the automated image capture and analysis of autophagy perturbation by small molecule compounds. We used stably transfected GFP linked LC3 reporter cancer cell lines to follow the autophagic process by quantifying the number of autophagosomes per cell (FIGURE 4) (124). For our high throughput screen, we selected U2-OS cells on the basis of their large cytoplasmic region which allowed

ease of automated segmentation of different subcellular regions for detection and quantification of LC3 punctae in cells.

Using known inducers of autophagy Gleevec (Imatinib; STI571) (125), 2-deoxyglucose (2-DG) (126), temozolomide (127), (127) , aminoimidazole carboxamide ribonucleotide (AICAR) , metformin, and rapamycin (128), we set up a prototype experiment to develop the imaging and analysis protocols and algorithms of automated imaging and analysis of autophagosomes using the LC3 reporter. Using this training data set, we were able to develop the parameters which correctly identified the LC3 autophagosomal marker in each cell to quantify autophagy upregulation which correctly measured the dose response effects of our treatments. We also determined that Gleevec (Imatinib; STI571) and 2-deoxyglucose (2-DG) were the strongest inducers of autophagy tested and therefore were used as the positive controls in our screen (FIGURE 7). We validated our assay in several prototype experiments using these algorithms and determined that our assay was robust, and reproducible. Since most compound libraries, including the Prestwick Chemical Library used here, are solubilized in DMSO, it was necessary to determine the DMSO tolerance of the cells in the developmental stage of our study and work within the identified range in our screen as well as in subsequent studies. DMSO and untreated cells served as controls to determine basal autophagy levels in the cells assayed.

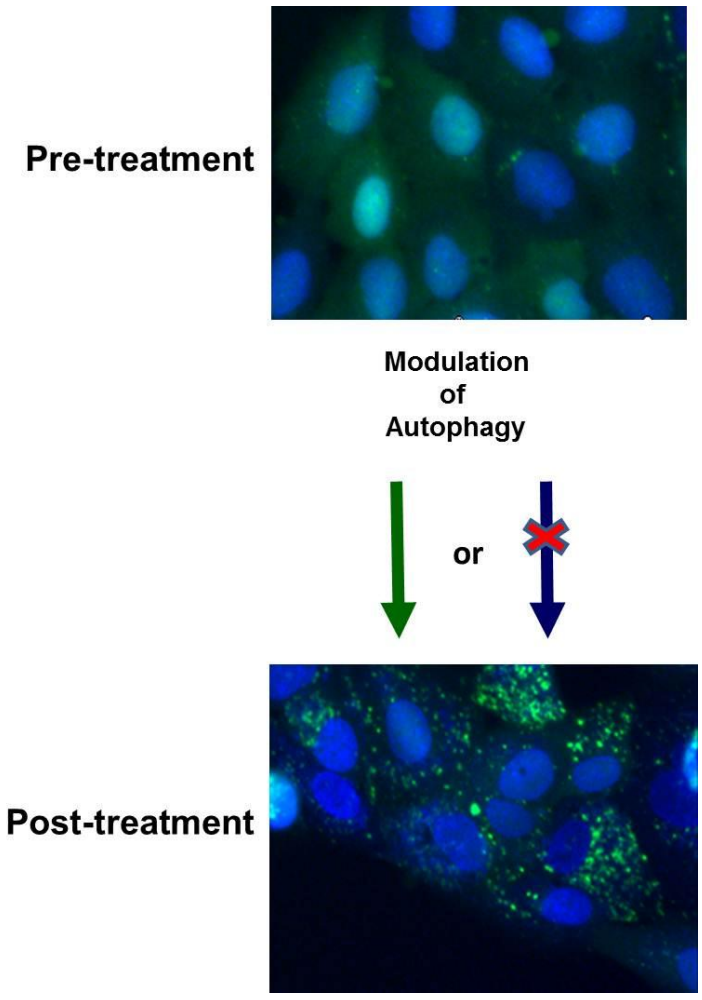

FIGURE 4: GFP-LC3 fluorescent reporter for autophagosomes in cells. U2-OS cells were stably transfected with GFP-LC3 for identifying autophagosomes in the cells. LC3 is diffusely distributed throughout the cell cytoplasm. Upon activation of autophagy, it undergoes various steps of modification to ultimately be lipidated and associated with autophagosomes, changing its diffuse pattern to a distinct punctate or granular appearance. This change in phenotype allows comparison of the number of punctate formations between untreated and treated conditions to determine if the autophagic process has been modulated. Since autophagy is a dynamic process, both increase in flux or blockage will lead to increase in number of autophagosomes seen as punctae in the cells with the GFP-LC3 reporter.

We captured 5 randomly selected fields in each of the 96 wells in the tissue culture plate using the automated fluorescent microscope to ensure that more than 200 cells are assayed per condition (FIGURE 5). The optimal concentration at which compounds in the Prestwick library would modulate autophagy was not known at the onset of our screen. To ensure that we captured the activity window in which the compounds modulated autophagy, we conducted our screen at 3 concentrations: 0.1 µM, 1 µM, 5 µM with each concentration on a separate 96 well plate. Each of the plates included 4 replicates of each of our controls: non- treated, DMSO, Gleevec, and 2-DG treated cells.

Once the images were captured, we developed and optimized an algorithm for automated demarcation or segmentation for each of the cellular components: cytoplasm, cell nuclei, and each punctate formation in the cell, on a cell by cell basis. Since the compound library solvent was DMSO, we used the DMSO control as the baseline for our screen. Any number above this threshold was used to define a cell in which the compound treatment modulated autophagy (FIGURE 6).

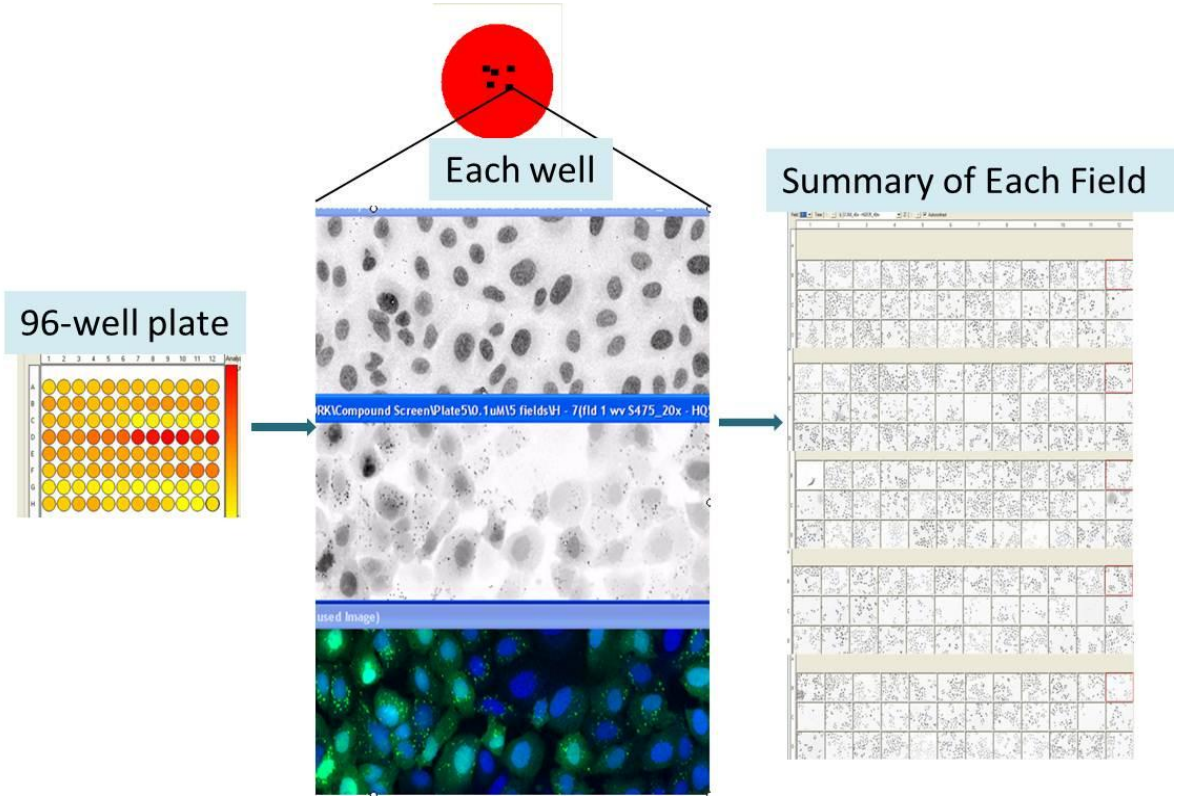

FIGURE 5: **Automated image capture of each well in a 96-well microplate.**

Five fields were imaged per well at 20X magnification to ensure enough cells were sampled. The fields were selected randomly by automated software to prevent bias.

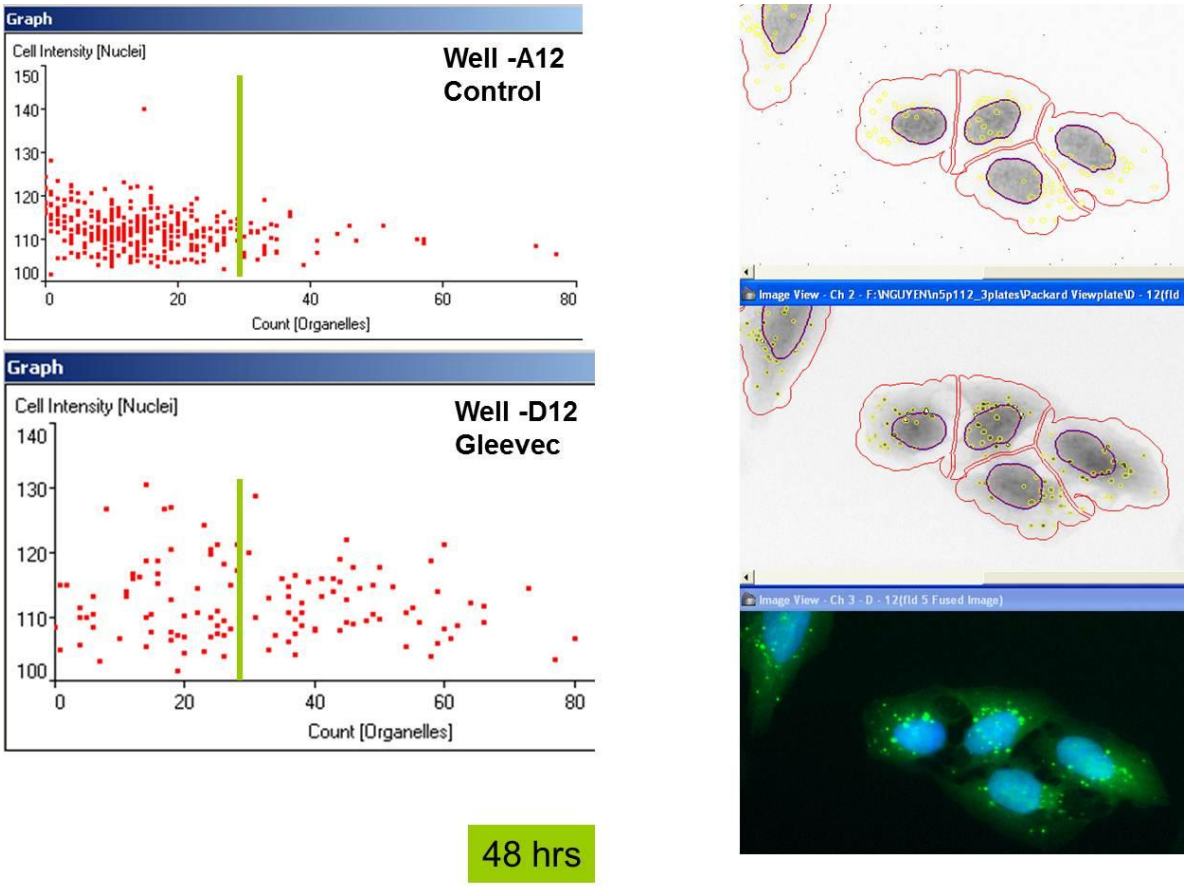

FIGURE 6: Automated segmentation of different cellular components. The nuclei are identified by the Hoechst stained regions. The green fluorescent signal was used to detect the gradient drop off for the demarcation and identification of the cellular boundaries.

		1 2 3	4 5 6	7 8 9	10 11 12
A	NT Control	RPMI 5% FBS			
B	Rapamycin	100nM	100nM	200nM	200nM
C	AICAR	0.25mM	0.50mM	1.0mM	2.0mM
D	Gleevec	5uM	10uM	20uM	40uM
E	2-DG	1mM	2mM	4mM	8mM
F	TMZ	75uM	150uM	300uM	600uM
G	Metformin	1.25mM	2.5mM	5.0mM	10mM
H	NT Control	RPMI 5% FBS			

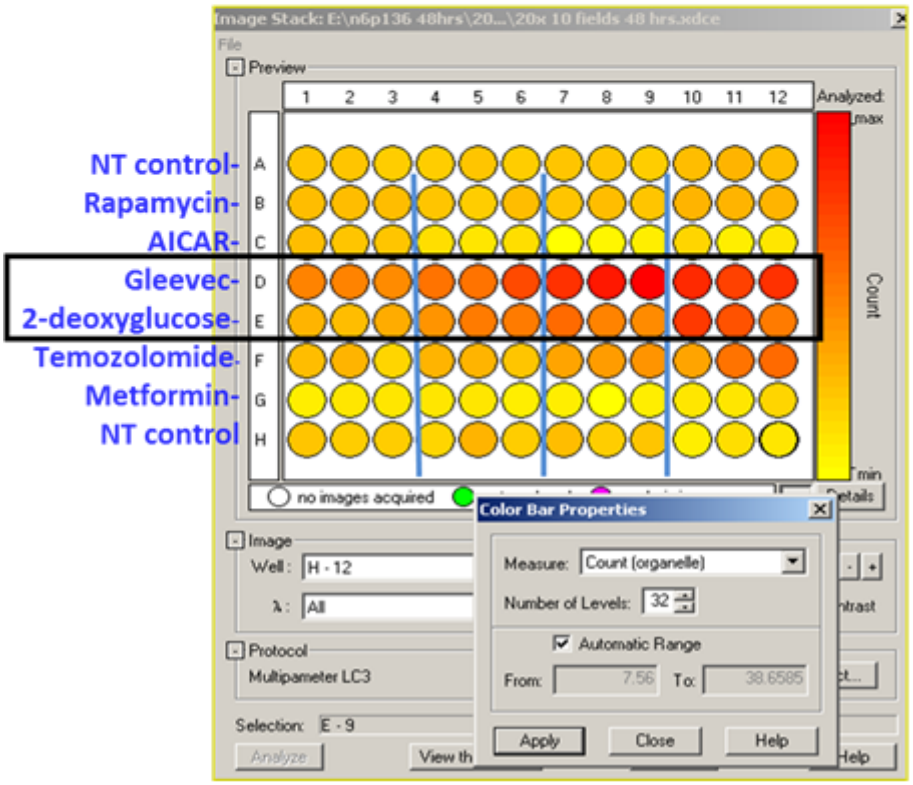

FIGURE 7: Identification of positive controls for a high-throughput cell-based imaged screen for modulators of autophagy. Several known modulators of autophagy (rapamycin, AICAR, Gleevec, 2-Deoxyglucose, temozolomide, and metformin) were assayed at different doses in U2-0S (GFP-LC3) cells at 48 hr time points to identify positive controls and doses for screening autophagy modulators.

RESULTS

Phenothiazines were the largest group of modulators of autophagy

Based on the 5% hit rate threshold, we identified 58 modulators of autophagy based on changes to GFP-LC3 fluorescence distribution, from a diffuse cytosolic to an increase in punctate or granular phenotype (APPENDIX 1). These compounds perturb the autophagic network resulting in an increase in the number of autophagosomes in the cells either by inducing increase in activation of autophagy or blocking the autophagic process from going to completion (autophagic flux). The compounds identified represented diverse groups of drugs with different pharmacological applications. In collaboration with Drs. David Maxwell and William Bornmann from the Department of Experimental Therapeutics, we clustered the positive hits identified in our screen into separate groups based on their 3-D steric structural characteristic. Ten of the 58, or 14% of the compounds identified by our autophagy modulation screen belonged to the phenothiazine family (FIGURE 8- 9). Phenothiazines identified as positive hits in our screen included different phenothiazine sub-groups based on different side chain modifications of the core tricyclic phenothiazine structure. We selected phenothiazines from each chemical clustering based on their 3 dimensional steric structures as grouped by Dr. David Maxwell to characterize in our follow up studies. Some of the hits identified in our screen have been recently reported independently by other groups as modulators of autophagy. These include camptothecin, thioridazine and colchicine (119), (129).

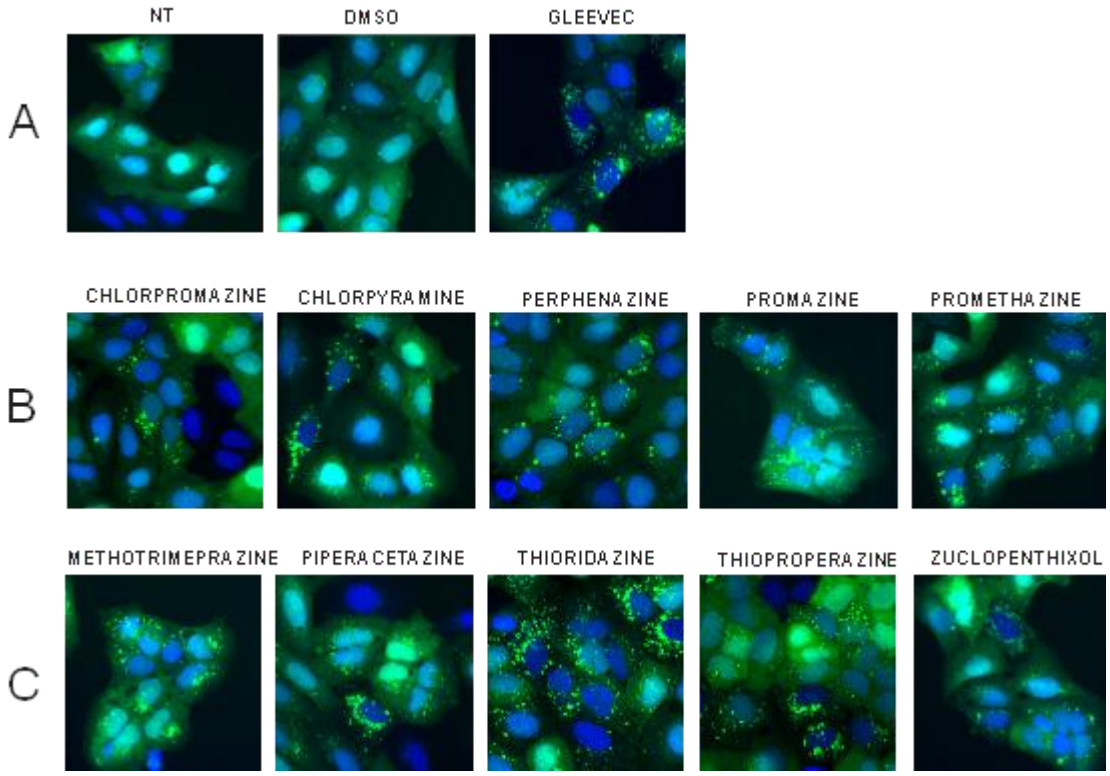

FIGURE 8: Phenothiazines identified as modulators of autophagy in HTS screen. U2-OS stably transfected with GFP-LC3 were assayed for autophagy modulation. Panel (A) are the control conditions, NT is non-treated cells, DMSO is the vehicle for our drugs, and Gleevec served as positive control. Our screen read-out is based on diffuse GFP distribution in normal untreated cells with few punctate formations. DMSO treatment was used to establish the basal autophagy in our cells. Autophagy induction or inhibition results in increased punctate formations which is indicative of autophagosome formations. Panel (B) are phenothiazines, which have been validated by subsequent studies. Panel (C) are phenothiazines that have not been validated in secondary assays.

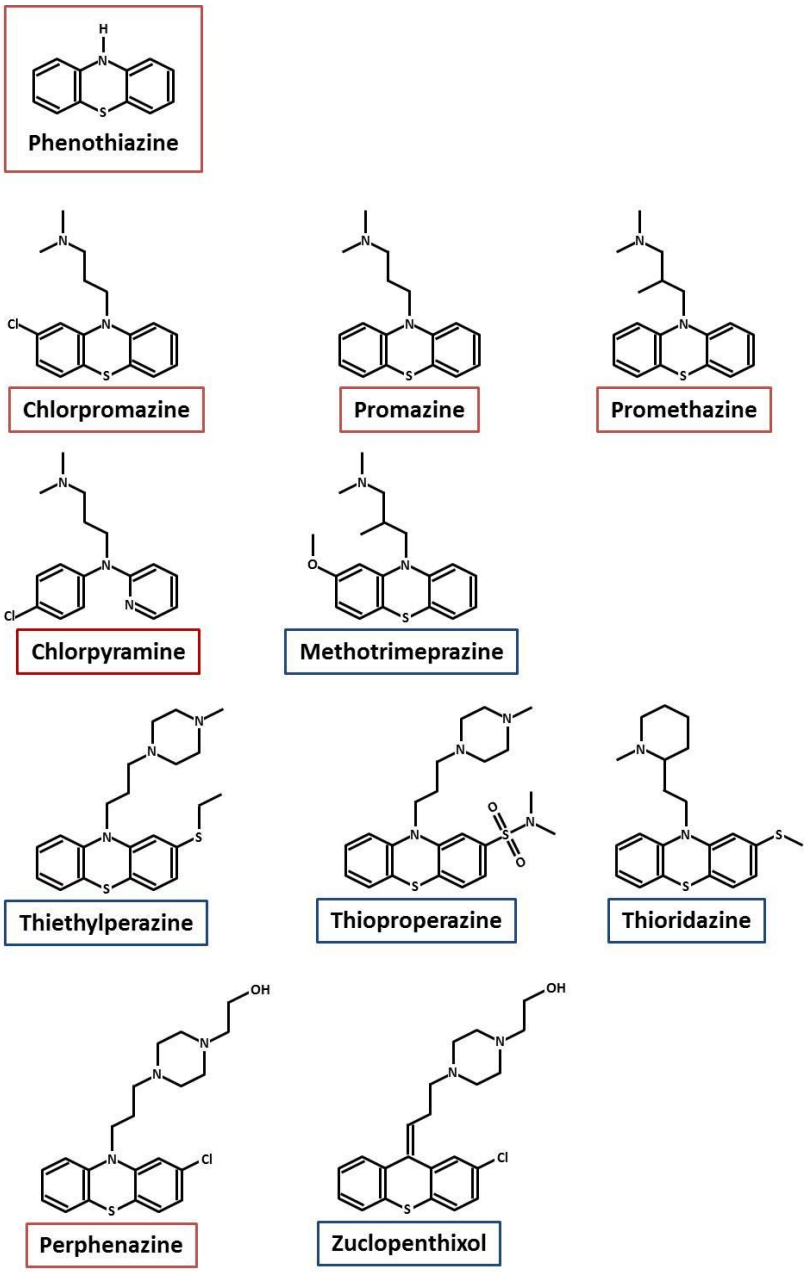

FIGURE 9: Phenothiazines identified as active modulators of autophagy by HTS screen.

10 of the 58 compounds identified by HTS screen for autophagy modulators belonged to the phenothiazine family. Phenothiazines used in follow up studies were boxed in red. The parental phenothiazine compound was not in the Prestwick Chemical Library.

Other studies have identified phenothiazines as modulators of autophagy using different compound libraries (119). The overlap in the findings that phenothiazines are modulators of autophagy by other research groups using different libraries further strengthens our findings that phenothiazines and structurally related compounds are robust modulators of autophagy.

Validation of chlorpromazine as modulator of autophagy in secondary assays

Of the phenothiazines identified in our screen, chlorpromazine was the oldest and most commonly used phenothiazine in the clinics for the treatment of schizophrenia. It is considered the prototype phenothiazine and is often used for studies because of the abundance of clinical data available related to safety, efficacy and dosing. We therefore selected chlorpromazine for the validation of the findings of our primary screen and for follow-up studies. We validated our positive hits in the U2-OS cells as well as in breast cancer cell lines with the GFP-LC3 reporter (FIGURE 10). Since our screen was conducted in the U2-OS osteosarcoma cell line, we sought to determine if the effects of chlorpromazine modulation were generalizable in breast cancer cells (the focus of our cancer model). We thus conducted a dose-response study in the MCF-7 breast cancer cells. Using the MCF-7/ GFP-LC3 stable cell line, we were able to follow the upregulation of LC3-II in cells treated with increasing doses of chlorpromazine. Chlorpromazine increased the punctate formations in a dose dependent manner (FIGURE 11). This was confirmed by Western blot analysis to occur with MCF-7 endogenous LC3 proteins as well (FIGURE 12).

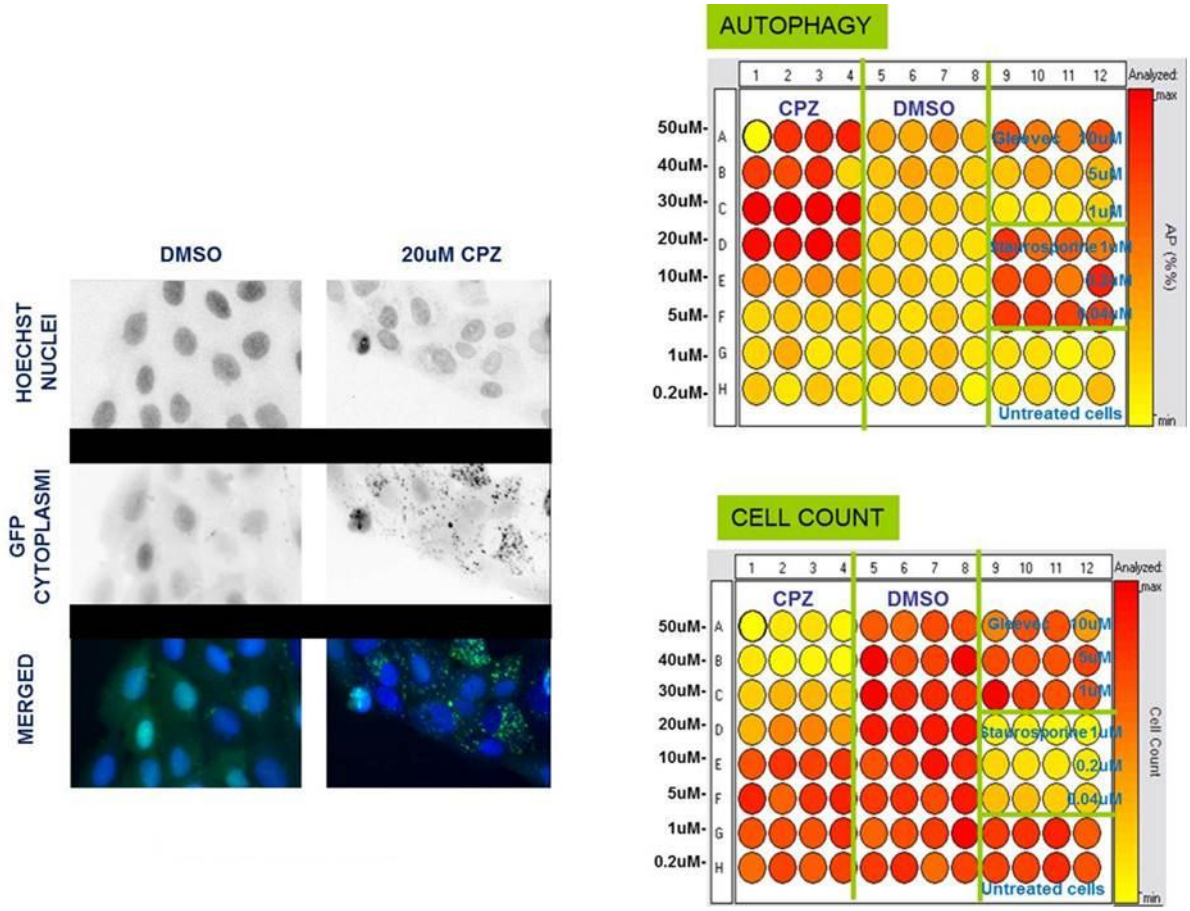

FIGURE 10: Validation of up-regulation of LC3- II by compound identified as positive hits in drug screen.

MCF-7 with stable transfection of GFP-LC3 were treated with selective compounds identified as active modulators by the screen of autophagy modulators in a dose gradient to validate the hits. The right top panel is a plate map of the quantified autophagy marker of cells treated with chlorpromazine, DMSO and with the positive controls Gleevec and Staurosporine in a dose gradient. The bottom plate map shows cell number quantification.

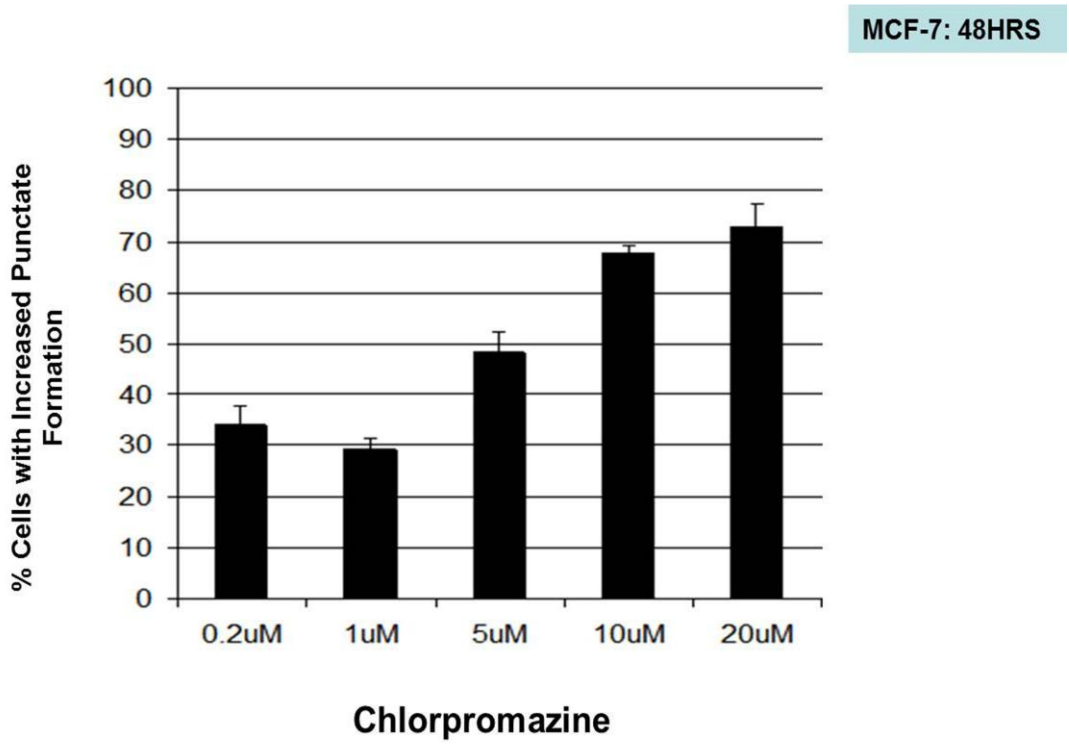

FIGURE 11: MCF-7/ GFP-LC3 Cells treated with chlorpromazine.

MCF-7 cells stably transfected with GPF-LC3 were treated with chlorpromazine for 48 hr at various concentrations. The formation of LC3-II marker as indicated by punctate formation was monitored. The increase in percent of cells with punctate formation above the basal level as set by the DMSO condition was used to indicate increased punctate formation. The percent of cells with increased punctate formation relative to DMSO is represented.

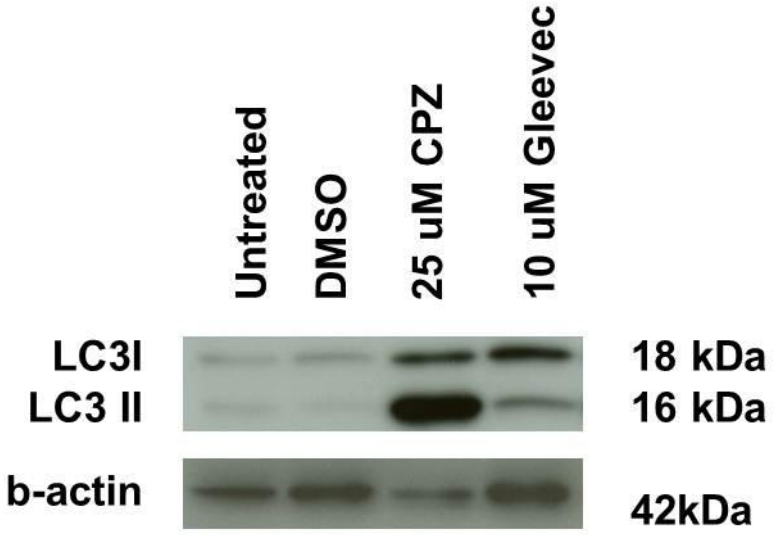

FIGURE 12: Western blot analysis for the formation of endogenous LC3-II. MCF-7 cells were treated with 25 µM chlorpromazine (CPZ) for 48 hr. The level of endogenous LC3-II was monitored by Western blot analysis.

Chlorpromazine mediates decreased cell viability in breast cancer cells without affecting viability of non-tumorigenic breast cells

We determined that chlorpromazine perturbed the autophagic pathway as it increased the number of autophagosomes per cell in a dose dependent manner. This was assessed using our automated fluorescent microscopy imaging and analysis protocol. As part of the analysis protocol, each cell in the image field is identified and counted. Our automated quantification of cells treated with chlorpromazine showed a decrease in cell number in a dose dependent manner. This decrease in cell number could possibly be due to a decrease in cell viability. We thus sought to determine if autophagy modulation by phenothiazines decreased cell viability. We assayed cell viability in a panel of breast cancer cells; MCF-7, T47-D, ZR75-1, BT549, SKBr3 and a non-tumorigenic breast line MCF10-A (FIGURE 13). These cell lines were chosen to represent different clinical sub-types of breast cancers.

Our study showed that autophagy modulation by phenothiazines lead to decreased cell viability in a dose dependent manner in various clinical sub-types of human breast cancers: MCF-7, ZR75-1, T47D, BT549 and SKBR-3 cells (TABLE 2). Thus the effects of phenothiazines are generalized to different clinical sub-types of human breast carcinomas. It has been previously reported that autophagy levels differed between tumorigenic and non-tumorigenic cells; therefore we included the MCF10-A cells which are a non-tumorigenic human breast cell line in order to determine if there is a difference in phenothiazines' effect on cell viability of non-tumorigenic breast cells when compared to tumorigenic breast cells.

Chlorpromazine treated MCF10-A did not exhibit decreased cell viability as compared to untreated cells. Several other studies have shown that phenothiazines mediate cell death in cancer cells while sparing normal cells (103). Zhelev *et al.* showed that phenothiazines induced apoptosis in leukemic cells but not in normal lymphocytes (130).

Chlorpromazine increases caspase-7 activation in MCF-7 cells

Viability assays measure cell viability which could be attributed either to decreased cell proliferation or increase in cell death, we sought to determine if the decrease in cell viability in cells treated with phenothiazine was due to cell death. We treated the MCF-7 human breast carcinoma cells with various concentrations of chlorpromazine and assayed apoptosis activity. MCF-7 cells have a deficiency in caspase-3, we therefore measured the caspase-7 activity as a biomarker of apoptotic cell death in these cells. We determined that chlorpromazine treatment increased caspase-7 activation in a dose dependent manner in MCF-7 cells (FIGURE 14).

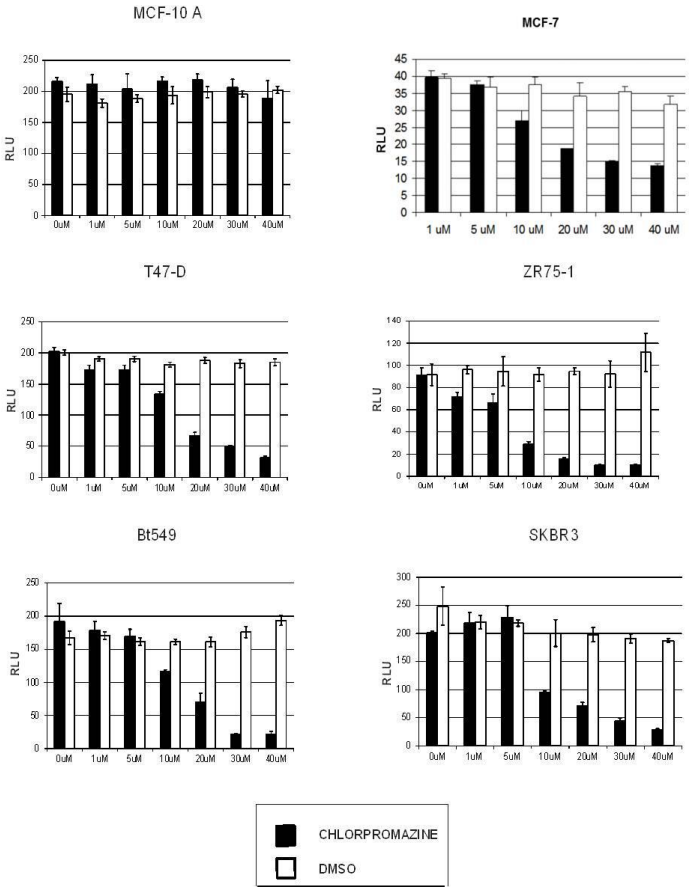

Classification	Immunoprofile	Other characteristics	Example cell lines
Luminal A	ER^+ $PR^{+/-}$ $HER2^-$	Endocrine responsive, often chemotherapy responsive	MCF-7 T47-D
Luminal B	ER^+ $PR^{+/-}$ $HER2^+$	Usually endocrine responsive, variable to chemotherapy. $HER2^+$ are trastuzumab responsive	ZR-75-1
Basal	ER^- PR^- $HER2^-$	$EGFR^+$ and/or cytokeratin $5/6^+$, endocrine nonresponsive, often chemotherapy responsive	MDA-MB-468
Claudin-low	ER^- PR^- $HER2^-$	E-cadherin, claudin-3, -4, & -7 low. Intermediate response to chemotherapy	BT549 MDA-MB-231
HER2	ER^- PR^- $HER2^+$	Trastuzumab responsive, chemotherapy responsive	SKBR3

TABLE 2: Mutational status and clinical classification of breast lines use and response to current therapies

Adapted with permission from Holliday and Speirs. Breast Cancer Res. V 13:4

FIGURE 13: Cytoxicity of chlorpromazine in normal and breast cancer cells. A panel of human breast cancer cell lines representing different molecular mutations (TABLE 2) and clinical sub-types were treated with a dose gradient of chlorpromazine for 48 hr, with a DMSO equivalent dose curve. MCF-10A is a non-tumorigenic human breast line. Cell viability was measured using CellTiter-Blue.

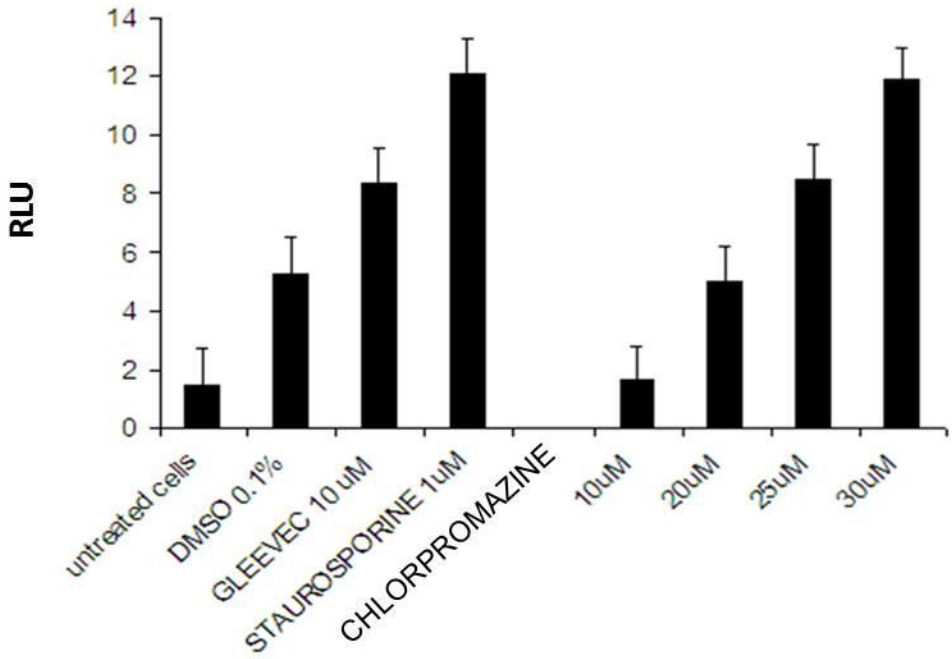

FIGURE 14: Treatment with chlorpromazine increased caspase-7 activation in cancer cells.

MCF-7 cells were treated with increasing dose of chlorpromazine and assayed for activation of effector caspase -7 after 48 hr treatment.

DISCUSSION

The primary aim of the studies in this chapter was to identify small molecule modulators of autophagy to study how perturbations of autophagy affect cancer cell viability. To accomplish this aim, we developed and executed a high-throughput drug screen and identified positive hits. We identified 58 active modulators of autophagy, most of which were heterocyclic compounds.

Interestingly, a group of tricyclic compounds belonging to the phenothiazine family emerged as the largest group of positive hits in our screen. Coincidentally, phenothiazines were also identified as active autophagy compounds by several independent studies using different compound libraries (119), (120). This suggested that phenothiazines are robust modulators of autophagy and therefore the logical choice to focus of our studies of autophagy modulation in cancer cells.

Anti-tumorigenic potentials of phenothiazines in cancers were alluded to by early epidemiologic reports that patients treated with phenothiazines had decreased cancer incidence as compared to patients receiving other antipsychotic regiments or compared to the general population (131), (132). Although several studies report that phenothiazines have cancer prevention potential and antitumor activities, the mechanism by which they mediate them have not been fully determined. Reported targets of phenothiazines for suppression of cancer cell growth include calmodulin (133), mitochondria (134) , P-glycoprotein efflux transporter (135), and PDK1(136), (137). Choi *et al.* showed that several phenothiazines, including chlorpromazine, fluphenazine, and thioridazine inhibited cell viability in the OVCAR-3 ovarian cancer cell line. They demonstrated that phenothiazines did not mediate

cell death through their function as calmodulin inhibitors because calmodulin inhibitors included in their study did not have any effect on OVCAR-3 viability. In their study, they've included haloperidol, a potent antipsychotic which does not belong to the phenothiazine family, to determine if phenothiazines mediated cell death through their antipsychotic properties. Haloperidol, like phenothiazine is a dopamine receptor type 2 (D2) antagonist (138), (139). The authors found that even at the highest dose of 130 µM – haloperidol did not inhibit cancer cell growth suggesting that dopamine receptors were not phenothiazine's target for exerting anti-proliferative potentials in cancer cells. Since haloperidol did not inhibit cell viability in OVCAR-3, they suggested that phenothiazines did not exert cell death through their antipsychotic functions (136). In our screen of the Prestwick Chemical Library, which contained haloperidol, we did not see autophagy induction at the highest dose of 5 µM. Additional supporting evidence suggesting that phenothiazine mediated autophagy modulation was not through their antipsychotic or action on the dopamine receptors will be discussed in chapter 5.

Based on the findings that phenothiazines emerged from non-biased screens from other groups as well as ours, and the finding by Choi *et al.* that phenothiazines did not exert cell death through their dopamine receptor antagonist or anti-calmodulin function, we will further explore how phenothiazines modulate autophagy to mediate cancer cell death.

CHAPTER 4

Comparative Studies of Phenothiazines' Effects on Cell Viability and Tumorigenic Potentials of Cancer Cells

EXPERIMENTAL RATIONALE AND GOALS

In the previous chapter we determined that 14 % of our positive hits belonged to the phenothiazine family. Since so many phenothiazines emerged as active compounds in our drug screen for autophagy modulators, we aimed to determine structure function relationship as pertaining to mediating effect on autophagy. The parental phenothiazine core structure has been reported to have many diverse pharmacological activities and has been used extensively to synthesize new compounds (31). We sought to determine if the unsubstituted or unmodified phenothiazine core structure was sufficient to modulate autophagy. Additionally, we aimed to determine relative potencies of different phenothiazines in modulating autophagy and their effects on cell viability.

RESULTS

Perphenazine and chlorpromazine are the most potent modulators of autophagy

Although we selected chlorpromazine to conduct validation assays of our autophagy screen, we sought to determine the relative potencies of different phenothiazines in augmenting the LC3-II levels in cancer cells. We conducted a comparative Western blot study of several breast cancer cells treated with various phenothiazines identified in our screen as autophagy modulators, shown here in MDA-MB-468 cells (FIGURE 15). The selected phenothiazines: perphenazine, chlorpromazine, chlorpyramine, promethazine, and promazine have different side chain substitutions and represented each of the 3 sub-groups of the phenothiazine families. The phenothiazine core ring was not in our screen but was included to determine if the parental tricyclic structure was sufficient to exert effects on autophagy. Immunoblotting for LC3 showed perphenazine was the strongest inducer of LC3-II upregulation, followed by chlorpromazine. The phenothiazine parental ring did not show an increase in LC3-II levels relative to the untreated cells or to other phenothiazines tested, and is therefore not an active autophagy compound. Therefore the phenothiazine parental ring will be used as the negative control in our follow-up studies.

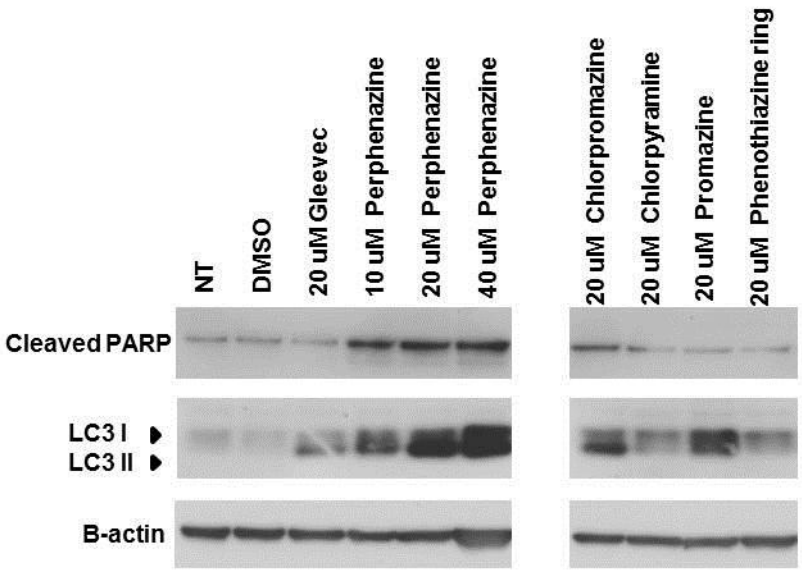

FIGURE 15: Relative potencies of different phenothiazines in modulating autophagy and inducing apoptosis.

MDA-MB-468 cells were treated for 24 hrs with different phenothiazines to determine relative strength of autophagy modulation and inducing apoptosis. Cells were treated at different concentrations of perphenazine (10 µM, 20 µM, 40 µM) and 20 µM of several phenothiazines identified in our drug screen: Chlorpromazine (CPZ), Chlorpyramine (CPY), Promazine (PMA), and Phenothiazine core ring (PTZ). The relative levels of LC3-II, and cleaved PARP were determined by Western blot analysis. All samples were on the same Western blot, and extraneous non-pertinent information was removed for clarity.

Perphenazine and chlorpromazine are the most potent phenothiazines in reducing cell viability in a dose dependent manner

The results of our Western blot study demonstrated that perphenazine and chlorpromazine were the most effective up-regulators of LC3-II levels. This upregulation of LC3-II correlated with an increase in cleaved PARP in the phenothiazine and chlorpromazine treated cells. Promazine showed increase in LC3-I and LC3-II levels but did not show a corresponding increase in cleaved PARP level. In order to have a quantitative analysis of the relative potencies of the different phenothiazine in mediating cell death, we conducted a dose response study using the following selected drugs: perphenazine, chlorpromazine, chlorpyramine, promethazine, promazine and the core phenothiazine ring (FIGURE 16). Cells were treated for 48 hr and viability was assessed using CellTiter-Blue (Promega). Of the phenothiazines studied, perphenazine was the most cytotoxic phenothiazine, followed by chlorpromazine. Promazine decreased viability in this assay. Further studies would be needed to determine the reason for the failure of promazine to induce PARP cleavage (FIGURE 15) and to decrease cell number (FIGURE 16). The parental phenothiazine structure had no cytoxicity relative to the DMSO treated cells. Based on these findings, we selected perphenazine, chlorpromazine, and the phenothiazine parental ring structure to conduct further studies.

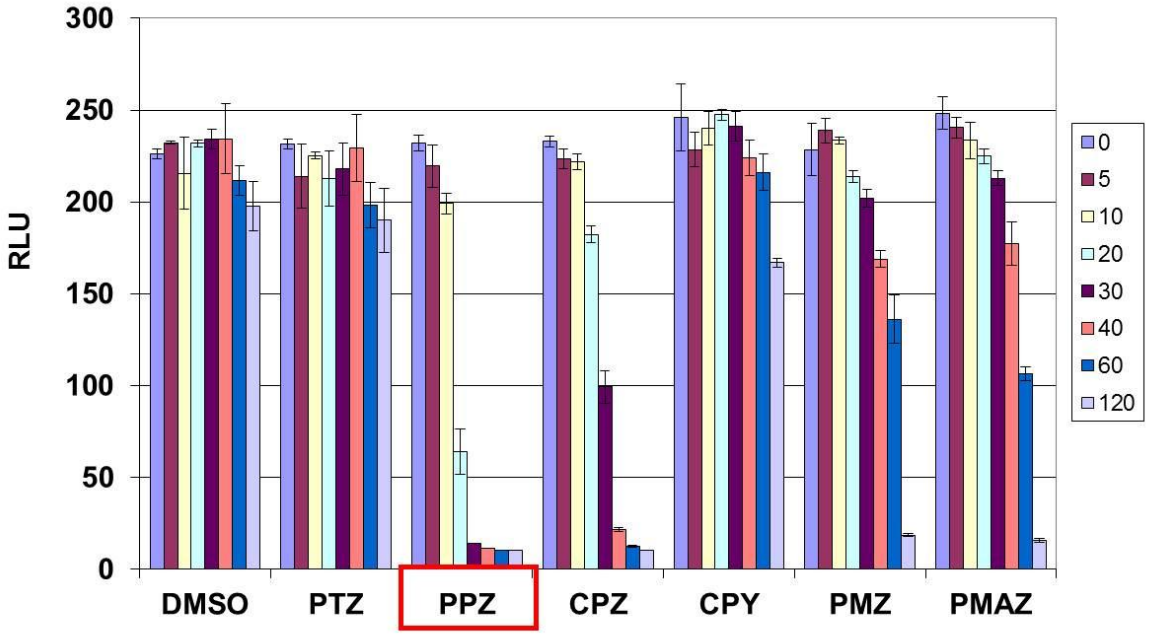

FIGURE 16: Comparative analysis of phenothiazines in decreasing cell viability.

MDA-MB-231 cells were treated with increasing doses (0, 5, 10, 20, 30, 40, 60, 120 µM) of DMSO and phenothiazines for 48 hr. PTZ: phenothiazine core ring structure, PPZ: Perphenazine, CPZ: Chlorpromazine, CPY: Chlorpyramine, PMZ: Promethazine, PMAZ: Promazine.

Perphenazine increases LC3 II expression and PARP cleavage in a time dependent manner

In comparing the relative potencies of various phenothiazines from our screen, we established that perphenazine was more effective in decreasing cell viability in MDA-MB-231 cells than chlorpromazine and other phenothiazines included in our study. We sought to determine if perturbation of autophagy by the strongest phenothiazine tested correlated with decreased viability through apoptosis. In the previous chapter, we determined that chlorpromazine induced apoptosis in the MCF-7 cells by measuring caspase-7 activation, and demonstrated that the concentration dependence of induction of LC3-II and caspase cleavage induced by perphenazine were similar. Here, we assessed activation of apoptosis by monitoring the status of poly (ADP-ribose) polymerase (PARP) (140) in MDA-MB-231 cells treated with 20 µM perphenazine at 24 hr and 48 hr (FIGURE 17). We conducted immunoblotting using an antibody specific for the cleaved PARP protein; this antibody detects the cleaved form of PARP, but not the full length PARP. We determined that perphenazine caused a time dependent increase in cleaved PARP levels which correlated with the increase in LC3-II protein level. This suggests that perturbation of autophagy by perphenazine led to apoptotic cell death in MDA-MB-231 cells, or alternatively, that a common effector was upstream of both processes.

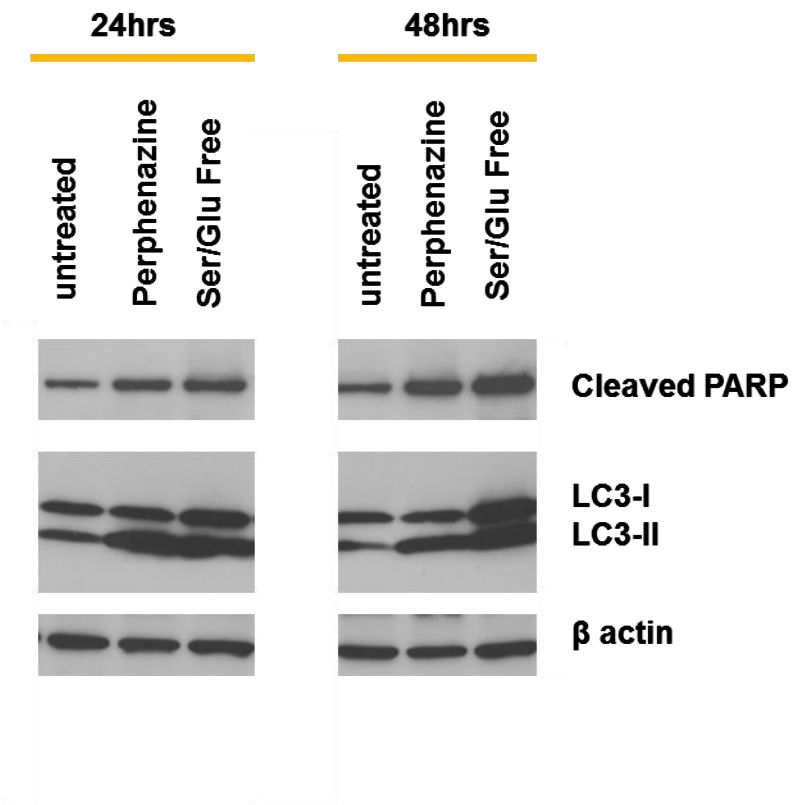

.

FIGURE 17: Perphenazine treated cells have increased cleaved PARP and LC3-II in a time dependent manner.

MDA-MB-231 cells were treated with 20 µM perphenazine or grown under the cell starvation condition of serum and glucose free medium for 24 hr and 48 hr. Cells treated with perphenazine exhibited increased cleaved PARP levels as well as LC3-II levels in a time dependent manner.

Phenothiazine mediated cell death is attributed in part by apoptosis

Based on our previous studies, which showed phenothiazines induced apoptosis as measured by caspase-7 activation in MCF-7 cells, and cleavage of its substrate, PARP in MCF-7 and MDA-MB 231 cells respectively, we next sought to determine if apoptotic cell death was the main mechanism by which cells treated with perphenazine underwent cell death. We treated several types of cancer cells with perphenazine or co-treated with the wide spectrum caspase inhibitor, Z-VAD, at concentrations shown to inhibit apoptosis in other systems, and determined that inhibition of caspase pathway partially abrogated cell death mediated by perphenazine. This suggests that perphenazine mediates cell death partially through apoptosis, but cell death was also mediated through a different mechanism (FIGURE 18).

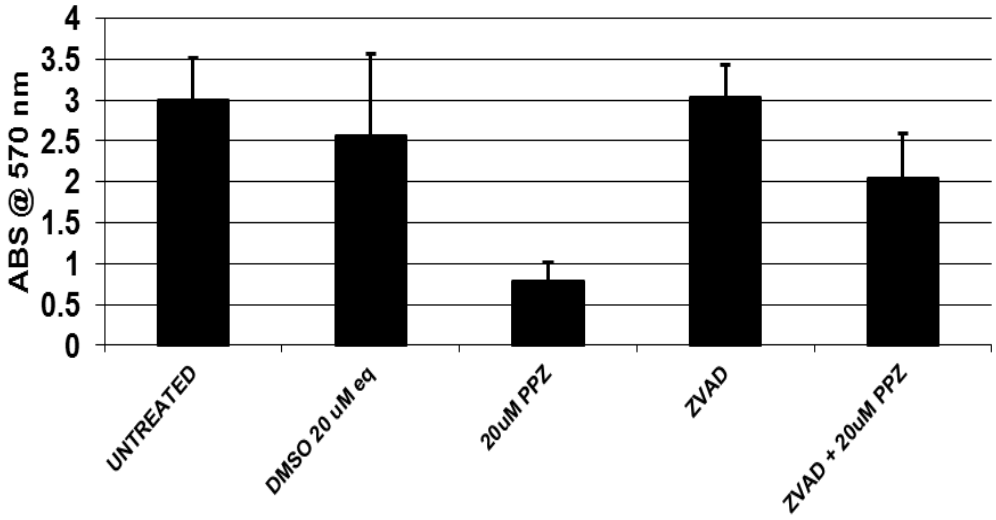

FIGURE 18: Perphenazine mediated decreased cell viability is contributed by apoptosis.

Several cancer cell lines were treated with 20 µM perphenazine or co-treated with the wide spectrum caspase inhibitor ZVAD (100nM) for 48 hr. (Shown here, the U2-OS cells). Cell viability was measured by crystal violet viability assay.

Perphenazine mediates apoptotic cell death through loss of transmembrane mitochondrial potential

At the early stages of apoptosis, the mitochondrial proton gradient across the mitochondria is lost. Loss or collapse in membrane potential is frequently used as a marker of apoptosis. 3, 3′-dihexyloxacarbocyanine iodide ($DiOC_6$) is a green lipophilic cationic fluorochrome used to measure the mitochondrial trans-membrane potential. When used with PI, live cells only fluoresce green. PI dye is non-permeable in live cells. Dead cell have damaged plasma membrane that leads to the uptake of PI dye and thus fluoresce red. Using fluorescent activated cell sorting, we identified the subpopulation of dead cells. We conducted a time course of MDA-MB-231 cells treated with 20 µM perphenazine (our most potent phenothiazine). At the 24 hr time point only 6.6% of the cells were dead, with an increase to nearly 17% at the 48 hr timepoint, and to a final cell death of nearly 70% at 72 hr (FIGURE 19).

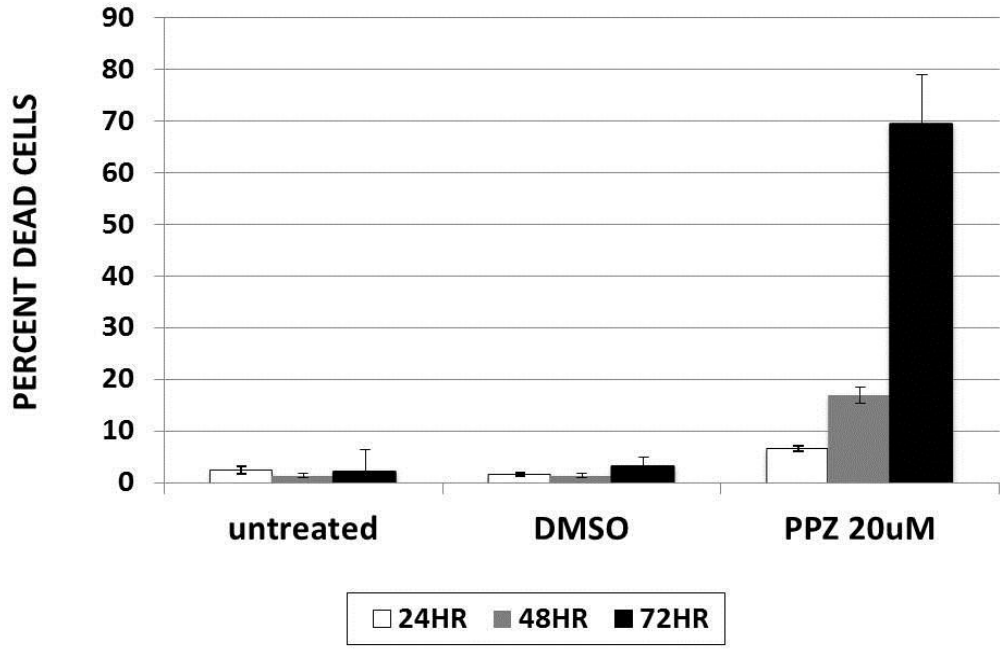

FIGURE 19: Measure of loss of mitochondrial potential in PPZ treated cells. MDA-MB-231 cells were treated with 20 µM perphenazine for 24 hr, 48 hr, and 72 hr to determine a cell death timeline. Cell death was measured using relative PI levels as described in materials and methods. DMSO was the vehicle control.

Perphenazine and chlorpromazine induce an increase in double membraned vacuoles as determined by EM

Christian de Duve first observed and used the terms ‘autophagy’ and ‘autophagic vacuoles’ to describe the process of autophagy using electron microscopy in 1963 (141). More than 50 years later, electron microscopy continues to be the gold standard in determining the presence of autophagosomes (142) (143). We used transmission electron microscopy (EM) to confirm our Western blot analysis and fluorescent microscopic studies which showed accumulation of autophagosome markers LC3-II. We selected MDA-MB-231 breast carcinoma cells of the triple negative clinical subtype (ER-/PR-/HER2-), to conduct our follow-up studies, and later *in vivo* animal studies. This subtype of breast cancer has the poorest clinical outcome (144). We treated the cells with 20 µM of phenothiazine core ring (PTZ), chlorpromazine, perphenazine (PPZ), or the DMSO equivalent to determine the presence of autophagosomes by ultrastructure analysis of the cells through EM. Perphenazine was also treated with 10 µM in addition to the 20 µM for dose response assessment. In comparing the potency of the different phenothiazines in increasing the number of autophagosomes per cell, we determined that the parental phenothiazine core ring (PTZ) had no effect, while chlorpromazine (CPZ) had modest effect, and perphenazine (PPZ) was the most potent in upregulating the number of vacuolar vesicles containing condensed cell materials, as indicative of autophagosomes (FIGURE 20). EM data showed that the parental phenothiazine ring structure was not sufficient to potentiate the accumulation of autophagosomes.

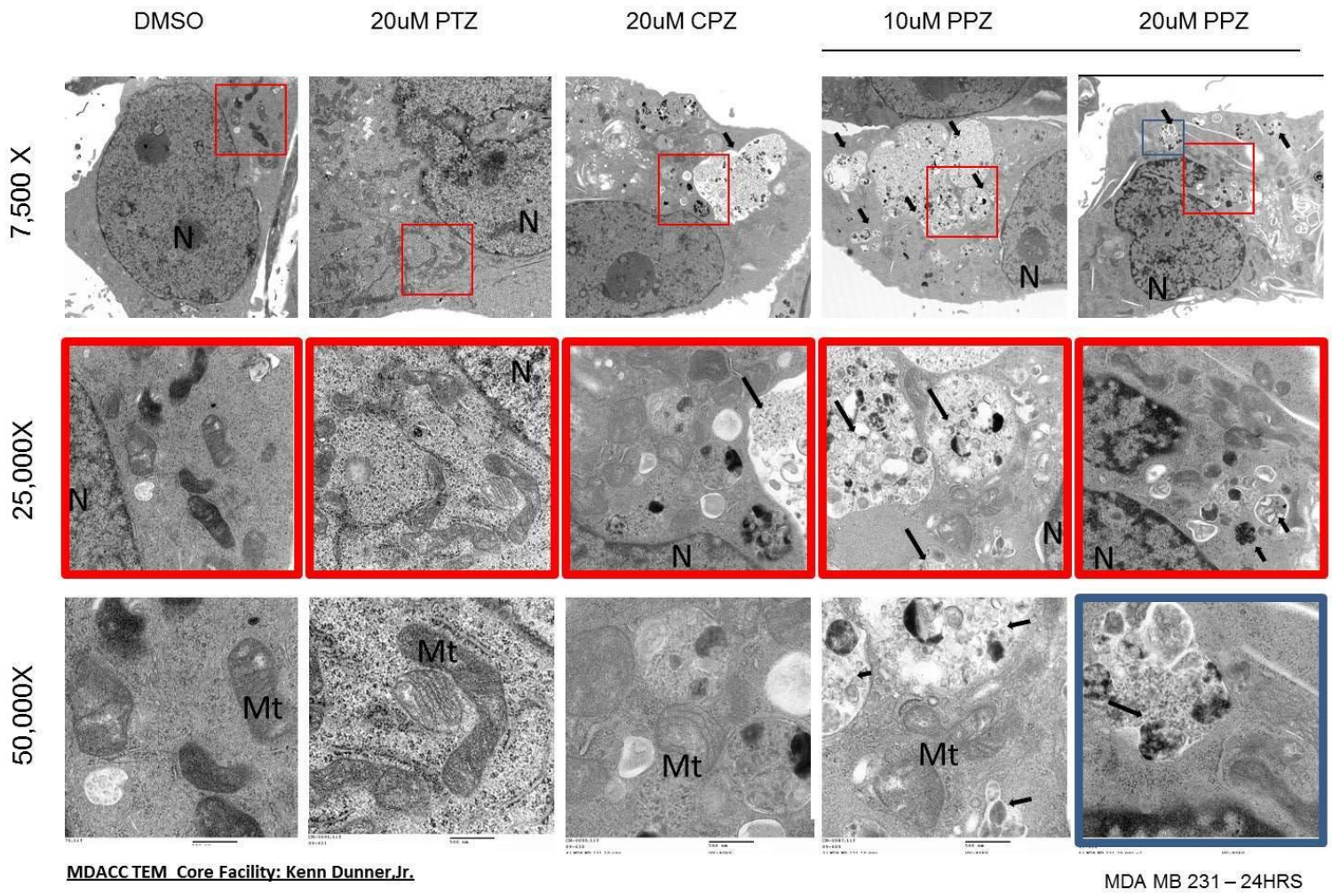

FIGURE 20: Ultrastructural analysis of autolysosomes by EM. MDA-MB-231 cells were treated with the parental phenothiazine ring structure (PTZ), chlorpromazine (CPZ), perphenazine or DMSO for 24 hr for ultrastructural analysis for the presence of autolysosomes**.** Ultrasctructures are labeled as: **N** nuclei, **Mt** mitochondria**, arrows** autolysosomes

Perphenazine was the most potent phenothiazine in decreasing cellular ATP in cancer cells

Since autophagy is a catabolic mechanism which sequesters cytoplasmic contents and organelles to generate substrates for generation of energy in the cells, agents which perturb this pathway could potential affect cellular energy. We therefore sought to determine the energy status of cells treated with phenothiazines. MDA-MB-231 cells treated with the 20 µM chlorpromazine, perphenazine and phenothiazine core ring for 24 hr and cellular levels of ATP was assayed (FIGURE 21)**.** Perphenazine was the most potent in decreasing cellular ATP, followed by chlorpromazine, while the phenothiazine core ring had no effect on cellular ATP levels. The decrease in ATP levels in cells treated with PPZ was observed at the effective dose which mediated decreased cell viability and upregulation of autophagosomal number as assessed by our EM study.

One key function of autophagy is maintenance of cellular energy levels. Through its catabolic activity, it provides amino acids and lipids for production of acetyl-CoA for the TCA cycle for the generation of ATP. Disruption of autophagy impairs mitochondrial function, potentially resulting in production of reactive oxygen species (ROS) and causing mitochondrial damage. Additionally, impaired autophagy leads to toxic buildup of defective mitochondria in the cells, resulting in cell death.

Zelev *et al.* proposed that the selective cytotoxicity of phenothiazine in lymphoblastic leukemia is due to inhibition of mitochondrial DNA polymerase and decreased ATP production. Sachlos *et al.* noted that mitochondria DNA

polymerase (although present in lymphoblastic leukemia cells) is present in normal lymphocytes and therefore may not be the reason for decreased ATP production (145). Previous studies have proposed that the mechanism whereby phenothiazines decrease the ATP levels in the cells were mediated by inhibition of calmodulin. However, Ruben *et al.* reported that this is not the case based on their findings that in phenothiazines still mediated decrease in ATP in mitochondrial extract lacking calmodulin. Instead, they proposed that phenothiazines mediated decrease in ATP production through inhibition of the mitochondrial ATPases (146).

Since tumors are rapidly proliferating, they have higher metabolic demands than normal cells, and more sensitive to energy perturbations than normal cells. This could potentially explain the selective toxicity of phenothiazine against cancer cells while sparing normal cells, seen in our study of breast cancer cells and the non-tumorigenic MCF10-A cells in earlier in this chapter.

Studies in mice have shown that chemoagents which deplete cellular ATP enhance the therapeutic efficacy of antitumor agents (147), therefore it is important to further explore the mechanism behind phenothiazines' ability to decrease cellular ATP.

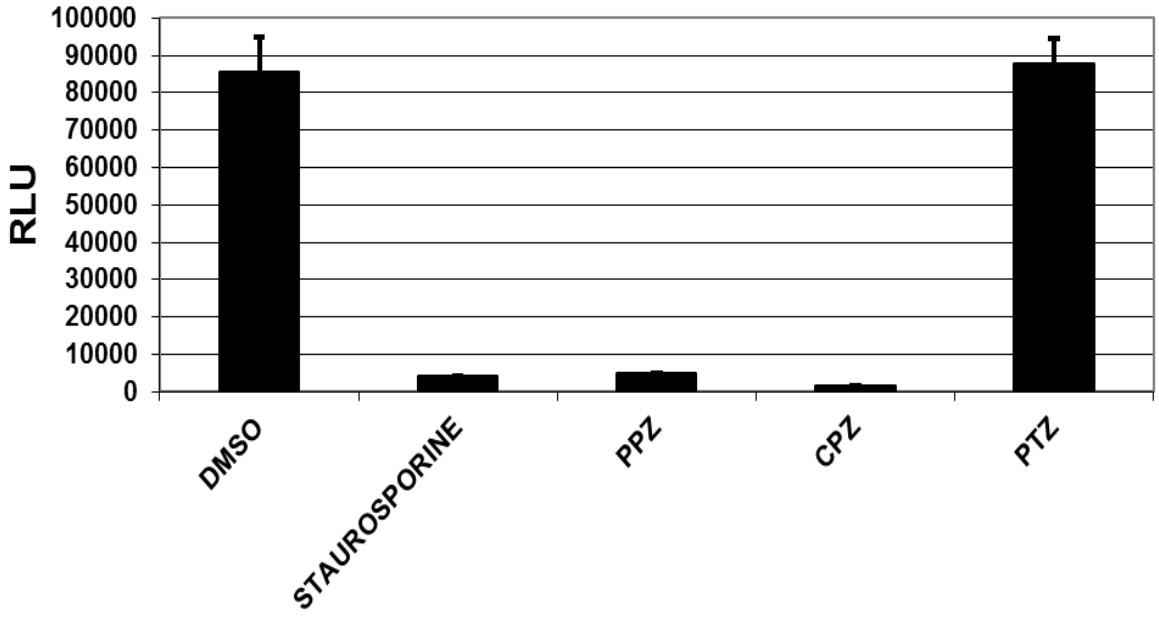

FIGURE 21: Perphenazine decreases cellular ATP. The cellular ATP status was determined in MDA-MB-231 cells treated with 20 µM perphenazine, chlorpromazine, and the phenothiazine core ring structure for 24 hr. Previous timecourse studies of cell death showed that cell death did not occur until after 48 hr at the 20 µM dose used.

Perphenazine decreased the invasive potentials of cancer cells

Aggressive cancer cells must digest through the basement membrane in order to disseminate to distant sites to form metastatic tumors. We used the Boyden chamber migration assay to quantitate the inhibitory potential of perphenazine on cell invasion requiring enzymatic degradation of the Matrigel matrix (148), (149). The coating on the membrane mimics the *in vivo* extracellular basement membrane, and functions as a barrier to the passage of non-invasive cells. The chambers consist of 8 µm micro-porous Matrigel coated membranes to assay tumor cell invasion for assessment of the anti-metastatic potential of phenothiazines.

Invasive potentials of MDA-MB-231 cells were determined after 16 hr treatment with different doses of perphenazine, phenothiazine core ring, or DMSO (FIGURE 22). Previously, our timecourse study for cell death determined that at 24h, MDA-MB-231 cells treated with 20 µM PPZ only had 6.6% decreased cell viability. We therefore assayed the invasive potential of MDA-MB-231 cells after 16 hr drug treatment to ensure that any observed reduction in number of invaded cells through the Matrigel was due to inhibition of invasive potential rather than cell death.

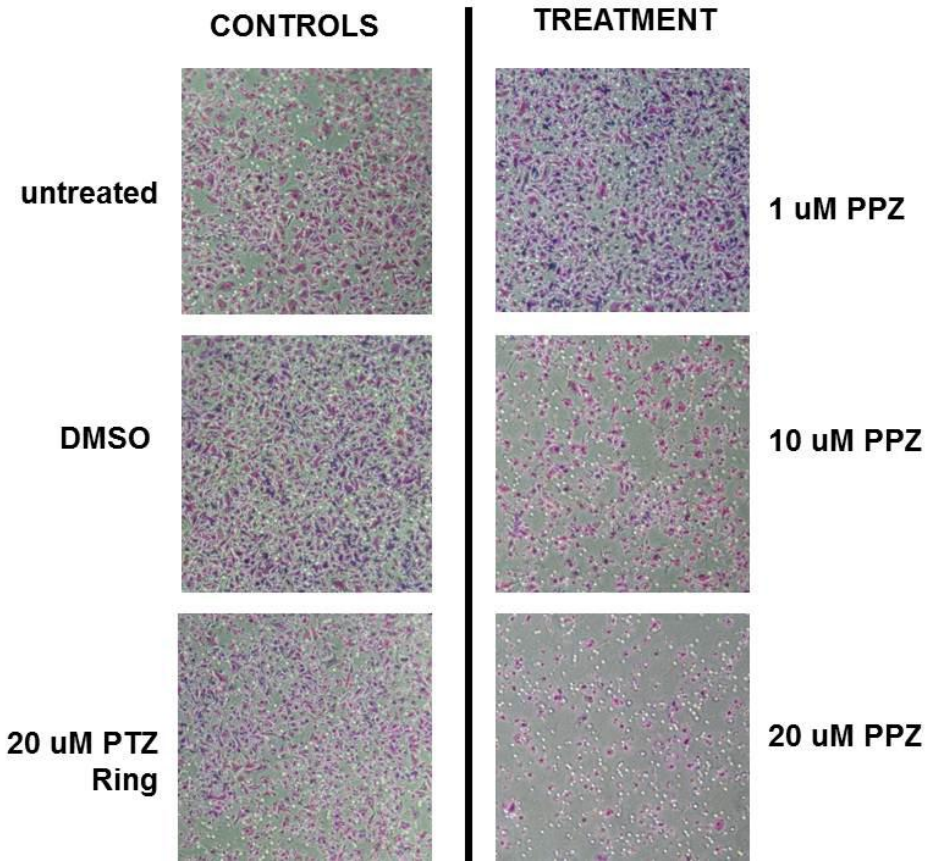

FIGURE 22: Effects of perphenazine on the invasive potential of cancer cells. MDA-MB-231 cells were treated for 16 hr with various doses (1 µM, 10 µM, and 20 µM) of perphenazine (PPZ) and assayed for invasive potential through a Matrigel matrix as compared to untreated, DMSO treated controls or 20 µM phenothiazine core ring structure (PTZ Ring). Experiment was conducted in duplicate, and repeated three times.

Perphenazine and chlorpromazine decreased the clonogenic potentials of cancer cells.

We measured the cell viability, with dye reduction assays, of cells treated with different phenothiazines, which assessed the number of metabolically active cells. Cancer cells must be able to proliferate and form colonies of hundreds and thousands of cells in order to form a tumor or to metastasize. In an *in vitro* clonogenic assay, cells are plated at a low density to assess the ability of single cells to proliferate and form a colony (150), (151). Using this assay, we determined the effectiveness of perphenazine in reducing the clonogenic potential of MDA-MB-231 cancer cells. We compared the relative potency of the core phenothiazine ring, chlorpromazine, and perphenazine as anti-clonogenic agents (FIGURE 23). Our clonogenic survival study showed that treatment with the core phenothiazine ring alone did not mediate decrease in clonogenic potential of the cells at our highest dose of 20 µM. Both CPZ and PPZ inhibited the clonogenic potential of MDA-MB-231 cells at 10 µM.

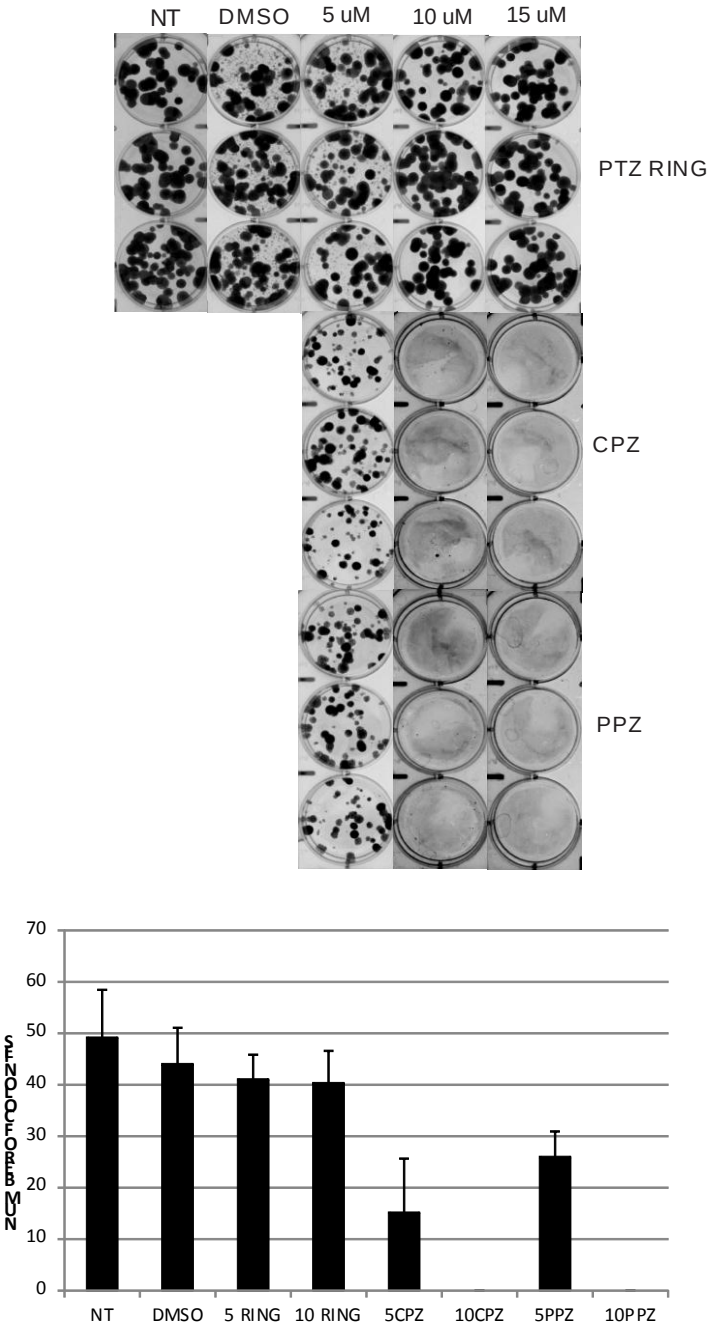

FIGURE 23: Effects of different phenothiazines on clonogenic potential of cancer cells. MDA-MB-231 cells were seeded at 100 cells/ well in a 3 ml volume of media in 6-well tissue culture plates. The cells were treated with different concentrations (5 µM, 10 µM, and 20 µM) of phenothiazine ring, chlorpromazine, and perphenazine to assess the relative potencies of the different phenothiazines in inhibiting clonogenic potential in MDA-MB-231 cells.

DISCUSSION

Understanding the biological effects of phenothiazine modulation of autophagy is important in understanding how phenothiazine can be used within the context of cancer treatment in a clinical setting. We and others have shown that treatment of cancer cells with different phenothiazines mediate cancer cell killing in a dose and time dependent manner. Since several phenothiazines were identified as positive hits in our screen, we sought to determine if these activities were inherent to the core phenothiazine structure itself. The parental phenothiazine ring is a pharmacologically active drug with many reported activities; however, we determined that without additional modification and substitution, it was not sufficient in mediating the measured antitumorigenic effects in the cell lines assessed. Perphenazine and chlorpromazine have been reported to be the most cytotoxic phenothiazines relative to other phenothiazines in different cell lines, including glioma and fibroblasts (103). Our comparative studies showed that perphenazine was more potent than chlorpromazine in inducing of apoptotic cell death through caspase activation. This is consistent with findings by Kanzawa *et al.* that side chain substitution on the parental phenothiazine which contain a piperazine heterocyclic ring conferred higher antitumor activity than aliphatic chain substitution (152) (FIGURE 24).

Our timecourse study of cell death showed that PPZ caused loss of mitochondrial membrane potential at 72 hr. We therefore conducted our invasion assay at 16 hr to ensure that the decreased number of invasive cells were in fact due to inhibition of invasive potential as opposed to decreased cell viability. In

addition to decreasing cell viability by apoptosis through caspase activation with subsequent PARP cleavage, perphenazine and chlorpromazine attenuated the cells' invasive capacity as measured by invasion through the Matrigel membrane of the Boyden invasion chambers. Decreased invasive potential of MDA-MB-231 treated cells could be attributed to the fact that phenothiazines mediate decrease in cellular ATP. Chlorpromazine has previously been observed to both decrease cellular ATP and inhibit the ability of tumor cells to generate ATP (153). Decrease in cellular energy can impact several cellular processes which are important for cancer cell survival. Because cancer cells are rapidly growing and are under metabolic stress, they are more sensitive to energy perturbations that normal cells.

Autophagy degrades macromolecules and organelles to provide amino acids, fatty acids which are used to produce ATP through the tricarboxylic acid (TCA) cycle. Abedin *et al.* reported that 45-50% of mitochondria were co-localized with autophagosomes after cells were treated with activators of autophagy (74). This suggests that mitochondria were sequestered within the autophagosomes. Functional autophagy regenerates ATP through degradation of macromolecules and organelles. The decrease in cellular ATP in cells treated with phenothiazines suggests that phenothiazines disrupted autophagy.

Additionally, perphenazine and chlorpromazine inhibited the ability of MDA-MB-231 single cells to form colonies at 10 μM as assessed by clonogenic potential assays. This inhibition of the ability for the cancer cells to form colonies is especially important in context of *in vivo* cancer formation as it prevents single cells which have shed to distant sites from establishing new tumors. Although

perphenazine and chlorpromazine mediated their decreased viability effects at doses of 20-30 μM at 48 hr treatment, they were effective in mediating the inhibition of clonogenic potential at a lower dose of 10 μM. This difference could be attributed to the fact that the measure of clonogenicity is clearly different than that of viability measure. Viability assays measure metabolically active, viable cells, without distinguishing if these viable cells are capable of forming colonies from single cells.

In all our measures of inhibition of tumorigenic potential of PPZ and CPZ, PPZ was more potent relative to CPZ. Interestingly, this correlates with the antipsychotic potentials of these drugs, with PPZ being more potent, and the dose which it is prescribed to patients is one forth to one sixth of that prescribed for CPZ (154). The difference in relative potencies of PPZ and CPZ may be attributed to the side chain substitution on the phenothiazine tricyclic core structure. Although phenothiazines are amphiphilic cations and can readily interact with cellular membranes (155), the side chain substitution on the parental ring influences how easily they cross cellular membranes. Perphenazine's piperazine substitution is more lipophilic than chlorpromazine's aliphatic substitution and thus perphenazine can better interact with cellular membranes and more effectively cross through them to reach their cellular targets.

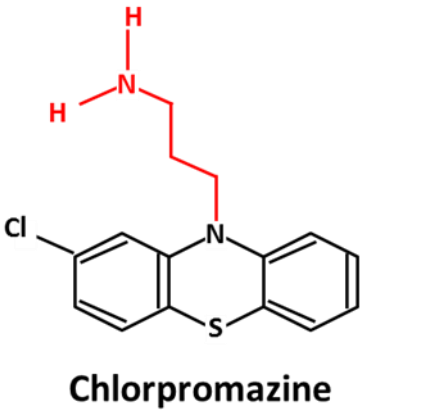

Chlorpromazine

Aliphatic substitution

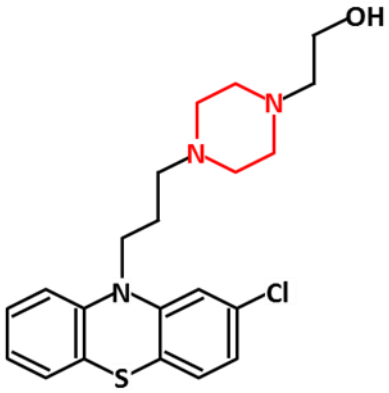

Perphenazine

Piperazine substitution

FIGURE 24: Substitution on phenothiazines affects lipophilic activity.

Aliphatic substituted phenothiazines are less soluble than phenothiazines with piperazine substitution.

CHAPTER 5

Identification of Perphenazine's Target in the Autophagy Signaling Network

EXPERIMENTAL RATIONALE AND GOALS

An increase in LC3-II and the appearance of autophagosomes in cells following treatment with phenothiazines could occur as a consequence of an increase in autophagosome formation, blocked autophagosome turnover, or blocked autophagic flux (156). We sought to determine the status of autophagic flux by using p62 which is a normally long lived protein that is targeted for degradation in the final steps in the autophagy pathway. Thus p62 is often used for as indicator of autophagic flux. Cells growing in nutrient replete conditions have low levels of p62; treatments which block the autophagy pathway increase cellular levels of p62 (157). We used pharmacologic inhibitors of the autophagy signaling network to assess where along the pathway perphenazine targets to upregulate LC3-II. Many inhibitors targeting different proteins in the autophagy signaling network are non-specific and have other cellular targets. We therefore, used RNA silencing and MEFs cells with knockout of the autophagy gene Atg5 to complement our studies.

RESULTS

Perphenazine treatment blocks autophagic flux and increases p62 and LC3-II

In order to understand how perphenazine perturbs the autophagy signaling pathway, we determined the expression status of the core regulators of the autophagy machinery in MDA-MB-231 cells before and after treatment with perphenazine.

We first determined if autophagy is induced or blocked. p62 levels were used to determine autophagic flux. MDA-MB-231 cells subjected to perphenazine (PPZ) treatment for 48 hr had increased p62 and LC3-II protein levels (FIGURE 25). Increased p62 levels in the cells treated with PPZ indicate that autophagic flux is blocked, likely contributing to the increased LC3-II levels in the cells.

Next, we sought to identify targets along the autophagy signaling pathway that could explain the effects of PPZ on autophagic flux. Induction of autophagy involves the activation of the class III PI3K/Vps34/Beclin 1 complex (158), and LC3-II recruitment to autophagosomal membrane is Atg5 dependent (159). Immunoblotting for Beclin 1 and Atg5 showed that the Beclin 1 and Atg5 levels were not altered following perphenazine (PPZ) and phenothiazine (PTZ) treatment, suggesting that these proteins are not the primary targets of phenothiazines in MDA-MB-231 cells. Additionally, this suggests that cells treated with phenothiazines may undergo autophagy through alternative autophagy pathways that are not dependent on changes in Beclin 1 and Atg5 levels.

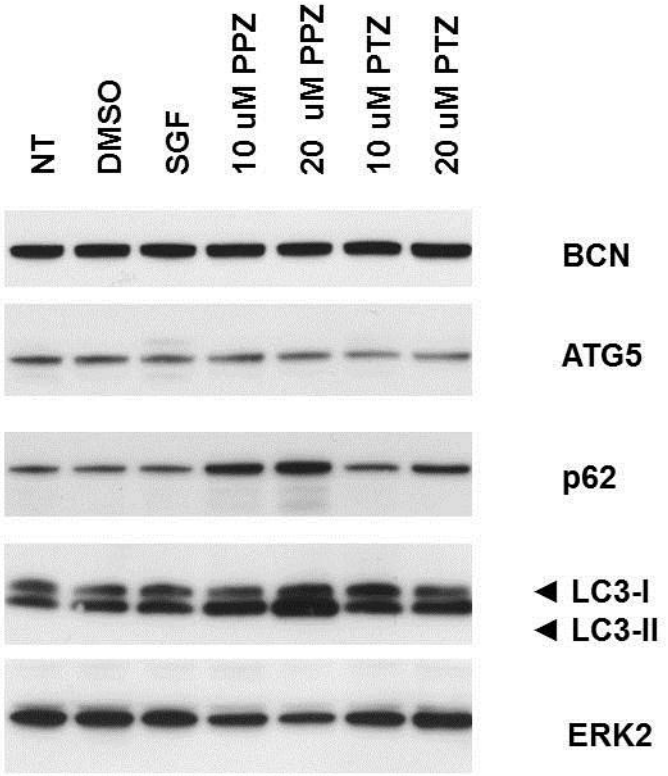

FIGURE 25: Effects of perphenazine treatment on the autophagy signaling pathway. MDA-MB-231 cells were treated with perphenazine, phenothiazine ring at 10 µM and 20 µM and compared to the non-treated, serum and glucose free starved condition for 48 hr for the analysis of changes in protein levels of the autophagy signaling network by Western blot. Immunoblotting was carried out with antibody against: Beclin 1 (BCN), Atg5, p62, LC3-I/II, ERK2 (loading control).

Pharmacological inhibition of the different steps of the autophagosomal signaling pathway elicit potential sites of action of phenothiazines

In order to determine where perphenazine affects the autophagosomal pathway to cause increases in LC3-II protein levels and to block autophagy flux, we used pharmacological inhibitors known to target different steps of the autophagy pathway. We targeted multiple steps from the formation of the autophagosome to the later stage where fusion of the autophagosome with the lysosomes occurs (FIGURE 26). We treated MDA-MB-231 cells with 3-MA, a class III PI3K inhibitor, which inhibits the nucleation of autophagosomes (160), Bafilomycin A1 (Baf A1), an H^+ ATPase inhibitor which can increases the pH of lysosomes and decreases the fusion of autophagosomes with lysosomes (161), and the E64d protease inhibitor, which inhibits lysosomal proteases, thus decreasing protein degradation in the lysosome (162), (163).

Inhibition of the autophagosome nucleation step with 3-MA in MDAMB231 cells did not alter the ability of PPZ to increase LC3-II levels. This is unexpected as the initial phases of autophagy are through to be required for processing of LC3 to LC3-II. This could be due to incomplete inhibition of the autophagosome nucleation step by 3-MA or alternatively could potentially be explained by autophagy activation occurring through an alternative autophagy pathway, known as the non-canonical autophagy pathway(164).

As expected, inhibition of autophagosomes and lysosomes fusion by Baf A1, lead to augmentation in LC3-II levels in MDAMB231 cells in the absence of phenothiazines, due to blockade of LC3-II degradation. Co-treatment with PPZ and

Baf A1 slightly augmented LC3-II levels compared to either agent alone. LC3-I was converted to LC3-II as seen by decreased LC3-I in the presence of PPZ and Baf A1 as compared to Baf A1 treatment alone. E64D, a protease inhibitor that blocks protein degradation in the autophagosome and lysosome was sufficient to increase LC3-II alone, a process that was modestly augmented by addition of PPZ. These studies are compatible with phenothiazines altering the later stages of autophagy at the level of the lysosome, or potentially acting upstream of lysosomal function.

In examination of the levels of autophagy regulators Beclin 1 and Atg5, we determined that PPZ treatment only caused a modest decrease in Atg5 levels, and no detectable changes in Beclin 1 levels as compared to the untreated MDA-MB-231 cells. These effects were insufficient to explain the effects of phenothiazines on LC3-II or autophagy flux.

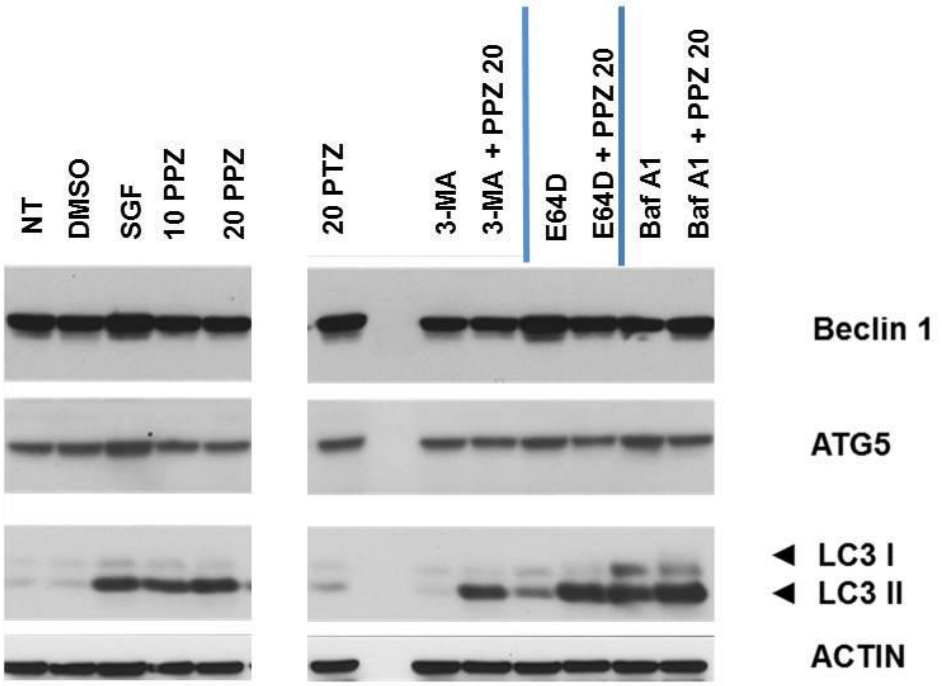

FIGURE 26: Pharmacologic inhibition of core regulators of the autophagosomal pathway. MDA-MB-231 cells were treated with 20 µM perphenazine with and co-treated with each of the inhibitors targeting different steps of the autophagy core signaling pathway; 3-MA (5 mM), E64d (10 µM), and Bafilomycin A1 (50 nM) for 24 hr.

siRNA knockdown of autophagy core signaling regulators

Since chemical inhibitors of the autophagy pathway are not always specific and may have additional cellular targets, it was necessary to confirm the above observations by genetic inhibition of the various steps of autophagy using RNA silencing (165).

We complemented our pharmacological inhibition study of the various steps of autophagy with knockdown of target genes essential for autophagy using short interfering RNA (siRNA). The experimental controls were untreated cells, the cells treated with the transfection agent (mock), RISC-free siRNA (RF), and serum and glucose free medium (SGF). Beclin 1 is required for the formation of the phagophore and the Atg12-Atg5 complex is required for maturation of autophagosomes and in particular formation of LC3-II. Beclin 1 knockdown with siRNA in MDA-MB-231 cells showed that despite marked Beclin 1 silencing, the ability of perphenazine (PPZ) to increase LC3-II levels was not ablated. We next sought to determine if PPZ mediated its effects through Atg5-Atg12 step of autophagy regulation. Using siRNA targeting Atg5 and Atg12, we silenced the expression of both proteins and treated the cells with PPZ. Again, RNAi knockdown of Atg5 and Atg12 did not abrogate the increase in LC3-II levels following PPZ treatment (FIGURE 27). Thus similar to 3-MA treatment above, blocking the autophagosome formation steps with RNAi knockdown of Beclin 1, Atg5 and Atg12. The lack of effect of inhibition of the early steps in the autophagy cascade on LC3-II formation was puzzling as these are proposed to be obligatory steps in the classical autophagy cascade described in the introduction. This raises the possibility that the

3-MA and the knockdown of autophagy pathway members was not sufficient to completely block initiation of the classical pathway. In the presence of block of autophagy flux by phenothiazines, sufficient autophagy initiation occurred to result in accumulation of LC3-II and p62. Alternatively, it is possible that cells underwent autophagy activation through a non-classical or non-canonical autophagy pathway.

Together, our studies of the effects of PPZ on components of the autophagy cascade are most compatible with PPZ mediating its effects on later steps in the autophagy pathway and thus blocking autophagy flux rather than autophagy initiation. One possibility is that PPZ may potentially target the autophagosome and lysosome fusion step to inhibit lysosomal degradation of autophagosome contents. This would increase both LC3-II and p62 are they are both degraded following autophagosome-lysosome fusion. We therefore proceeded to examine the fusion of the autophagosomes with the lysosomes and lysosome function.

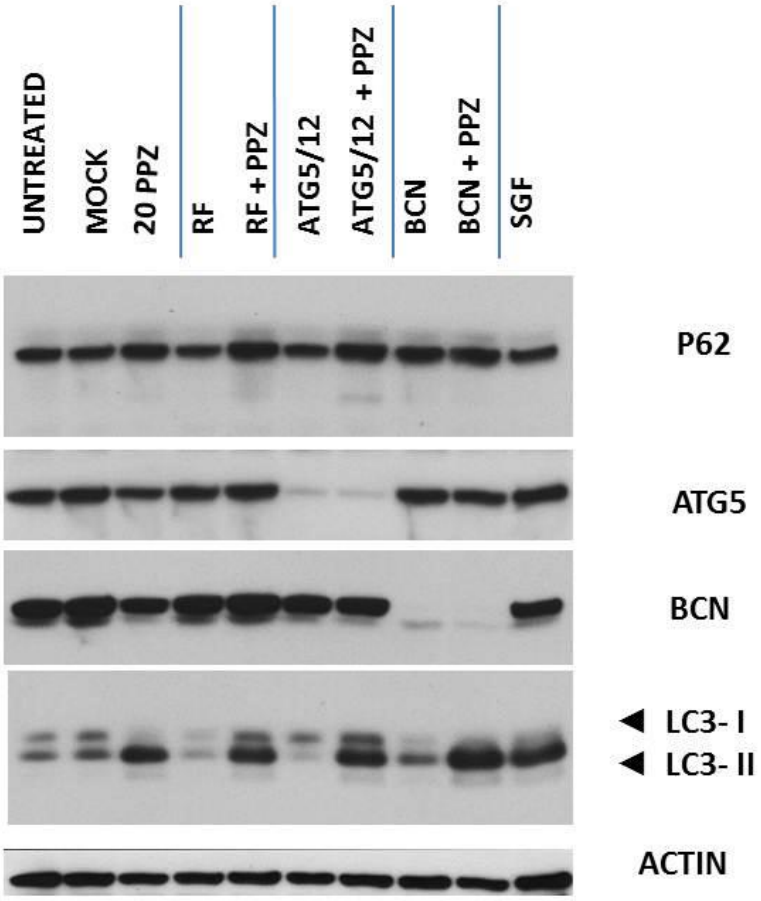

FIGURE 27: Inhibition of autophagy signaling network fails to inhibit accumulation of LC3. MDA-MB-231 cells were transfected with siRNA targeting Beclin 1 or Atg5 and 12 for 48 hr followed with treatment with perphenazine for 24 hr.

Effects of phenothiazines on cell viability is independent of Atg5 activation

Our RNA knockdown approach to silence the activity of different core regulators of the autophagy signaling network determined that increased LC3-II levels were not dependent of the classic early steps in upregulation of autophagy. Since knockdown of the Atg5/Atg12, or Beclin 1 genes may not been completely effective, we also used autophagy deficient cells, mouse embryonic fibroblasts (MEFs) lacking Atg5 genes, Atg5 -/- MEFs to complement our study. Recently, it was reported that MEFs lacking Atg5-/- were be able to undergo autophagy through an Atg5 independent pathway. When starved or treated with etoposide, these cells were able to form vacuoles which did not have LC3-II lipidation (166). We have confirmed that PPZ treated MEFs Atg5 double knockout cells had LC3I which were not converted to LC3-II (data not shown). Using these classic autophagy pathway deficient cells, we aimed to confirm that the decrease in viability mediated by PPZ is not dependent on activation of the classis autophagy pathway. Wild type MEFs and Atg5 -/- mutant cells were treated with increasing concentrations (5, 10, 20, or 40 µM) of PPZ for 48 hr and cell viability was assayed (FIGURE 28). PPZ treatment decreased cell viability in both cell lines, but there were no significant differences in cell viability based on the cells' ability to activate autophagy. This suggests that PPZ mediated decrease in cell viability is not dependent of Atg5 activation. We've previously shown in chapter 3 (FIGURE 13) that chlorpromazine did not have any cytotoxic effect on the non-tumorigenic human breast cells MCF10-A up to 40 µM. Here, however, wt MEFs, non-tumorigenic fibroblast cells have marked decrease in cell viability when treated with perphenazine. The differences in sensitivity to

phenothiazine treatment between these cell lines may be due to MCF-10A being a human cell line, whereas the MEFs cells were of mice origin. Another potential underlying difference is that MCF-10A cells are breast cells whereas MEFs are fibroblast cells. The level of basal autophagy in each of the cell types may also contribute to final outcome on cell viability upon drug treatment.

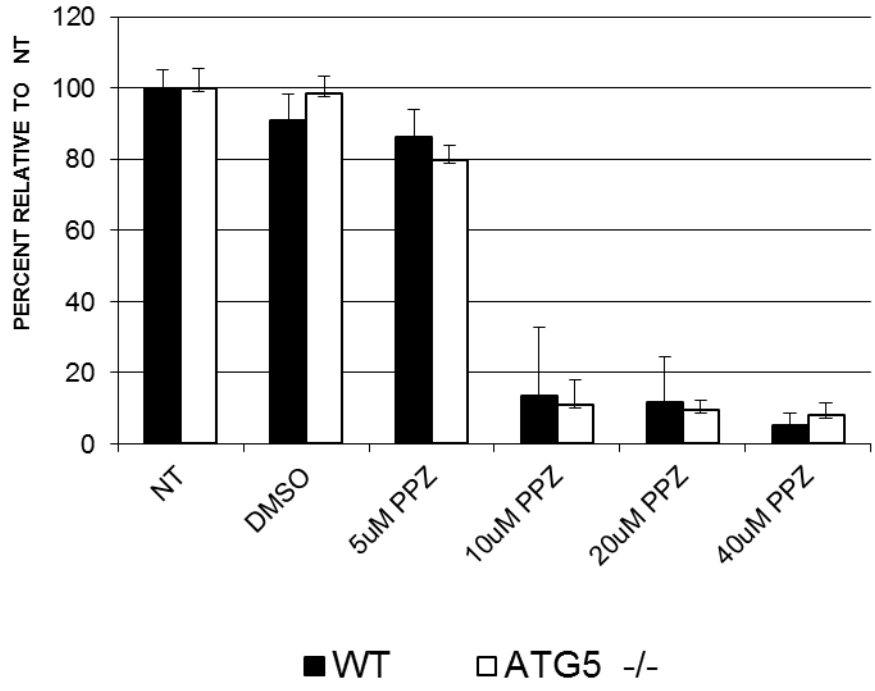

FIGURE 28: Perphenazine mediated decrease in cell viability is independent of Atg5 activity. Mouse Embryonic Fibroblast (MEFs) wild type, or Atg5 double knock-out (Atg5 -/-) cells were treated with 5, 10, 20, or 40 µM of perphenazine (PPZ) or DMSO for 48 hr. The cell viability was assayed by crystal violet assay. The data is represented as percent relative to the untreated control cells.

Perphenazine causes non-productive autophagy at the autophagosomal lysosomal fusion step of the autophagy cascade

To determine if phenothiazines affect lysosomal degradation of proteins by lysosomes at the final step of autophagy, we utilized a plasmid construct of LC3 tandemly expressed with red fluorescent protein (RFP) and green fluorescent protein (GFP), or tf-LC3. The tf-LC3 constructs are commonly used to study the fusion step of autophagosomes to lysosomes. GFP and RFP have different sensitivity towards the acidic lysosomal environment with GFP being more sensitive to lysosomal pH than RFP (61). Hence, autophagosomes show both RFP and GFP signals, but upon fusion with lysosomes, the GFP signal is attenuated and only the RFP signal remains. MDA-MB-231 cells were transiently transfected with the tandemly expressed RFP and GFP LC3 plasmid (tf-LC3) and subjected to treatment with 20 µM perphenazine (PPZ), DMSO, Baf A1, or EBSS medium (for starvation condition) (FIGURE 29). DMSO served as the control to show the basal autophagy condition in the cells. Under basal conditions, the RFP signal will be dominant as LC3 exists mostly in the cytoplasmic form with little being delivered to the lysosomes (FIGURE 29). Starvation upregulates autophagy and results in the delivery of autophagosomal bound LC3 to the lysosomes for degradation. EBSS medium was used as the starvation condition to show upregulation and completion of autophagy. In this condition, it would be predicted that the GFP signal would be attenuated leaving mainly the RFP signal, which is what was observed (FIGURE 29). Baf A1, the lysosomal proton pump inhibitor, disrupts lysosomal pH and inhibits the fusion of autophagosomes with lysosomes, therefore leaving GFP intact.

As expected, in Baf A1 treated cells, both GFP and RFP signals remained intact as indicated by the dominant yellow color in the merged image (Figure 29). When MDA-MB-231 were treated with 20 µM PPZ for 24 hr both the RFP and GFP signals persisted resulting in a mimic of the effects of Baf-A1. There are three possibilities as to why both the RFP and GFP signals remained intact: impairment of maturation of autophagosomes into autolysosomes, aggregation of autophagosomes, or successful fusion but defective lysosomal enzyme function. Defective lysosome function, either as a consequence of non-functional proteases or loss of acidification would result in their inability to degrade proteins and an accumulation of the yellow signal. Together the data, particularly when combined with accumulation of LC3-II and p62, argues that PPZ blocks the degradative step of autophagy, resulting in non-productive or abortive autophagy.

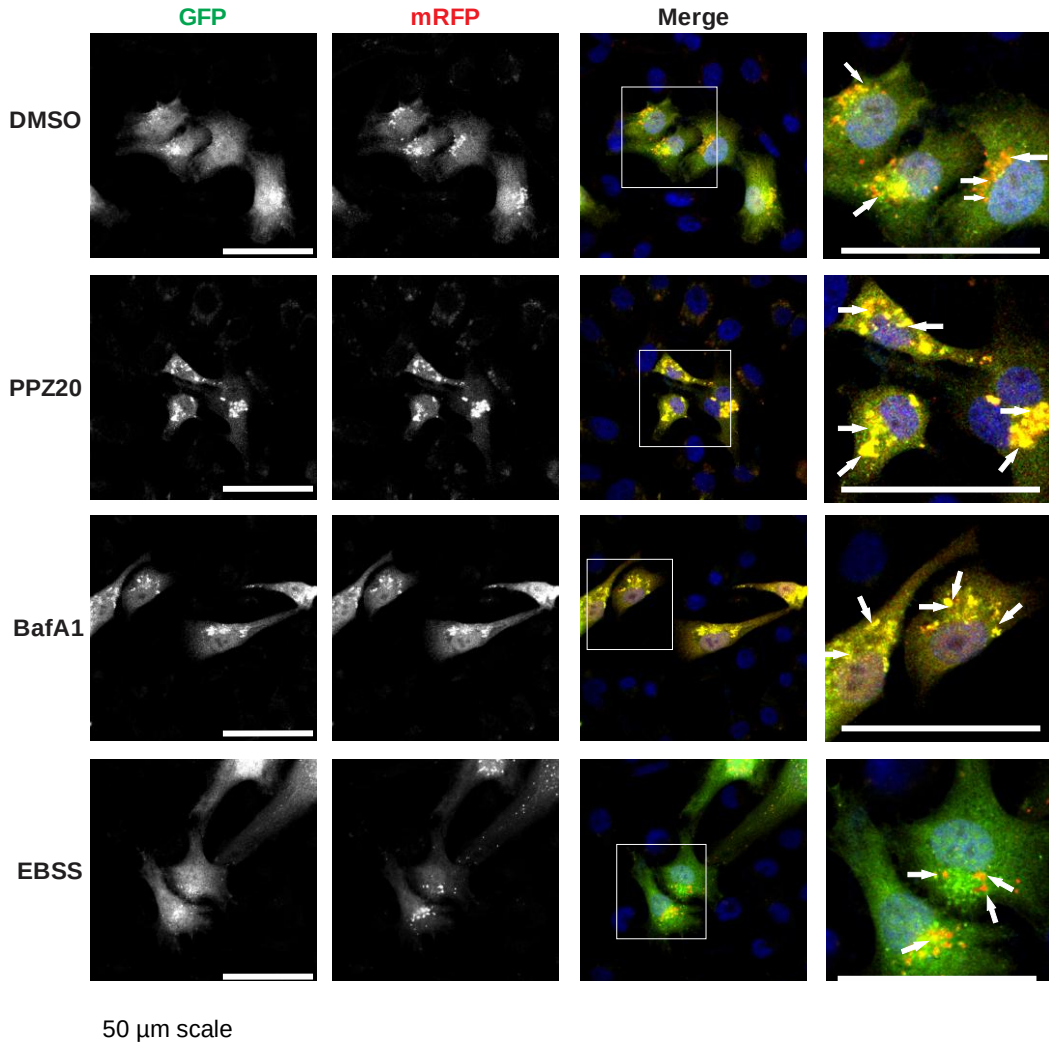

FIGURE 29: tf-LC3 showing perphenazine treatment blocks LC3 degradation. MDA-MB-231 cells were treated with 20 µM perphenazine (PPZ), DMSO, or 50 nM Baf A1 for 24 hr, and EBSS treatment for 4 hr. tf-LC3 is a tandemly expressed red fluorescent protein (RFP) and green fluorescent protein (GFP) to the LC3. Scale bar, 50 µm.

Perphenazine causes lysosomal volume expansion Based on the above findings that GFP signals of the tf-LC3 construct persisted in perphenazine treated cells, we sought to determine if autophagosomes co-localized with lysosomes to deliver their cargo to autolysosomes for degradation. We assessed the sub-cellular localization of these organelles by confocal microscopy using MDA-MB-231 cells stably transfected with GFP-LC3 in conjunction with the LAMP-2 antibody, a marker of lysosomes (FIGURE 30). In control cells, lamp 2 stained vesicles whereas LC3 was cytosolic. In PPZ treated MDA-MB-231 cells both LC3 and LAMP-2 were located in vesicles which are some cases overlapped. However, the autophagosomes and lysosomes has distinctly different appearance as compared to untreated cells. PPZ increased LC3 amount, as well as increased LC3 puncta size in the cells; indicative of increased in both number and size of autophagosomes. Additionally, PPZ caused expansion in lysosomal volume compared to untreated counterparts. These findings suggest that PPZ, at least in part, targets lysosomes prior to their fusion with autophagosomes. Indeed, perphenazine and chlorpromazine have been reported to induce increase in lysosomal vacuole expansion in lung carcinoma cells (167). Recently, Funk *et al.* studied drugs containing amine groups and their effect on lysosomal volume. They observed that imipramine, a weakly basic amine, which is similar to the weakly basic amines in phenothiazines, increased the lysosomal volume 4-fold (168).

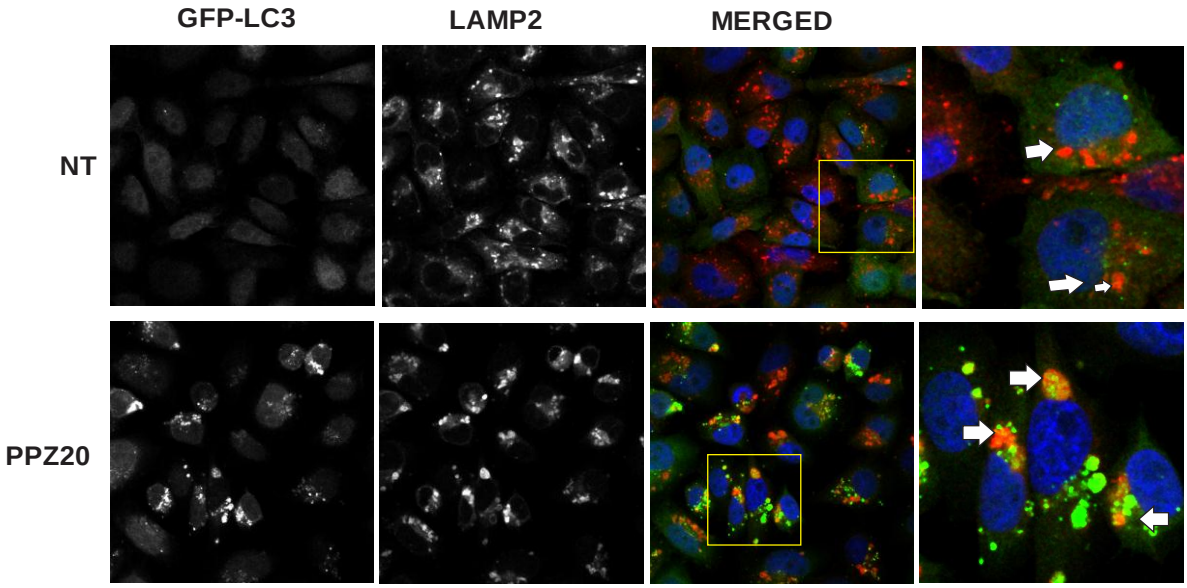

FIGURE 30: Perphenazine treatment causes lysosomal volume expansion (immunofluorescence). MDA-MB-231 cells stably expressing GFP-LC3 were treated with 20 μM perphenazine (PPZ) for 24 hr. The cells were immunostained with lysosomal marker LAMP-2 (red). Perphenazine treated cells exhibited lysosomes (red) with enlarged surface areas (indicated by the arrows) as compared to the untreated cells.

Perphenazine causes expansion in autophagy vacuoles and lysosomal number and size

We sought to determine whether the expansion of autophagosomal and lysosomal size and number observed in the fluorescent immunohistochemistry study could also be detected by EM, which is considered the “gold standard” for analysis of organelle structure including autophagosomes, autolysosomes and lysosomes. MDA-MB-231 cells were previously shown to have increased autophagosomal vacuoles containing cellular debris when treated with chlorpromazine and perphenazine in chapter 4. Perphenazine treatment also leads to extensive increase in the number of lysosomes and autophagosomes (FIGURE 31). Phenothiazines are weakly basic amines, which preferentially localize to lysosomes. Amines have been reported to induce vacuolization which can take up to 30% of the cell volume (169). More detailed discussion of mechanism of action of lysosomotropic agents will be undertaken in the next section.

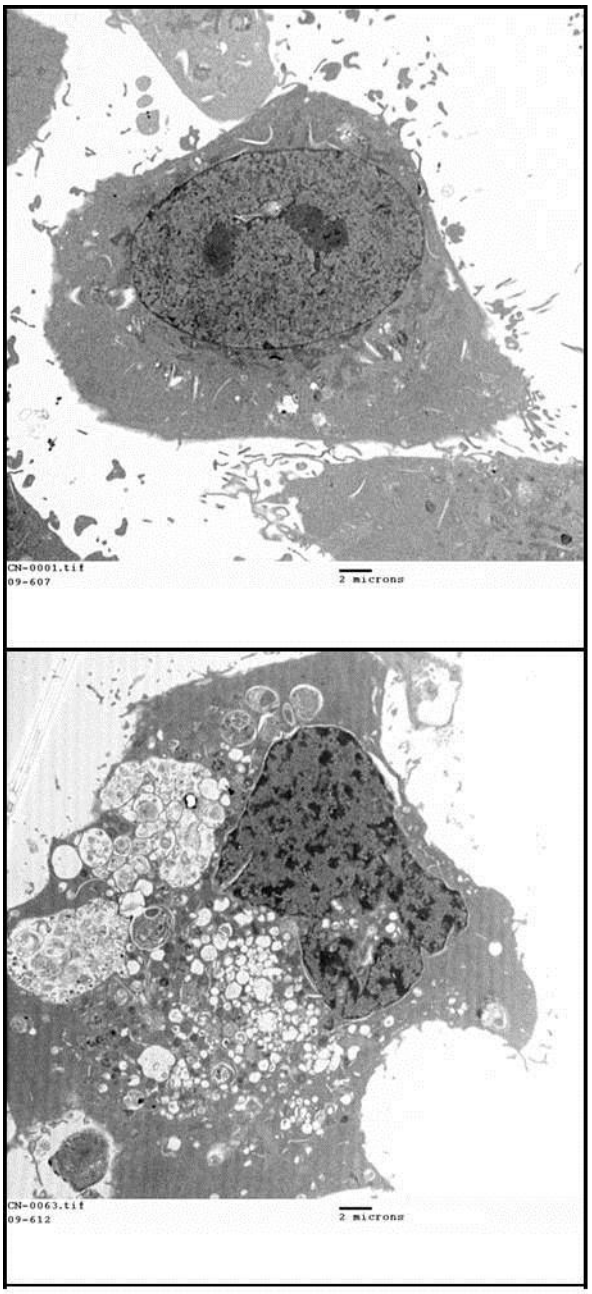

FIGURE 31: Perphenazine treatment causes autophagosomal vacuole expansion (EM). Ultrastructural study of MDA-MB-231 cells treated with 20 µM perphenazine (PPZ) for 24 hr showed extensive vacuolization –seen as increase in the number and size of lysosomes and autophagosomes.

DISCUSSION

In this chapter, we have shown that perphenazine blocked autophagic flux as measured by increase in p62 levels in cells. This blockage would be expected to result in the previously observed increase in LC3-II levels. Since LC3-II accumulation could be attributed to aggregated autophagosomes, inhibition of fusion of autophagosomes to lysosomes, or inhibition of LC3-II autolysosomal degradation, we systematically determined the status of autophagy regulators for each step of the autophagy pathway.

We determined that pharmacological inhibition of autophagy initiation with 3-MA did not decrease LC3-II levels in cells treated with perphenazine. In contrast, inhibition of acidification of lysosomes and the activity of lysosome proteases increased LC3-II levels independent of the presence of phenothiazines. Because autophagy inhibitors may not be fully effective in inhibiting their target and are known to have non-specific targets beyond the autophagy signaling network, we complemented this approach by systematically blocking key steps of the autophagy signaling pathway using siRNA. siRNA knock-down of regulators of early steps of autophagosomal formation, Beclin 1, Atg5 and Atg12, did not abrogate the effects of perphenazine on LC3-II accumulation. This could happen due to insufficient knockdown to completely inhibit pathway initiation. Indeed, since LC3-II accumulation did not occur on PPZ treatment of Atg5 knockout MEFs, inadequate knockdown with the siRNA may indeed be the case. Alternatively, PPZ treated cells may undergo autophagy through an alternative autophagy activation process that is

not Beclin 1, Atg5 or Atg12 dependent. Autophagy which is independent of Beclin 1 and Vps34 is known as non-canonical autophagy, as opposed to Beclin 1 dependent autophagy known as canonical autophagy. Scarlatti *et al*. showed that breast cancer cells treated with resveratrol activated autophagy and underwent cell death that was independent of Beclin 1, and therefore insensitive to 3-MA inhibition (170).

We used classical autophagy incompetent cells, Atg5 double knock-out MEFs to determine whether the effects of perphenazine were dependent on Atg5-mediated autophagosome formation. Nishida *et al.* have demonstrated that MEFs Atg5 -/- were able to form autophagosomes when treated with etoposide, thus providing evidence of yet another alternative autophagy pathway with Atg5 independent formation of autophagosomes. However these autophagosomes do not contain LC3-II. Cell death mediated by PPZ was not dependent on autophagy activation through Atg5. In order to confirm if MEFs which are deficient in Atg5 undergo autophagy when treated with PPZ, EM studies, or other approaches independent of LC3-II formation will need to be conducted.

However, these studies have major consequences in interpretation of the mechanisms by which phenothiazines cause cell deaths. As indicated in previous chapters, cell death, LC3-II accumulation and blockage of autophagic flux demonstrated similar structure function and concentration dependencies. Thus, we hypothesized that the block in autophagic flux was the cause of death. However, as PPZ causes death in cells lacking Atg5 and unable to undergo classic autophagic flux, it is possible that the cell death induced by PPZ is, at least in part, independent

of the block in autophagic flux. Alternatively, at least in MEFs cells, a non-classic autophagy pathway may contribute to cell death.

Using co-localization studies using the lysosomal marker LAMP-2 with LC3 autophagosomal marker, we were able to determine that the autophagosomes and the autolysosomes co-localized. We determined that PPZ disrupted lysosomal function and autophagic flux as the GFP signal was not attenuated. GFP is sensitive to low pH. Since its signal was not attenuated, this suggests that perphenazine increased lysosomal pH or ablated the functions of its hydrolases. Another possible explanation for the persistent GFP signal is that the autophagosomes did not fuse with the lysosomes to deliver the GFP linked LC3 for degradation. Lysosomal fusion to autophagosomes requires and acidic lysosomal pH. Thus in future mechanistic studies more direct assays of the accumulation of phenothiazines in lysosomes, effects on the pH of lysosomes, enzyme activity of lysosomal hydrolases and the formation of autolysosomes would need to be completed.

Lysosomes degrade cellular macromolecules through hydrolases, which are delivered as precursors by the trans-Golgi system to the lysosomes. There are over 50 lysosomal hydrolases which are activated through autocatalytic activity or processing by other proteases in the lysosomes. These require acidic pH in order to be activated. Lysosomal pH ranges from 4.5 to 5 as compared to the cytosolic pH of 7. The difference in pH is maintained by H^+ ATPases which pump protons from the cytosol to the lysosomal lumen (171).

Drugs or compounds which accumulate in the lysosomes are defined as lysosomotropic drugs (172). Lysosomotropic drugs have a lipophilic and basic component. The lipophilic component allows them to interact with the phospholipid membranes of cellular organelles such as lysosomes. Lipophilic weak base compounds accumulate more effectively than hydrophilic weak bases (173). Due to the pH difference between the cytosol and lysosomal lumen, weak bases move down their concentration gradient and accumulate in the lysosomes, often several orders of magnitude greater than the surrounding cellular environment (172), (174). In the cytosol, they are uncharged and cross freely into the lysosomes (175). Once inside the lysosomes they are protonated and become trapped due to the acidic lysosomal pH. This phenomenon was first described as ion trapping by de Duve and is also known as lysosomal trapping (172), (176). The basic compounds raise the lysosomal pH, disrupting the functions of the lysosomal hydrolases (177). Another means by which amphiphilic amines increase the lysosomal pH is through the inhibition of H^+ ATPases (178).

Recently, several phenothiazines, including chlorpromazine, promethazine, and thioridazine, were identified as lysosomotropic compounds through a drug screen by Nadanaciva and colleagues (129). The authors noted that many of the compounds identified in their screen had two common characteristics: basic pKa values ranging from 6.6 and 11, and a lipophilic component. Of the drugs identified by this study, chloroquine, and Gleevec (Imatinib) were previously reported to affect autophagy. Chloroquine (CQ) is a well-known autophagy inhibitor and a lysosomotropic drug that neutralizes the positive charge of the lysosomes, raising

their pH to abrogate their ability to fuse with autophagosomes (179). CQ has been reported to induce lysosomal volume dilation in retinal pigmentation epithelial (ARPE) derived cells (180) and other cells (181), (182).

Additionally, many compounds identified in the screen were antipsychotics of the phenothiazine and non-phenothiazine family. This was attributed to the fact that antipsychotics are lipophilic and effectively cross the blood brain barrier (183). Daniel *et al*. reported that many psychotic compounds including desimapramine, piperazine, piperidine undergo lysosomal trapping (184), (185). Lysosomal trapping could therefore be a plausible explanation as to why many of the positive hits identified in our screen included other, non-phenothiazine, antipsychotics as well.

Nadanaciva *et al.* proposed that lysosomotropic agents could disrupt the lysosomal degradative function by raising its pH, in doing so, inhibit the final step autophagy. Bafilomycin A1 and chloroquine are commonly used to inhibit autophagy and are described as lysosomotropic agents. Baf A1 inhibits the H^+ ATPase, which functions to acidify the lysosomes, this leads to an accumulation of autophagosomes in the cell due to the lysosomes' inability to degrade them (186).

Drugs which are more lipophilic cross the lysosomal membrane more easily than hydrophobic drugs. Chlorpromazine belongs to the aliphatic subclass of phenothiazines, having carbon chain substitutions and is not as lipophilic as perphenazine which has a piperazine substituted side chain. Perphenazine is therefore able to cross the cellular membranes more easily than chlorpromazine to reach its targets. The pKa value of phenothiazine (PTZ), chlorpromazine (CPZ), and perphenazine (PPZ) are: 0, 9.30, and 7.94 respectively (187). Weakly basic

amines with pKa values close to 8, in their unionized state freely cross membranes (141). PPZ's pKa value of 7.94 is the closest to 8 relative to CPZ and to PTZ and therefore would be expected to cross more easily into the cell and then into lysosomes. Lipophilic compounds which are weakly basic bases cross the lysosomal membranes freely and become trapped in the lysosomes through becoming ionized. In their ionized state, they are unable to cross back out of the lysosomes where they remain trapped and raise the lysosomal pH (FIGURE 32). The relative potencies of PTZ, CPZ, and PPZ in mediating cell death could be attributed to their lysosomotropic attributes such as ease of crossing membranes and ability to increase lysosomal pH. In addition to being better able to permeate membranes to reach the lysosomes, PPZ has 3 sites where it can be ionized, as compared to CPZ, which only has 2 sites, thus, it could be more potent in increasing the lysosomal pH.

Morissette *et al.* have shown that the concentration of bases which accumulate in the cells correlated with the extent of vacuolization observed. They've also found that the same drug caused different degrees of vacuolization in different cell types (188). The results of comparative studies of phenothiazines in the previous chapter demonstrated that PPZ was more potent in upregulating LC3-II, p62, and cell death than CPZ and the phenothiazine parental ring (PTZ). This suggests that the effects of phenothiazines on cancer cell viability may be due to lysosomal trapping as PPZ's physiochemical properties allows it to more effectively cross cellular membranes and increase lysosomal pH, consequently blocking autophagy at the lysosomal stage. This failure to complete the autophagy process,

sometimes described as abortive autophagy could then lead to cancer cell death. However, it is important to point out that PPZ induces death in ATG5 knockout MEFs. Thus the death induced by phenothiazines is not absolutely dependent on the classic autophagy pathway and, in MEFs, could be due to initiation of non-classical autophagy or interference with lysosomal function directly.

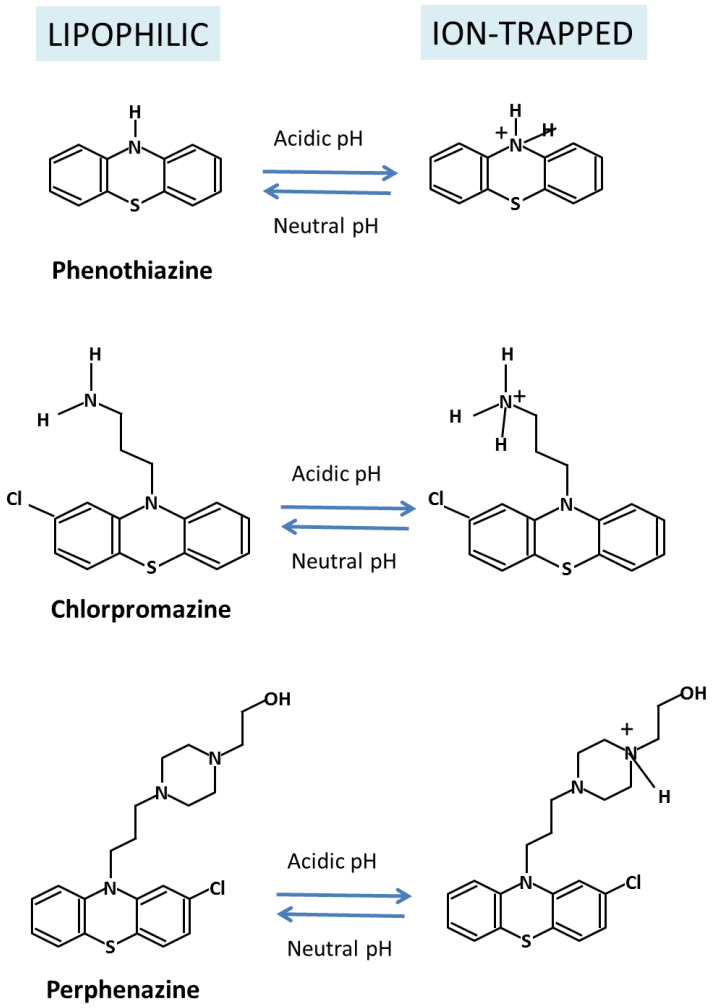

FIGURE 32: Phenothiazines contain weak amine base groups and undergo protonation in acidic environments. Phenothiazines have amines groups and are weakly basic. At neutral pH, they exist as non-ionized (unprotonated) species and cross freely through biological membranes but become ionized in acidic compartments such as lysosomes. Once ionized (protonated), they cannot cross back out of the lysosomes into the cytosol and become trapped. This phenomenon is known as ion trapping, or lysosomal trapping.

CHAPTER 6

Determination of the Effects of Perphenazine on Cancer Cell Signaling Pathways *in vivo* and in Other Cancer Cell Lines

RATIONALE AND EXPERIMENTAL GOALS

Although there are large numbers of *in vitro* studies of phenothiazines and cancer, *in vivo* studies are still lacking. Human tumor xenografts are routinely used to evaluate antitumor effects of drugs in a metabolically intact organism for the study of the effects of drugs on tumor versus normal tissues (189). In order to ascertain if perphenazine mediated abortive autophagy which resulted in cell death *in vitro* could be observed *in vivo*, we conducted an MDA-MB-231 xenografted mouse study.

RESULTS

In vivo study shows PPZ treatment elevated p62 protein expression is accompanied by increased cleaved PARP protein expression levels

We injected MDA-MB-231 cells into the mammary fat pads of 5 week old female athymic nude mice. The tumors were allowed to establish to a palpable size for one week. Once the tumor reached a minimum volume of 0.5 mm^3, the mice were randomly separated into 3 treatment groups: DMSO, PTZ ring, and PPZ treated group. Intraperitoneal (IP) drug treatment was delivered on alternate days with a starting dose of 25 mg/kg. This dose was ill- tolerated by the animals; the mice showed extreme lethargy and sedation through 4-5 hr post-treatment. Consequently, we decreased the dosage several times over the course of the next two weeks to a final dose of 2 mg/kg. At the conclusion of our study, we did not observe tumor mass reduction in the animal model, potentially due to being unable to deliver adequate doses.

Although the xenografted tumors did not show differences in growth rate or tumor volume among the treatment groups, we sought to determine if our drug treatment had any effect on the established tumors at the molecular level. Specifically, we sought to determine if the signaling effects on autophagy observed by *in vitro* studies were replicated *in vivo*. We therefore collected the xenografted tumors at sacrifice for frozen tissues preparation as well as for paraffin embedded preparations for our follow-up studies. Protein lysates were prepared from the frozen samples for studies using the reverse phase protein array (RPPA) platform

whereby we measured upregulation or downregulation of proteins commonly involved in regulation of cancer signaling. The analysis of the xenografted tumors showed that a subset of the tumors from PPZ treated mice had increased p62 protein levels (FIGURE 33). Tumors which expressed increased p62, also had increased cleaved PARP level (indicative of apoptotic cell death). This is consistent with the results from our *in vitro* studies where increased LC3-II formation and p62 levels correlated with increased cleaved PARP levels in a dose and time dependent manner. A more detailed study of the protein expression profiles comparing the responders against the tumors which did not respond to PPZ treatment could yield a better understanding of which additional signaling pathways, apart from the autophagic signaling pathway was targeted to bring forth cell death.

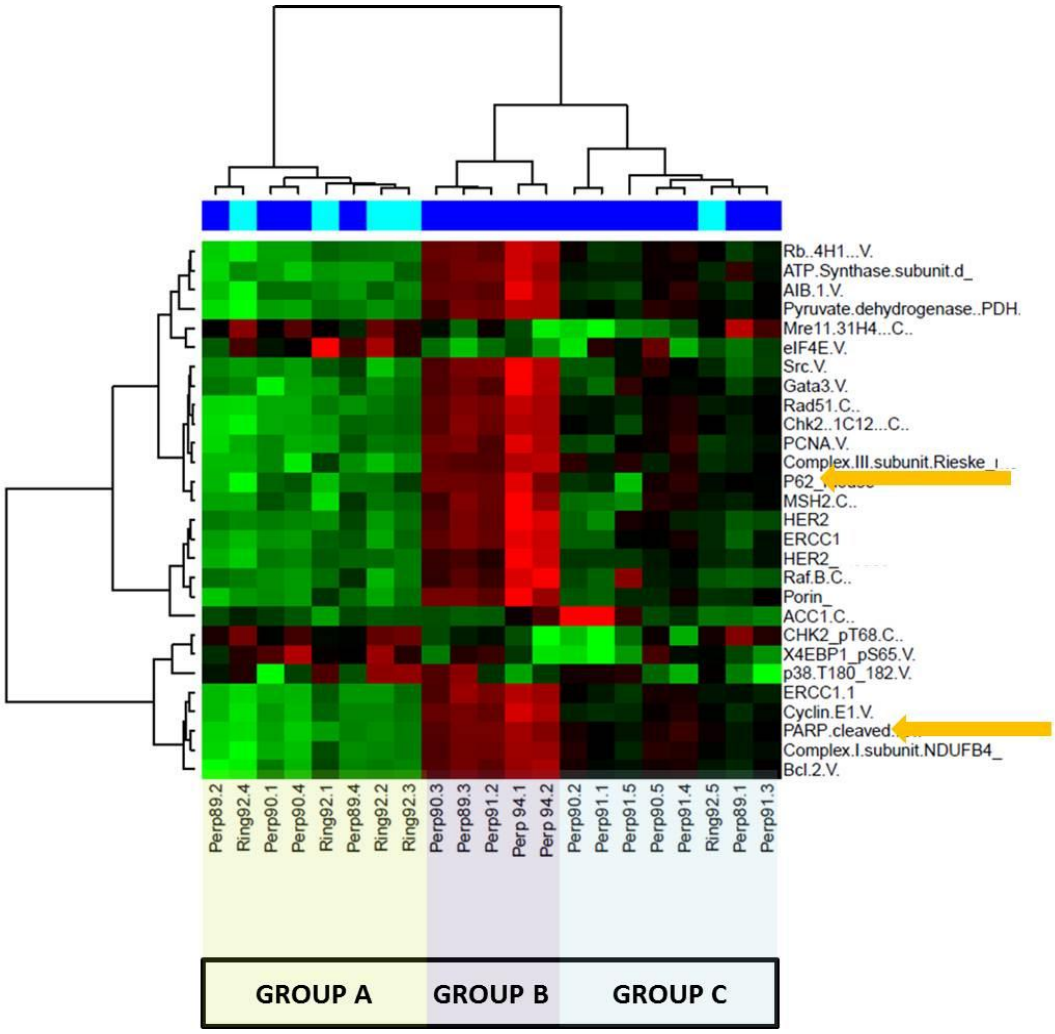

FIGURE 33: *In vivo* study of signaling events altered with perphenazine treatment. MDA-MB-231 xenografted tumors of two drug treatment groups were compared: perphenazine (blue color) and phenothiazine core ring (teal or light blue). The groups were clustered and 3 clear groups emerged. **Group A** consisted of 4 core phenothiazine ring treated and 4 perphenazine treated mice. **Group B** showed phenothiazine treated mice have increase in p62 and increase in cleaved PARP, which were consistent with *in vitro* studies. **Group C** consisted of 7 perphenazine treated mice and one phenothiazine core ring treated mouse. Mice in group C did not have increase in p62 nor increase in cleaved PARP.

RPPA study of perphenazine treatment of human cancer cells harboring different mutations

Cancer cells harbor mutations which influence how they respond to different therapeutics. We sought to determine if certain mutational background sensitizes cancer cells to PPZ treatment by assessing its effects on a panel of 16 human cancer cells of different tissue origins, including breast, ovarian, osteocarcinoma, prostate, melanoma and a non-tumorigenic breast line (TABLE 1). Cell lines selected included different mutational status commonly found in patient clinical samples to ensure that our findings would be clinically relevant. For example, breast cancer lines used in our studies have been shown by gene expression microarrays to have the same transcriptome profiles as patient samples and to be appropriate models for breast cancer studies (190). We used RPPA to measure protein levels and phosphorylation status of proteins in the cell lysates to measure upregulation or downregulation of signaling pathways commonly deregulated in cancer. A comprehensive time course study of cells treated with PPZ was conducted to generate protein expression profiles for each cell line (APPENDIX 2). We compared the effects of PPZ treatment on protein expression across the 17 cell lines using the 48 h timepoint of our study.

Perphenazine treatment elevates p62 levels accompanied by increased cell death proteins and decrease autophagy proteins in several human cancer cell lines

We studied the expression profiles of protein levels in our panel of cancer cells in response to 48 hr perphenazine treatment (FIGURES 34-35). We determined that p62, a long lived protein targeted for degradation during late stages of autophagy, is elevated in many of the cells lines, but to varying degrees. This is in agreement with our Western blot analysis of MDA-MB-231 and other cell lines which showed perphenazine treatment increased p62 levels. Our RPPA data also showed increase in the apoptotic cell death protein (caspases) levels in cell lines with the highest p62 levels.

Interestingly, in our RPPA panel, the cell lines most sensitive to perphenazine treatment – with the strongest increase (red) and decrease (green) in protein level relative to DMSO condition were two cell lines of melanoma origin: SKMEL-5 and WM-35. SKMEL-5 showed impaired or down-regulated autophagy as seen by p62 increase, indicating blocked autophagic flux. Additionally, SKMEL-5 exhibited the most decrease in 2 important autophagy genes, Beclin 1 and Atg7. More importantly, the decreased autophagy pathway activation was accompanied by increase in levels of cell death pathway regulators caspase-3 and caspase-7. These findings are consistent with reports that melanoma cancers harbor activating Ras mutations which lead to autophagy addiction for survival, thus rendering them sensitive to PPZ inhibition of autophagy relative to other types of cancers.

SKMEL-5 also exhibited the strongest upregulation of BiP (immunoglobulin heavy chain binding protein), also known as GRP78, which is a marker of UPR activation. UPR activation is mostly a cytoprotective mechanism, but sustained activation leads to apoptosis activation (191). Our RPPA study suggests that perphenazine inhibited autophagy seen as increased in p62 levels and mediated cell death through caspase activation. Perphenazine mediates abortive autophagy, blocking the final step of autophagy by inhibiting lysosomal function. We hypothesize that in doing so, it causes a bottleneck upstream, leading to accumulation of aggregated proteins. This places stress on the ER system, leading to activation of the UPR system. Our lab has previously shown that abortive autophagy activates ER stress which consequently causes cell death (30).

MSH2 and MSH6 are two proteins involved in DNA mismatch repair (MMR). Expression levels of both proteins are decreased in nearly all cell lines treated with perphenazine. This suggests that PPZ treatment impairs DNA repair in the cells. This is in concordance with previous studies which showed that phenothiazines potentiate the cytotoxic effects of DNA damage by bleomycin *in vivo* studies of high grade gliomas (192).

Our RPPA results showed that in our panel of breast cell lines, the MDA-MB-231 cells were one of the least sensitive cells to perphenazine treatment. This offers a potential reason as to why our MDA-MB-231 xenograft studies did not show tumor size regression or shrinkage. The breast cancer cell line most sensitive to PPZ treatment was SKBR-3; it had similar upregulated or downregulated protein profile as the SKMEL-5 cells. Based on these results, the SKBR-3 cell line may

have been a more appropriate line to initiate *in vivo* studies with. The non-tumorigenic breast line, MCF10-A, treated with PPZ had lower p62, caspase-3, caspase-7 and BiP protein levels relative to the tumorigenic cell lines. These results were consistent with the fact that tumor cells have higher metabolic needs and are under low levels of ER stress. When these tumor cells are faced with additional stress stimuli from chemoagents or radiation therapy, they undergo more intensive ER stress, and upregulate UPR to try to bring the cells back to homeostatic levels. Although UPR is an adaptive response to support cell survival in adverse conditions, sustained UPR activation leads to the activation of apoptosis thus results cell death (193). The waterfall graphs showed MCF-7 cells had low caspase-3 expression at the baseline, in agreement of the fact that MCF-7 cells have non-functional caspase-3 through base pair deletions (194).

SKMEL-5 cells which had the strongest upregulation of p62, caspase-3 and caspase-7, shows downregulation of autophagy genes Beclin 1, Atg7, and p760SK. p706SK is an effector of the mTORC1 signaling pathway that is required for autophagy (195),(196).

Due to time constraints, only a few of the strongest up and downregulated proteins were examined. More detailed studies of the time course of the proteins which showed the strongest upregulation or downregulation in our RPPA studies by Western blot analysis to confirm our findings will be necessary to gain in depth understanding of how PPZ perturbs the global protein signaling in the cells.

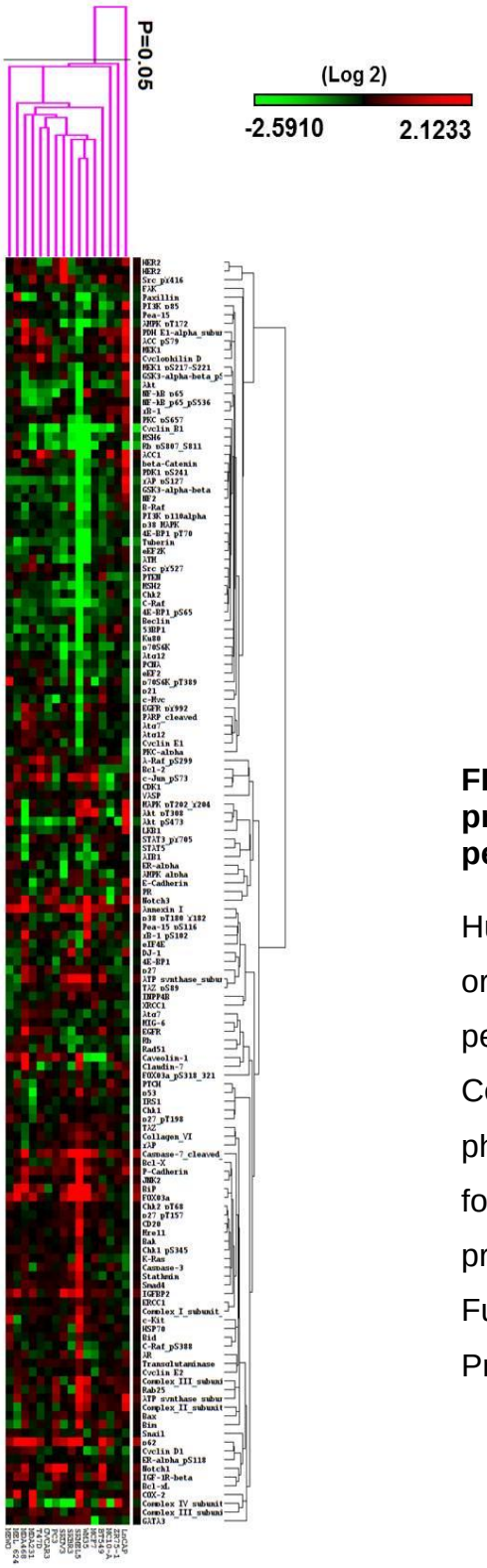

FIGURE 34: Protein expression profiles of cancer cells treated with perphenazine

Human cancer cell lines of different tissue origins were treated with 20 µM perphenazine and normalized to DMSO. Cell lysates were processed on a reverse phase protein array (RPPA) and stained for antibodies to each of the indicated proteins and phospho-proteins by the Functional Proteomics Reverse Phase Protein Array Core Facility.

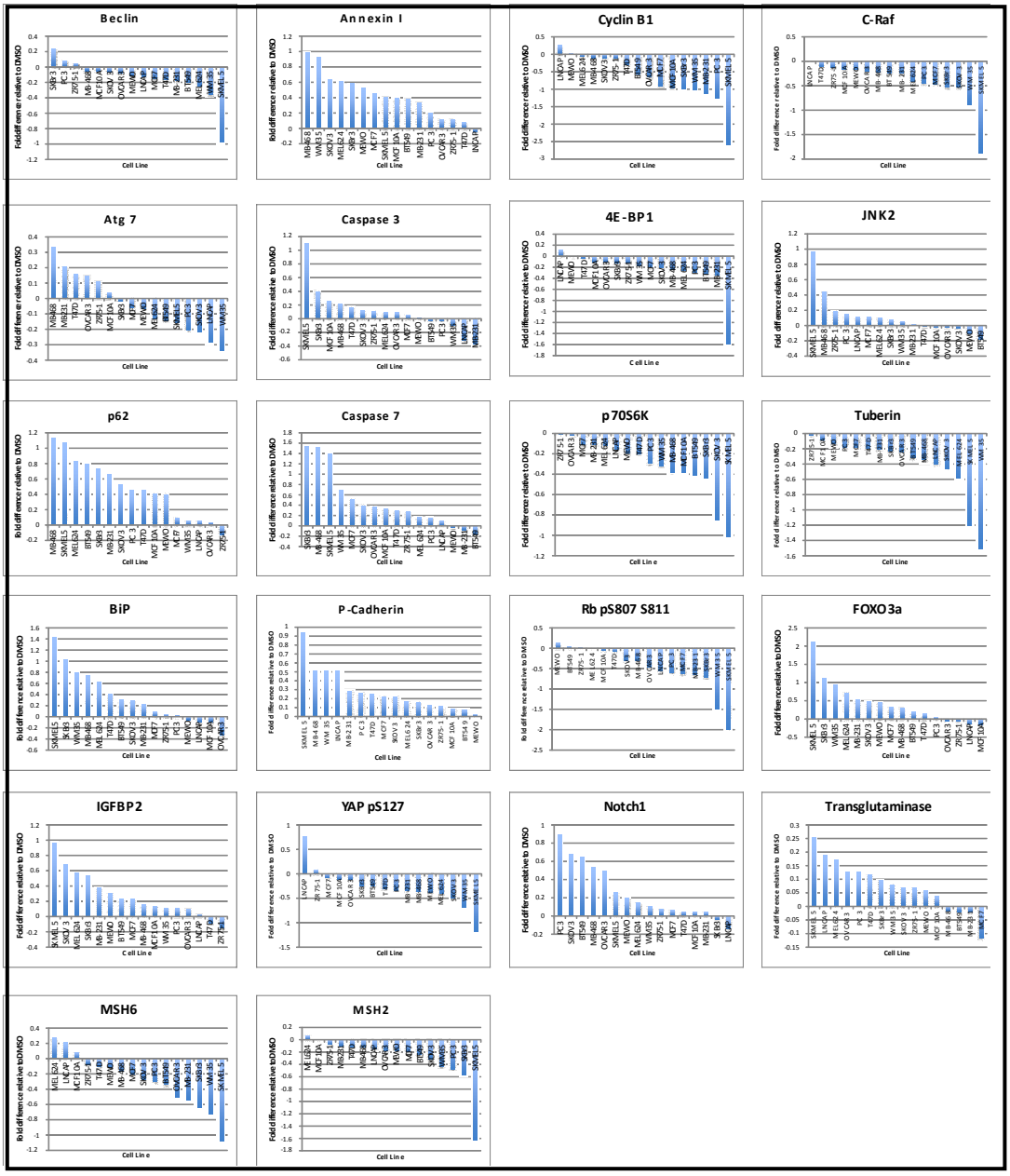

FIGURE 35: Waterfall graphs showing proteins with the strongest level of upregulation or downregulation due to perphenazine treatment. Proteins which showed the strongest increase or decrease in expression levels in our heatmap representation of our data were graphed to exhibit correlation in cell line clustering based on the different expression patterns.

DISCUSSION

One of the aims of the studies in this chapter was to determine if the *in vitro* findings of previous chapters could be observed *in vivo.* MDA-MB-231 xenografted into nude mice did not show tumor mass reduction, but analysis of protein levels of the different sub-group of tumors showed that some tumors responded to PPZ treatment. In these tumors, PPZ did block autophagy, as seen in elevated p62 levels compared to the group which consisted mostly of the core parental group, our negative control in the experiment. The tumors with elevated p62 levels had corresponding increase in cleaved PARP levels, indicative of cell death. These observations suggest that *in vitro* mediated anti-tumorigenic potentials of PPZ mediated through autophagy manipulations could be translated *in vivo.* Thus PPZ is a viable candidate for development of cancer therapy. The lack of growth inhibition in the mice may be due to it being relatively insensitive to phenothiazines even in vitro.

Mutational status or genetic background of cancer cells can potentially determine the outcome of autophagy inhibition (197). Although the focus of the studies of phenothiazines in the earlier chapters of this thesis were conducted in breast cell line MDA-MB-231 cells, we wanted to determine if certain mutational status or different types of cancers were more them sensitive to autophagy inhibition by perphenazine. Our study of a panel of 17 human cell lines of diverse mutational status and cell lineages showed that each cell line displayed different protein activation profiles (APPENDIX 2). Examination of the protein expression

status of the 48 hr treatment across cell lines showed that PPZ inhibited autophagy nearly all the cancer cells and mediated cell death through caspase activation.

Different degrees of sensitivity to PPZ treatment was observed in the different cell lines. SKMEL-5 and WM-35 melanoma cell lines were the most sensitive to perphenazine treatment as compared to the non-tumorigenic breast and other cancer cell lines in the study. This is in line with Motohashi and colleagues' findings that phenothiazines preferentially accumulate in melanoma tissues, and were more effective against these types of cancers (91). Others have also reported antitumor activity of phenothiazines in melanoma cells in *in vivo* mice studies (135). Additionally, both SKMEL-5 and WM-35 have B-Raf mutations, which confirm findings from John Weinstein's group. The Weinstein lab examined drug activity in context of mutational status of the NCI-60 cell lines and found that melanoma cells with the Ras pathway B-Raf gene mutation were sensitive to phenothiazines (102). These computational modeling findings were confirmed experimentally. Since melanoma cells have 40-60% activating B-Raf, and more than 90% of B-Raf mutations in melanoma cancers are V600E mutations, where valine to glutamine mutation occurred at codon 600 (V600E), phenothiazines could potentially be effective against these cancers. PLX4032 (vemurafenib) is a V600E B-RAF inhibitor currently approved for patients with melanoma (198). Combining PPZ with this inhibitor may potentially have synergistic effects to enhance the efficacy of both drugs.

Differences in toxicity to PPZ treatment as seen in relative upregulation levels of caspases could also be attributed to the different mutational status of cells

such as Ras driven cancer cells. These cells have been shown to be highly dependent on autophagy for survival. Inhibition of autophagy in these tumor cells result in synthetic lethality conditions which enhance cell death potentials of the drugs. However, this is not universal as MDA-MB-231 which has both RAS and BRAF mutations is relatively insensitive to phenothiazine.

In addition to mutational status of different cancer cells which may contribute to their sensitivity to perphenazine treatment, the number of lysosomes in different cell types could also contribute to differences in sensitivity. More comprehensive studies of the data is necessary in order to map out other pathways that are affected by perturbation of autophagy by perphenazine. Based on the findings in our previous chapters, we generated a proposed model of how perphenazine mediates cancer cell death (FIGURE 36). Through its properties as a weakly basic amine, perphenazine (PPZ) diffuses passively through cellular membranes to travel down its concentration and pH gradient into lysosomes. PPZ becomes ionized in the lysosome's acidic environment and remain trapped inside the lysosomes by a phenomenon known as lysosomal trapping. Since PPZ is converted from the un-ionized form after reaching the lysosomes, the concentration difference between the cytosol and the lysosomes is maintained. This difference functions as a driving force for diffusion of PPZ, allowing it to reach concentrations which are several fold higher in the lysosomes relative to the cytosol. In doing so, they also cause osmotic pressure to increase. Consequently, the lysosomes expand to relieve the increasing pressure which is as seen in dilated vacuoles observed by EM and by fluorescent microscopy. By raising the lysosomal pH, PPZ disrupts lysosomal

functions by inactivating lysosomal hydrolases which require low pH and prevent lysosome fusion to autophagosomes. By disrupting these lysosomal functions, PPZ prevents autophagy from going to completion, disrupting autophagic flux which results in abortive autophagy. Abortive autophagy has been shown by our group to activate ER stress (30).

In blocking autophagy's degradative step, PPZ causes increase in unfolded and aggregated protein concentrations in cells. The ER, which is also involved in protein quality control in the cell, becomes overwhelmed and undergoes ER stress resulting in the activation of UPR. Sustained activation of UPR activates apoptosis and results in cell death (193).

Additionally, by inhibiting the degradative step of autophagy, PPZ blocks the cells' ability to recycle damaged organelles, and cytoplasmic contents for energy to sustain proliferation and survival, thus leading to cell death.

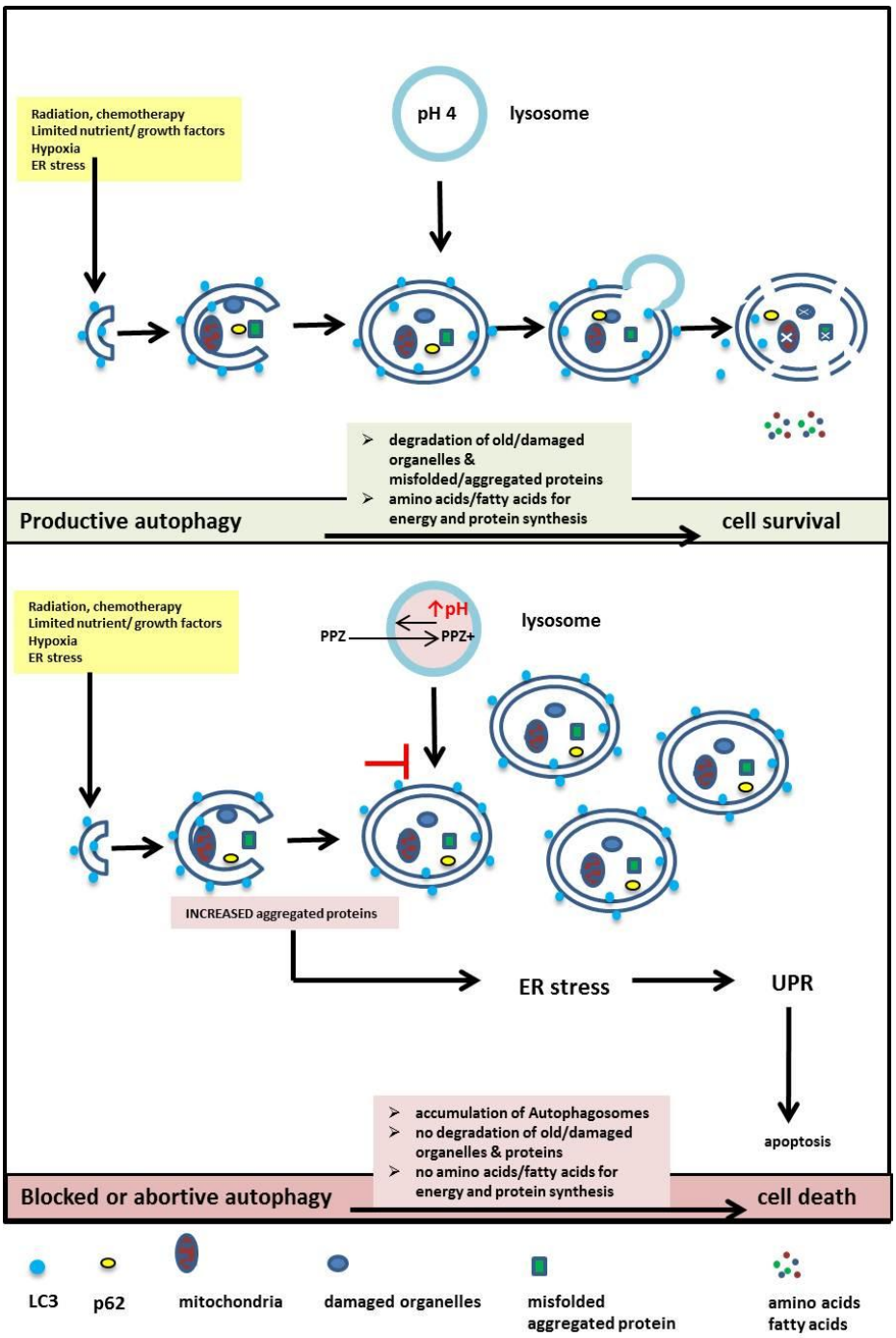

FIGURE 36: Model of proposed mechanism of perphenazine mediated cancer cell death.

CHAPTER 7

OVERVIEW, FUTURE DIRECTIONS

Many current therapies target apoptosis or programmed cell death type I (PCD I) as a mechanism of cell death. Taxanes commonly used to target apoptosis are paclitaxel and docetaxel, which bind to tubulin and stabilize the microtubule bundles and impairs mitosis (199). This causes cell cycle arrest and initiates apoptosis (200). Cancer cells develop resistance to these drugs by point mutations on the tubulins, or by expressing different isoforms of tubulins to impair taxane binding (201), (202). Other cancers acquire resistance by overexpressing P-glycoprotein efflux pumps to decrease drug concentration in the cells, thus decreasing their efficacy. Because autophagy is also known as programmed cell death type II (PCD), it became an attractive target to explore for cancer drug development. We therefore sought to understand how autophagy which is commonly known as a cell survival mechanism could be converted to a cell death mechanism in cancer cell.

The two main aims of this dissertation were: 1) to understand how modulation of autophagy in cancer cells affects their viability, and 2) to determine whether autophagy could be targeted for cancer therapy.

In order to accomplish the first aim, we conducted a HTS of small molecules to identify active autophagy modulators. We characterized the largest group, the

phenothiazines, and determined that in perturbing autophagy, they induced cancer cell death in a panel of breast cancer cells. We systematically examined different steps of the autophagy pathway through genetic and pharmacological inhibition as well as cells deficient in autophagy genes to determine where phenothiazines exerted their effect to mediate cell death. We determined that phenothiazines blocked the degradative step of autophagy by targeting lysosomes. We showed perphenazine disrupted the lysosomal phenotype, as indicated by marked increases in lysosomal volume as observed by immunofluorescence study and EM. Phenothiazines are weakly basic amines and accumulate in lysosomes through a mechanism known as lysosomal trapping. Once they reach the low pH in the lysosomes, they become ionized, gaining a proton, and raise the lysosomal pH to disrupt both the lysosomal hydrolase functions as well as the fusion step between autophagosomes and lysosomes. This effectively blocks autophagy flux, causing abortive autophagy.

Differences in the relative potencies of the phenothiazines in modulating autophagy and inhibiting proliferation correlated with how easily these cross the cellular membranes to reach their targets. Substitution on the parental ring influence solubility, and without any substitution, the parental ring had no autophagy activity. In comparing chlorpromazine with perphenazine's relative activity on autophagy and cell viability, perphenazine was more potent in mediating these effects. This could be attributed to chlorpromazine's aliphatic substitution being less lipophilic than perphenazine's piperazine substitution. Additionally, the pKa value of perphenazine is closer to 8, the optimal pKa value which allows amines to cross

freely across membranes. Perphenazine's ability to better induce abortive autophagy than chlorpromazine is likely through its ability to better disrupt lysosomal function based on its physiochemical properties which permitted ease of crossing through membranes to act as a lysosomotropic agent. Perphenazine was more potent than chlorpromazine in mediating antitumor activity in MDA-MB-231 cells and effectively decreased cancer cell invasion, and cellular ATP in these cells. Therefore, in aim one, we've determined that perphenazine mediated cancer cell death as a process which was associated with disrupting autophagy at the final step, by targeting lysosomal functions.

The coordinate effects of different concentrations on different structures of autophagy and cell death was consistent with the processes being potentially causal. However, the ability of perphenazine to decrease the growth of wild type and Atg5 knockout MEFs at similar concentrations suggests that classical autophagy which requires Atg5 may not be a prerequisite for perphenazine mediated death. However, non-classical forms of autophagy have been hypothesized. These may contribute to the ability of perphenazine to induce cell death. Additional studies will be necessary to elicit the mechanisms responsible for perphenazine mediated cell death.

The second aim of this dissertation was to determine if autophagy could be targeted for cancer therapy. In order to determine if the *in vitro* results of our studies would be applicable *in vivo*, and determine if our findings could eventually be brought to the patients, we conducted human xenograft MDA-MB-231 studies. We found that a sub-group of tumors responded to perphenazine treatment,

showing autophagy was inhibited as seen in the increased levels of p62. This inhibition was accompanied by cell death as indicated by increased cleaved PARP levels. Although we were not able to show tumor regression, our study provided us with a starting point for dosing, and design of future experiments.

In chapter 6, we also aimed to determine if certain mutations or types of cancers were more sensitive to autophagy inhibition by perphenazine. Through our study of a panel human cancer cell lines, we've determined that melanoma cancer cells (SKMEL-5 and WM35) with B-Raf mutations were more sensitive to autophagy inhibition by perphenazine relative to other types of cancers, including breast cancers. This confirms findings by the Weinstein lab that melanoma cells with specific B-Raf mutations having increased sensitivity to phenothiazines. Our findings were also consistent with findings from the White lab that Ras activated cancers were more sensitive to autophagy inhibition due to autophagy addiction. However, MDA-MB-231 cells which have both Ras and B-Raf mutations were comparatively less sensitive to the effects of perphenazine. Thus, other context dependent events contribute to sensitivity. Our reverse phase protein array (RPPA) study also showed cells that had the most decreased autophagy genes which were accompanied by highest increased expression of caspase proteins. Additionally, these cells also had upregulated expression of the ER chaperone BiP/GRP78 protein, indicative of unfolded protein response activation (UPR), known to induce apoptosis. Bip protein expression level was decreased in MCF10-A, the non-tumorigenic breast cell line which did show not decrease in cell viability when treated with chlorpromazine in chapter 2. Together, these findings suggest that

perphenazine induced abortive autophagy, which causes cancer cell death while sparing normal cells.

The potential utility of phenothiazines in the clinic as an anti-cancer treatment is underscored by findings from the studies presented here as well as findings previously reported by other groups. Pre-clinical studies have shown that phenothiazines are antitumorigenic against different types of cancers (131), (137), (203). Recently, a study showed that phenothiazines target cancer stem cells without killing normal cells, thus providing additional supporting evidence that phenothiazines are cytotoxic against tumor cells with limited toxicity to normal cells (145). Phenothiazines are attractive agents to explore in context of cancer therapies because in addition to many reported antitumorigenic potentials, they are relatively inexpensive and are widely available. Additionally, we've shown that perphenazine exerted the anti-proliferative activities at concentrations which are within reported plasma levels (2-36 μM) of patients treated with phenothiazines for psychotic conditions such as schizophrenia (130) (145).

Autophagy inhibition by phenothiazines could have clinical utility as numerous studies provide evidence that activation of autophagy by cancer cells decreases therapeutic potentials of many current cancer therapies (204), (205). Examples of how autophagy activation attenuates cancer treatments include glioma cells treated with temozolomide (TMZ) that activated autophagy and induced resistance to TMZ's cytotoxic effects. When Baf A1 was combined with TMZ to inhibit autophagy, the cells underwent apoptotic cell death (127). Cancer cells subjected to ionizing radiation (IR) undergo cell cycle arrest and autophagy

activation. Inhibition of autophagy by Baf A1 or 3-MA with IR treatment rendered the cells more sensitive to IR, resulting in more extensive DNA double-strand breaks than IR treatment alone (206). Human neuroblastoma cells treated with paraquat, an inducer of active oxidative stress, resulted in autophagy activation. When autophagy activation was inhibited with 3-MA, apoptotic mediated cell death was accelerated (207). Cancer cells treated with the DNA-damaging agent, doxorubicin, activate autophagy, attenuating doxorubicin efficacy; inhibition of autophagy by various agents led to increased cancer cell toxicity (208). Breast cancer treatment with tamoxifen, an estrogen antagonist, induces autophagy; inhibition of autophagy enhanced tamoxifen's efficacy (209), (210). Mefloquine toxicity in neuroblastoma cells is enhanced when autophagy is inhibited (211). Inhibition of autophagy impairs the cells' ability to repair DNA damage induced by radiation therapy or anticancer drug camptothecin or etoposide (topoisomerase I and topoisomerase II inhibitors), thus enhancing their cytotoxic potentials (212). Autophagy also confers resistance to dasatinib treatment in B-cell chronic lymphocytic leukemia (213). These are only few examples where autophagy activation interferes with anticancer treatments. Pre-clinical studies have shown phenothiazines enhanced efficacies of cancer drugs (108), (107). Perphenazine could potentially be introduced in combination therapies with the above anticancer treatments to inhibit autophagy and increase efficacy of these cancer treatments.

Presently, in the United States alone, there are more than 30 clinical trials involving combination of chemotherapy with the inhibition of autophagy with chloroquine (CQ) or hydroxychloroquine (HCQ) (199), (214). Chloroquine and

hydroxychloroquine inhibit lysosomal acidification, blocking the degradation step of autophagy. Since our studies suggest perphenazine exert its effects on autophagy in a similar manner as CQ, and may also act to increase pH in lysosomes this provides evidence that perphenazine could have real clinical potential as an inhibitor of autophagy and can be implemented with treatments which have been shown to have increased efficacy when combined with CQ to inhibit autophagy.

Autophagy is a complex mechanism with contradictory roles that are context dependent. Since autophagy has many important physiologic functions in the cells, manipulation of this process can impact normal cells adversely. It is therefore necessary to target key differences between cancer and normal cells to selectively affect tumor cells and limit toxicities to normal cells. Cancer cells have high energy requirements along with low oxidative phosphorylation to sustain their rapid growth. For these cancers, inhibition of autophagy could be a good strategy for cancer treatment. Our findings that cells treated with perphenazine have decreased ATP levels can have several consequences in the cancer cells, all of which leads to cell death. Cells need ATP to survive, and in conditions where there is nutrient deprivation, cancer cells will upregulate autophagy to survive the stress. Since cancer cells have a higher need for energy than normal cells in order to sustain their rapid growth, this may allow selective cancer cells killing with relatively low toxicity to normal cells.

Inhibition of autophagy must be approached with caution as dysregulation of autophagy has consequences in neurodegenerative diseases like Alzheimer's disease, Huntington, and Parkinson's disease due to toxic-intracellular protein

aggregates (215). Therefore, short term treatment or low dose treatment of autophagy inhibitors may be warranted to prevent acute accumulation of proteins which could cause neurodegenerative diseases. In this regard, perphenazine offers the advantage of having had a long history as an antipsychotic where its safety is already established. Our studies showed that autophagy inhibition and cell death occurred within achievable plasma levels, thus further supporting the utility of phenothiazines as an antitumor agent. Since the clinical trials for chloroquine are ongoing and the results are not yet available, it is important to continue to explore other inhibitors of autophagy (62). Together, these findings support previous studies that phenothiazines are viable compounds to pursue in the development of combination therapy for therapeutic strategy against cancers, cells with activating Ras or Raf mutations may be selectively sensitive, providing a potential biomarker.

Future Directions

We have demonstrated that phenothiazine may target lysosomes, disrupt their function which is associated with expansion of lysosomal volume. In our tandemly expressed GFP and RFP LC3 protein study, we determined that GFP persisted in PPZ treated cells which is consistent with increased lysosomal pH which prevented degradation of GFP by lysosomal hydrolases. It will be necessary to confirm the lysosomal pH changes mediated by phenothiazines through pH sensitive lysosomal probes.

Our xenograft studies showed that PPZ mediated autophagy inhibition in a subgroup of tumors which showed increased cleaved PARP levels. Analysis of

immunohistological samples of xenografted tumors could lead to better understanding of differences in response to perphenazine among different tumor groups of our *in vivo* experiment. Information gained would provide knowledge of how to design future experiments for animal studies for perphenazine for the development of therapeutic intervention against cancer.

Our comprehensive timecourse study of perphenazine treatment in 16 human cell lines (15 tumor, and 1 non-tumorigenic cell line) was a huge undertaking. It involved numerous months for the execution of the timecourse study, preparation of the RPPA samples for printing on the micro slides, followed by months of the data processing. We've examined the 48 hr timepoint as the endpoint of our study here to gain insight into which type of cancers were most sensitive to perphenazine, and determined which proteins were most strongly upregulated or downregulated as a consequence of perphenazine treatment. Comprehensive analysis of the data was not possible due to time constraints, and the complexity is beyond the scope of this study. It is included here in APPENDIX 2 to show that beyond perturbing autophagy, perphenazine also impacts other signaling networks. This comprehensive study is complex and requires use of signaling models to map out perturbations of signaling networks. More in depth analysis of the data could offer insights into the early and late signaling events which could be targeted in combination with inhibition of autophagy in order to allow development of more effective therapeutic strategy based on mutational status and cancer types.

APPENDIX 1

Compounds identified in our HTS of autophagy modulators were classified by 3 dimensional steric fingerprinting by Dr. David Maxwell, Department of Experimental Therapeutics, MDACC

CLUSTER 1

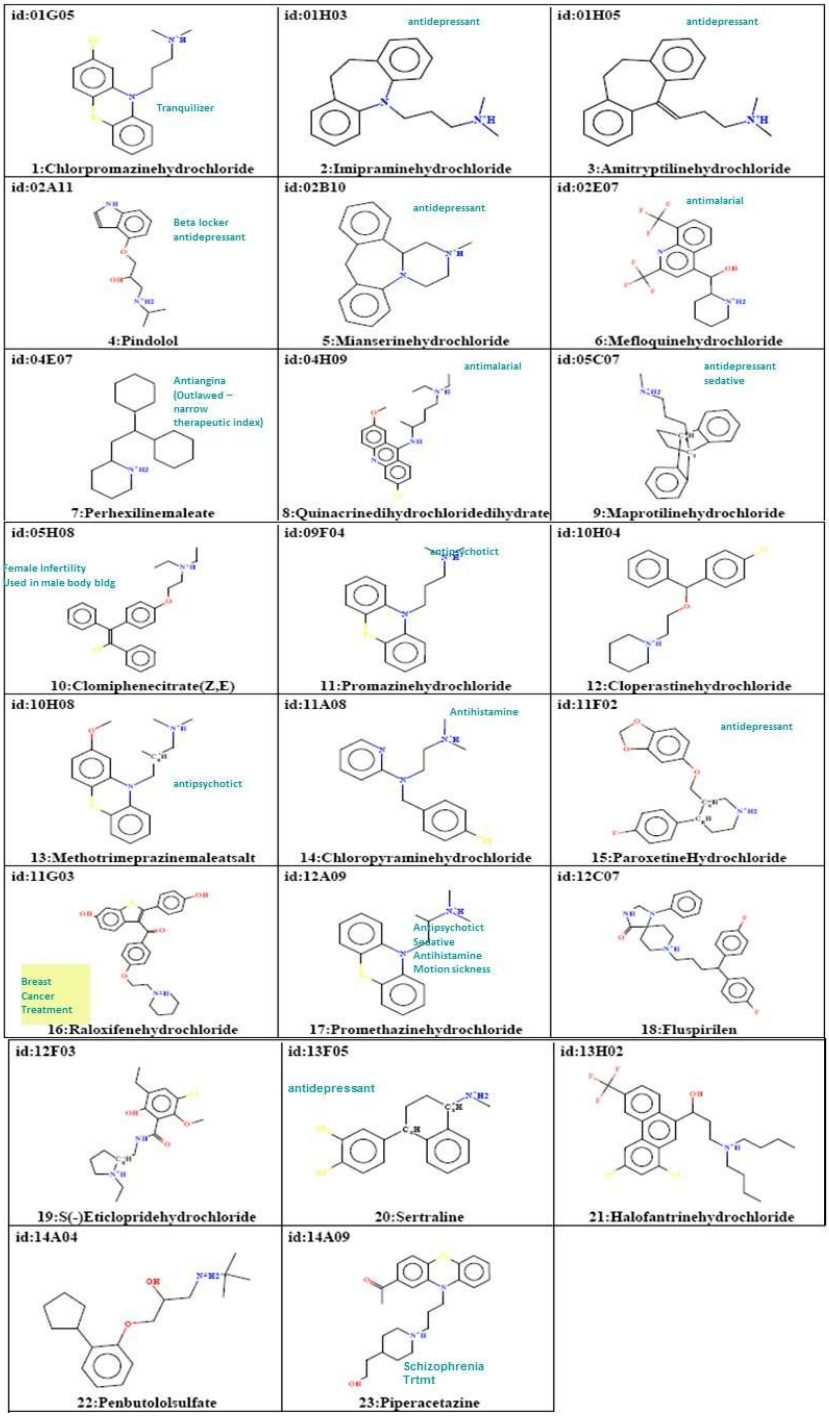

CLUSTER 2

id:01A02 acute leukemia. 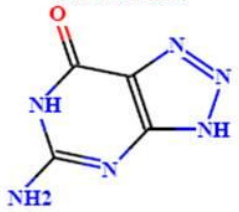 1:Azaguanine-8	id:01D11 antihelminthic  2:Niclosamide	id:03D11 anticancer 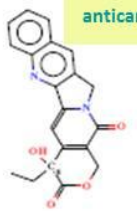 3:Camptothecine(S,+)
id:05C08 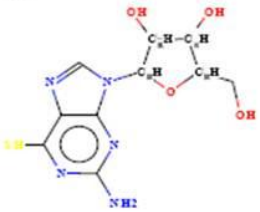 4:Thioguanosine	id:05H07 anticancer 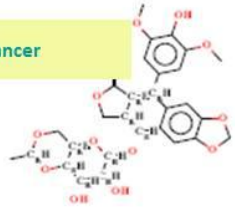 5:Etoposide	id:07G02 antifungal 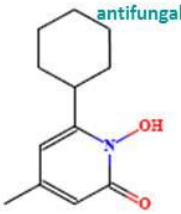 6:Ciclopiroxethanolamine
id:07G07 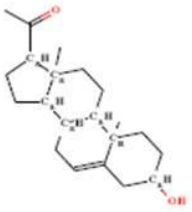 7:Pregnenolone	id:08F05 anticancer 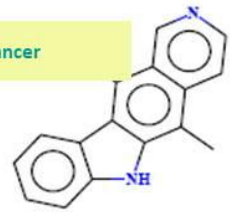 8:Ellipticine	id:10G03 trmt genital warts 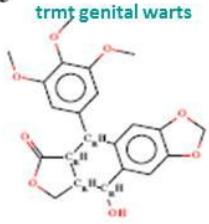 9:Podophyllotoxin
id:12D03  Depigmentation; Destr. melanocytes 10:Monobenzone	id:14A05 New type of cortisol 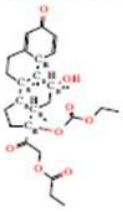 11:Prednicarbate	id:14A06 antifungal 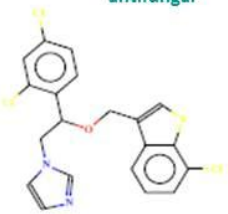 12:Sertaconazolenitrate
id:14B07 Anti-viral/Herpes 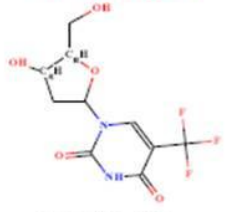 13:Trifluridine		

CLUSTER 3

id:02E06 antipsychotic  1:Perphenazine	id:02G10  antipsychotic 2:Thioproperazinedimesylate	id:05G06 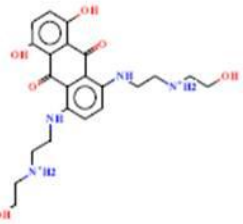 3:Mitoxantronedihydrochloride
id:09E06 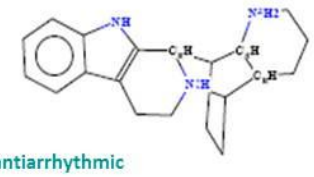 antiarrhythmic 4:Nitrarinedihydrochloride	id:13D09 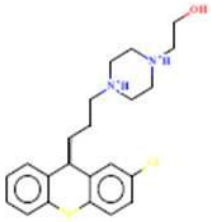 5:Zuclopenthixolhydrochloride	id:14C09 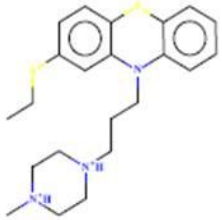 6:Thiethylperazinemalate

CLUSTER 4

id:01F09 anesthetic antipsychotict  1:Oxethazaine	id:02F09 antihistamine 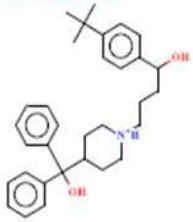 2:Terfenadine	id:12G06 Asthma trtmt 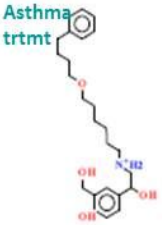 3:Salmeterol
id:13H11 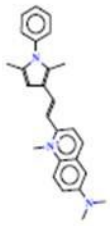 4:Pyrviniumpamoate		

CLUSTER 5

id:08A05	id:08A09	id:11H06
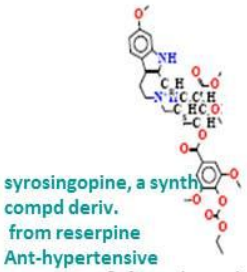 syrosingopine, a synth compd deriv. from reserpine Ant-hypertensive	Anti-hypertensive 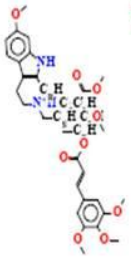	Antipsychotic hypertensive 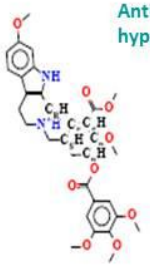
1:Syrosingopine	2:Rescinnamin	3:Reserpine

CLUSTER 6

id:05F04

Chemotherapeutic-leukemias

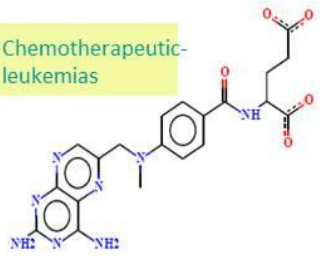

1:Amethopterin(R,S)

CLUSTER 7

id:11A06

Antibiotic

1:Piromidicacid

UNCLUSTERED COMPOUNDS

09B11	Avermectin B1 antiparasitic	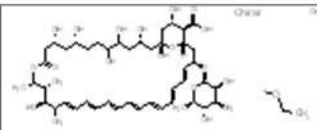
09G09	Benzethonium chloride (Hyamine) anticancer	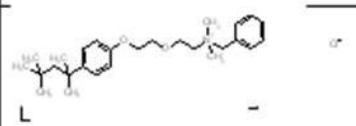
10C06	Spiramycin antiparasitic	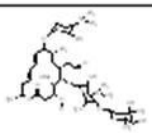
11C09	Lasalocid sodium salt antibiotic	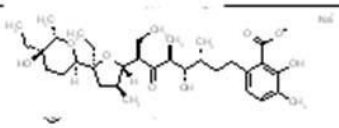
11F10	Fluvastatin sodium salt Cholesterol lowering	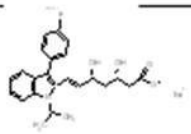
12E06	Thonzonium bromide Aids transdermal drug delivery	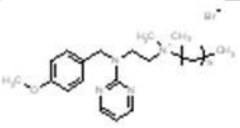

APPENDIX 2

Protein expression profile of cancer cell lines treated with perphenazine normalized to corresponding DMSO treatment at each timepoint (0, 0.5, 1,3,6,12,24 hr). Protein status is represented as: red for upregulated protein expression, and green for downregulated protein expression level.

	Tissue of Origin	Cell Line
1	Breast	BT-549
2	Breast	MCF-7
3	Breast	MCF-10A
4	Breast	MDA-MB-231
5	Breast	MDA-MB-468
6	Breast	SKBR3
7	Breast	T47D
8	Breast	ZR75-1
9	Melanoma	Mel 624
10	Melanoma	MEWO
11	Melanoma	SKMEL-5
12	Melanoma	WM 35
13	Osteosarcoma	U2-OS
14	Ovarian	SKOV-3
15	Ovarian	OVCAR-3
16	Prostate	LNCaP
17	Prostate	PC3

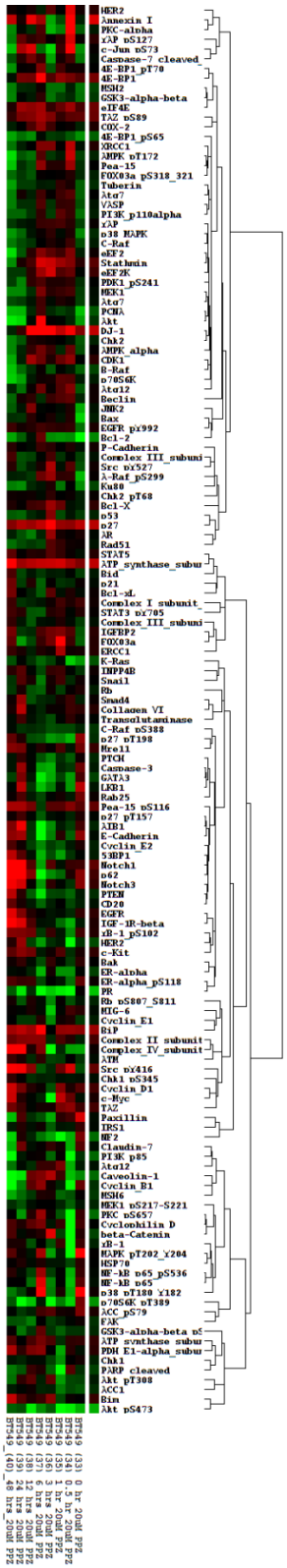

1*
BT549 / Breast

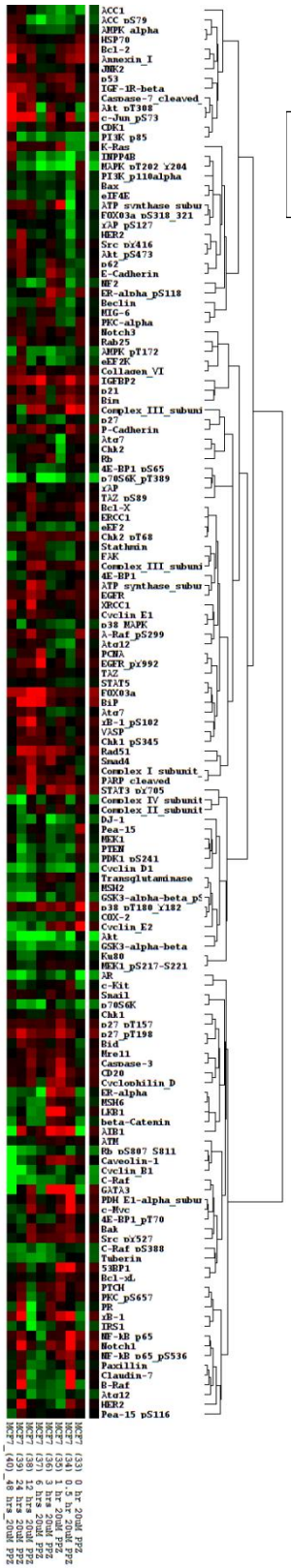

2*
MCF-7 / Breast

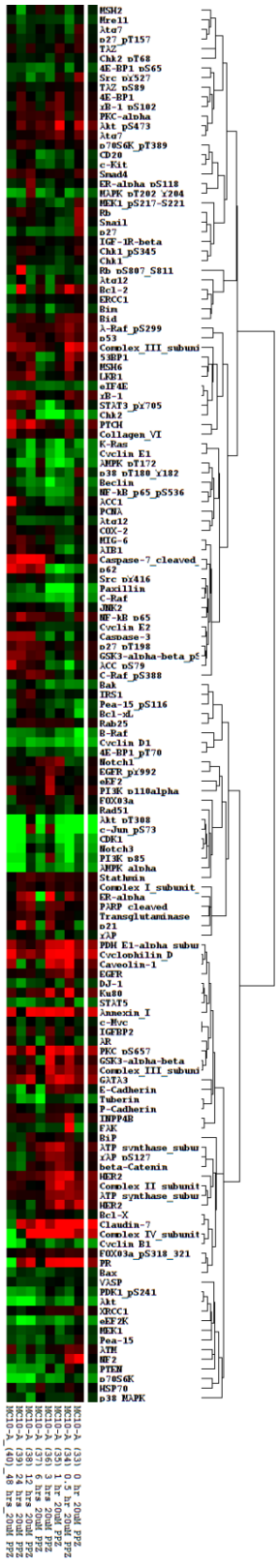

3*
MCF-10A / Breast

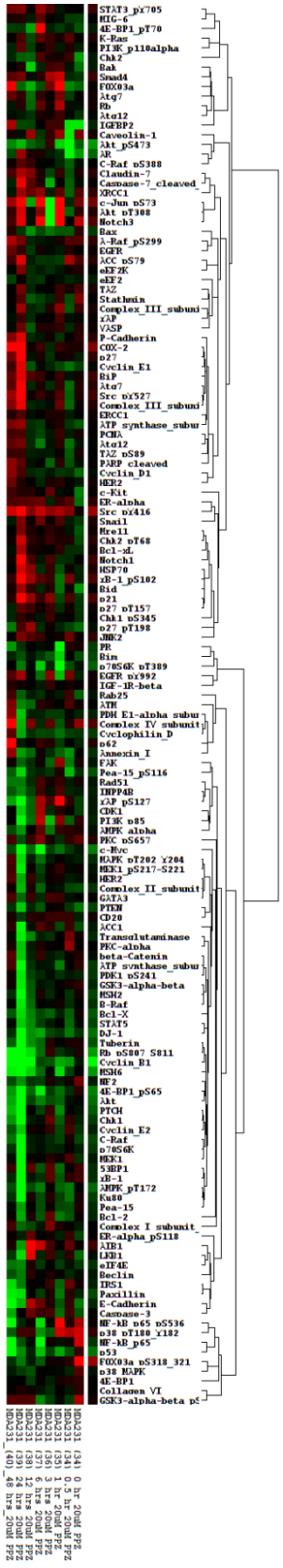

4*
MDA-MB-231 / Breast

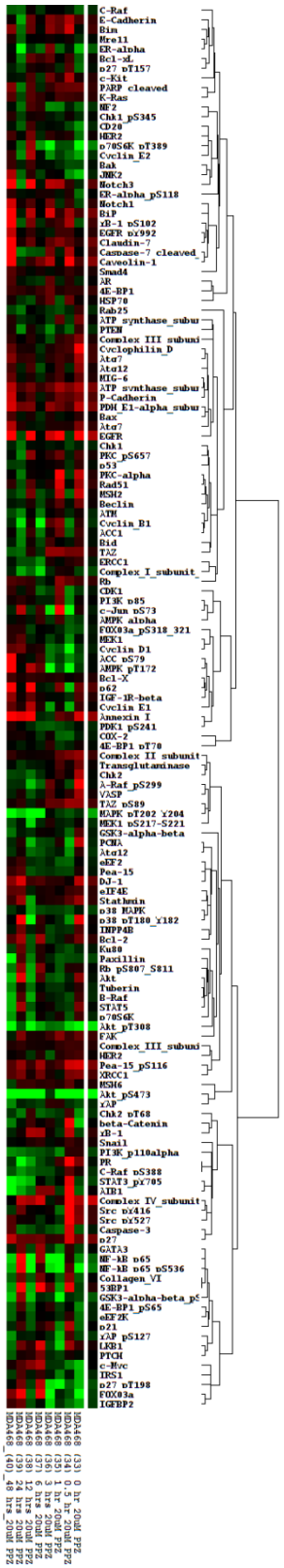

5*
MDA-MB-468 / Breast

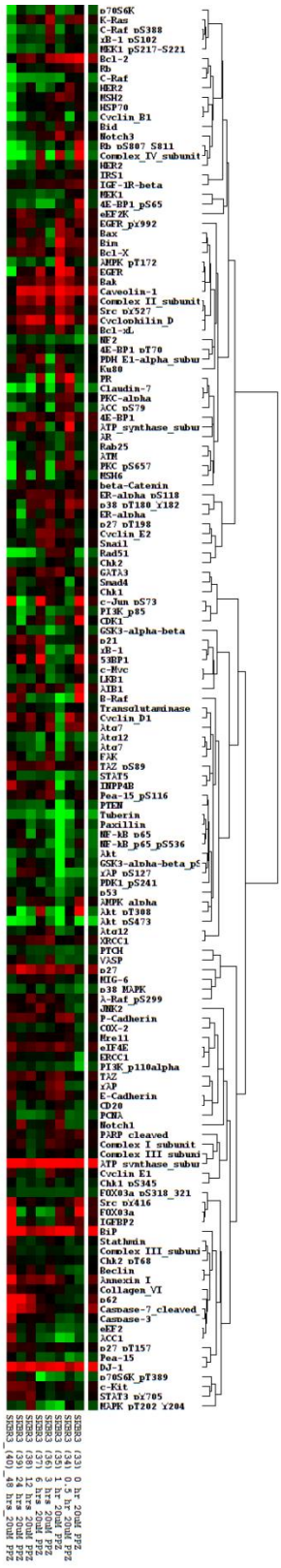

6*
SKBR3 / Breast

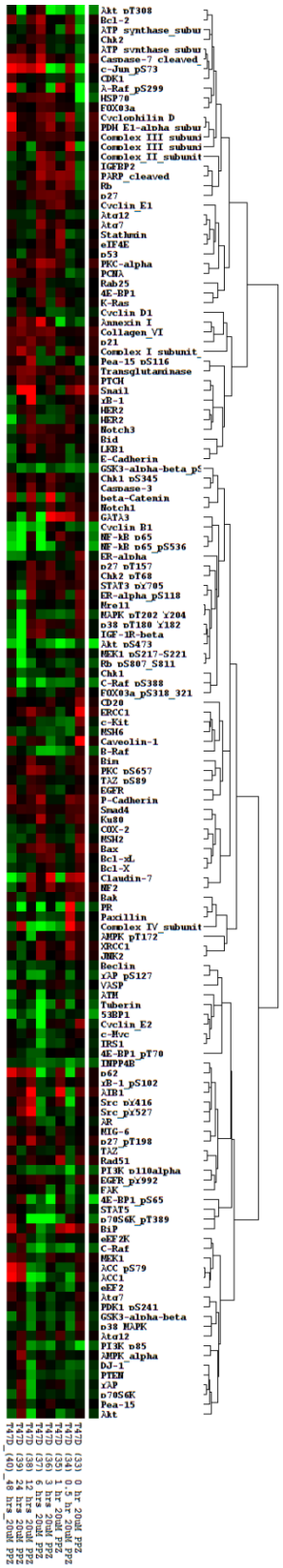

7*
T47D / Breast

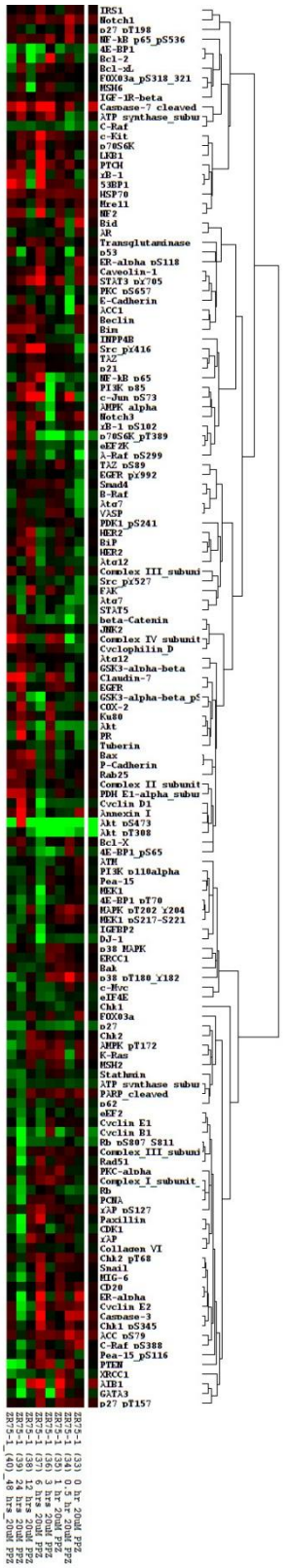

8*
ZR-751 / Breast

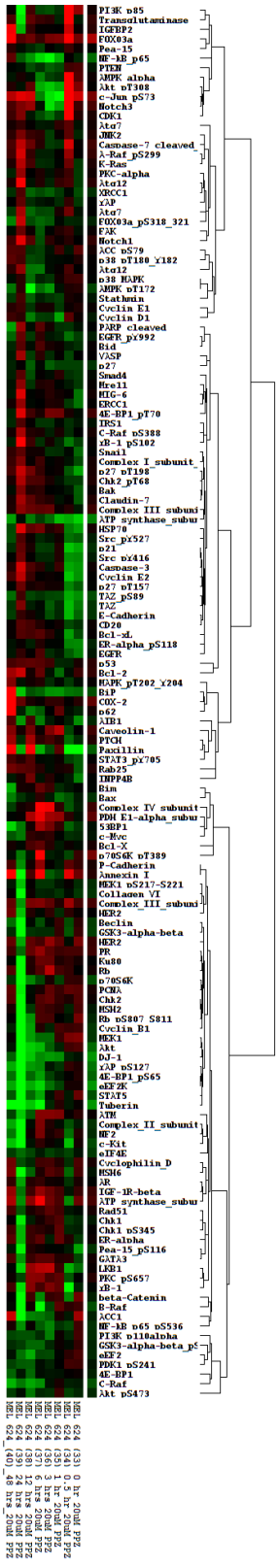

9*
Mel 624 / Melanoma

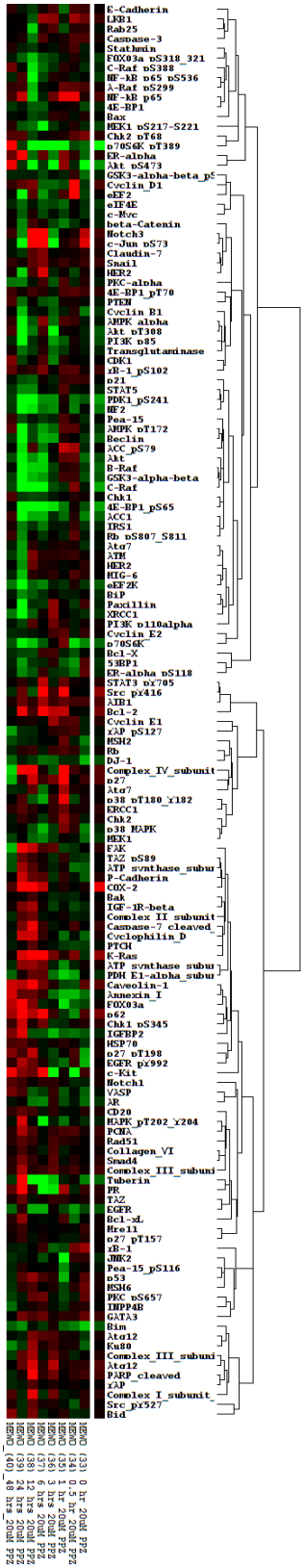

10*
MEWO / Melanoma

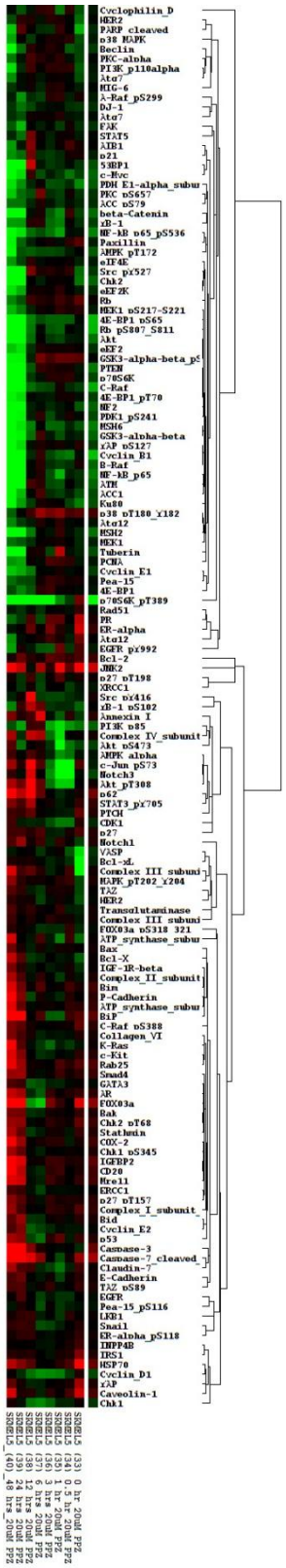

11*
SKMEL5 / Melanoma

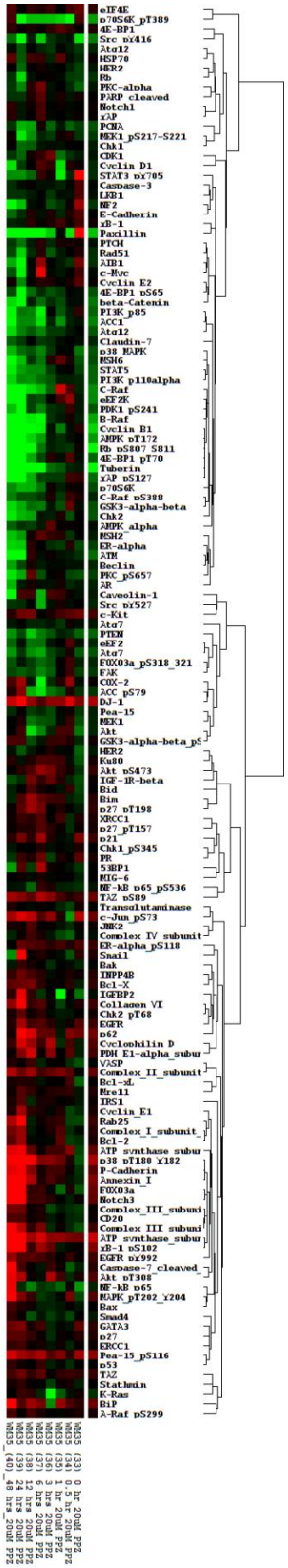

12*
WM35 / Melanoma

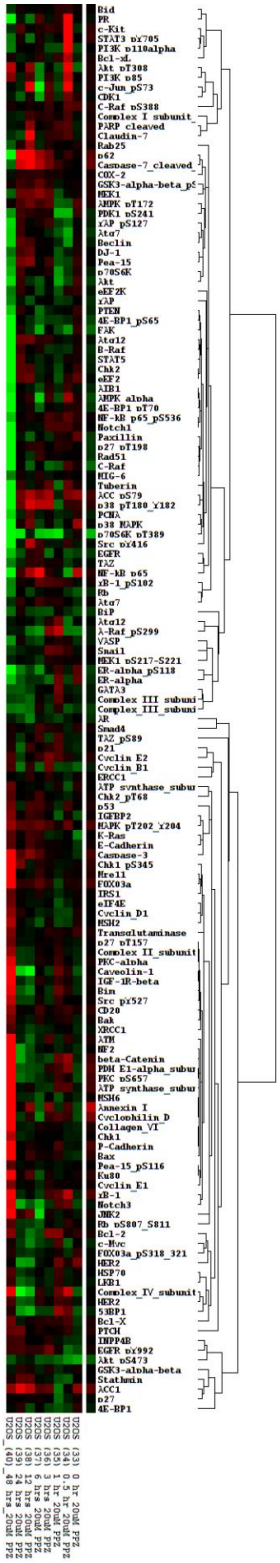
Bid
PR
c-Kit
STAT3 pY705
PI3K p110alpha
Bcl-xL
Akt pT308
PI3K p85
c-Jun_pS73
CDK1
C-Raf pS388
Complex I subunit
PARP cleaved
Claudin-7
Rab25
p62
Caspase-7_cleaved
COX-2
GSK3-alpha-beta_pS
MEK1
AMPK pT172
PDK1 pS241
XAP pS127
Atg7
Beclin
DJ-1
Pea-15
p70S6K
Akt
eEF2K
XAP
PTEN
4E-BP1_pS65
FAK
Atg12
B-Raf
STAT5
Chk2
eEF2
AIB1
AMPK alpha
4E-BP1 pT70
NF-kB p65_pS536
Notch1
Paxillin
p27 pT198
Rad51
C-Raf
HIG-6
Tuberin
ACC pS79
p38 pT180_Y182
PCNA
p38 MAPK
p70S6K pT389
Src pY416
EGFR
TAZ
NF-kB p65
xB-1_pS102
Rb
Atg7
Bid
Atg12
A-Raf_pS299
VASP
Snail
MEK1 pS217-S221
ER-alpha_pS118
ER-alpha
GATA3
Complex III subuni
Complex III subuni
AR
Smad4
TAZ_pS89
p21
Cyclin E2
Cyclin B1
ERCC1
ATP synthase subu
Chk2_pT68
p53
IGFBP2
MAPK pT202_Y204
K-Ras
E-Cadherin
Caspase-3
Chk1 pS345
Mre11
FOXO3a
IRS1
eIF4E
Cyclin D1
MSH2
Transglutaminase
p27 pT157
Complex II subunit
PKC-alpha
Caveolin-1
IGF-1R-beta
Bin
Src pY527
CD20
Bak
XRCC1
ATM
NF2
beta-Catenin
PDH E1-alpha subu
PKC pS657
ATP synthase subu
MSH6
Annexin I
Cyclophilin B
Collagen VI
Chk1
P-Cadherin
Bax
Pea-15_pS116
Rab9
Cyclin E1
xB-1
Notch3
xRCC2
Rb pS807_S811
Bcl-2
c-Myc
FOXO3a_pS318_321
HER2
HSP70
LKB1
Complex IV subunit
HER2
53BP1
Bcl-X
PTCH
IMPP4B
EGFR pY992
Akt pS473
GSK3-alpha-beta
Stathmin
ACC1
p27
4E-BP1
U2OS (33) 0 hr 20nM PP2
U2OS (34) 0.5 hr 20nM PP2
U2OS (35) 1 hr 20nM PP2
U2OS (36) 3 hrs 20nM PP2
U2OS (37) 6 hrs 20nM PP2
U2OS (38) 12 hrs 20nM PP2
U2OS (39) 24 hrs 20nM PP2
U2OS (40) 48 hrs 20nM PP2

13*
U2OS /

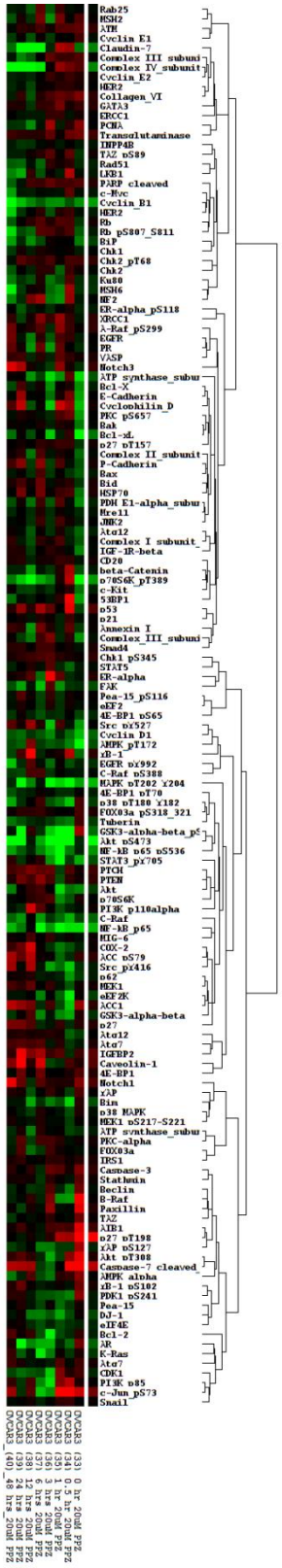

14*
OVCAR3 / Ovarian

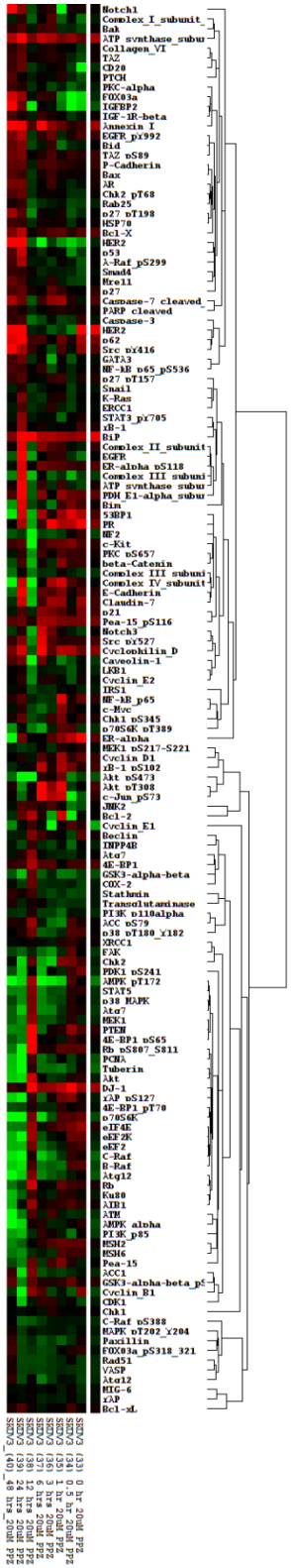

15*
SKOV3 / Ovarian

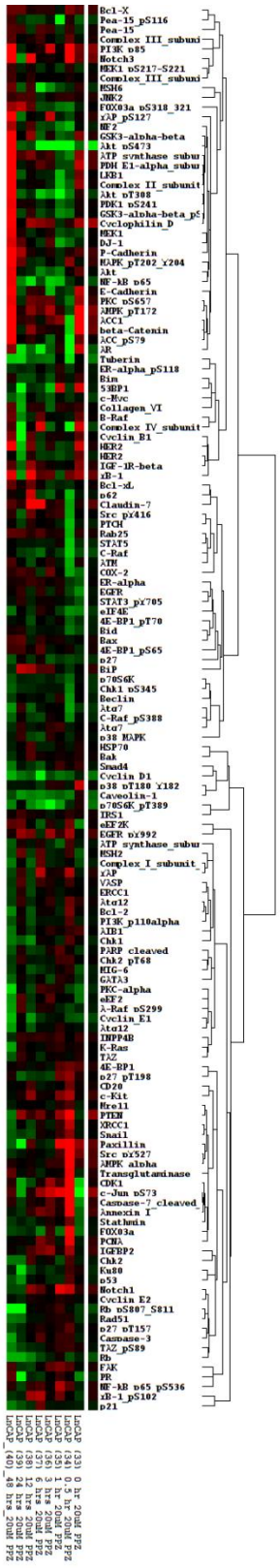

16*
LNCaP / Prostate

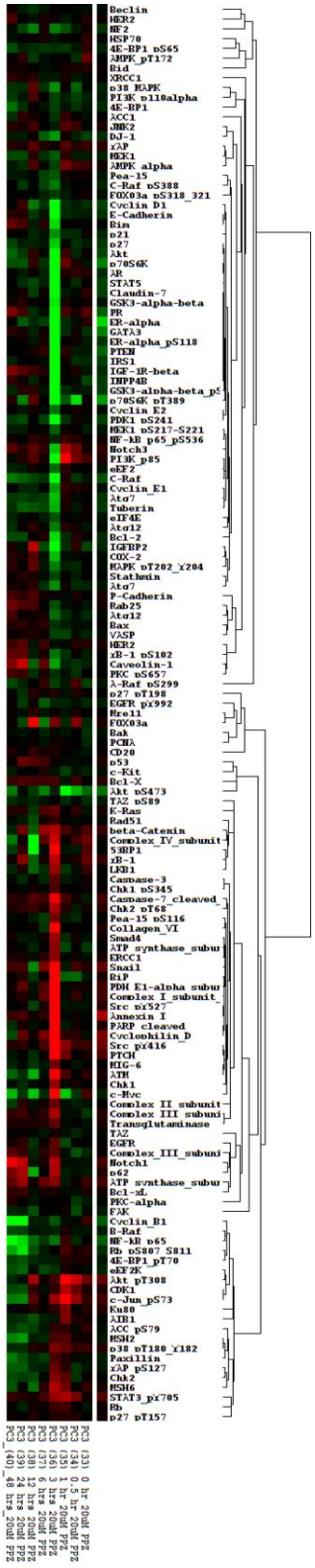

17*
PC3 / Prostate

REFERENCES

1. Holliday, D. L., and V. Speirs. 2011. Choosing the right cell line for breast cancer research. Breast Cancer Res 13:215.
2. Siegel, R., D. Naishadham, and A. Jemal. 2012. Cancer statistics, 2012. CA Cancer J Clin 62:10-29.
3. Coates, J. M., J. M. Galante, and R. J. Bold. 2009. Cancer therapy beyond apoptosis: autophagy and anoikis as mechanisms of cell death. J Surg Res 164:301-308.
4. Claerhout, S., L. Verschooten, S. Van Kelst, R. De Vos, C. Proby, P. Agostinis, and M. Garmyn. 2011. Concomitant inhibition of AKT and autophagy is required for efficient cisplatin-induced apoptosis of metastatic skin carcinoma. Int J Cancer.
5. Ohsumi, Y. 1997. [Autophagy in yeast, bulk protein degradation in the vacuole]. Seikagaku 69:39-44.
6. Mijaljica, D., M. Prescott, and R. J. Devenish. 2011. Microautophagy in mammalian cells: revisiting a 40-year-old conundrum. Autophagy 7:673-682.
7. Klionsky, D. J., and Y. Ohsumi. 1999. Vacuolar import of proteins and organelles from the cytoplasm. Annu Rev Cell Dev Biol 15:1-32.
8. Kerr, J. F., A. H. Wyllie, and A. R. Currie. 1972. Apoptosis: a basic biological phenomenon with wide-ranging implications in tissue kinetics. Br J Cancer 26:239-257.

9. Levine, B., N. Mizushima, and H. W. Virgin. 2011. Autophagy in immunity and inflammation. Nature 469:323-335.

10. Mizushima, N., and D. J. Klionsky. 2007. Protein turnover via autophagy: implications for metabolism. Annu Rev Nutr 27:19-40.

11. Mizushima, N. 2007. Autophagy: process and function. Genes Dev 21:2861-2873.

12. Mathew, R., C. M. Karp, B. Beaudoin, N. Vuong, G. Chen, H. Y. Chen, K. Bray, A. Reddy, G. Bhanot, C. Gelinas, R. S. Dipaola, V. Karantza-Wadsworth, and E. White. 2009. Autophagy suppresses tumorigenesis through elimination of p62. Cell 137:1062-1075.

13. White, E., C. Karp, A. M. Strohecker, Y. Guo, and R. Mathew. 2010. Role of autophagy in suppression of inflammation and cancer. Curr Opin Cell Biol 22:212-217.

14. Mathew, R., S. Kongara, B. Beaudoin, C. M. Karp, K. Bray, K. Degenhardt, G. Chen, S. Jin, and E. White. 2007. Autophagy suppresses tumor progression by limiting chromosomal instability. Genes Dev 21:1367-1381.

15. Mathew, R., V. Karantza-Wadsworth, and E. White. 2007. Role of autophagy in cancer. Nat Rev Cancer 7:961-967.

16. Karantza-Wadsworth, V., S. Patel, O. Kravchuk, G. Chen, R. Mathew, S. Jin, and E. White. 2007. Autophagy mitigates metabolic stress and genome damage in mammary tumorigenesis. Genes Dev 21:1621-1635.

17. Kiffin, R., U. Bandyopadhyay, and A. M. Cuervo. 2006. Oxidative stress and autophagy. Antioxid Redox Signal 8:152-162.

18. Berridge, M. J. 2002. The endoplasmic reticulum: a multifunctional signaling organelle. Cell Calcium 32:235-249.

19. Schroder, M., and R. J. Kaufman. 2005. The mammalian unfolded protein response. Annu Rev Biochem 74:739-789.

20. Fujita, E., Y. Kouroku, A. Isoai, H. Kumagai, A. Misutani, C. Matsuda, Y. K. Hayashi, and T. Momoi. 2007. Two endoplasmic reticulum-associated degradation (ERAD) systems for the novel variant of the mutant dysferlin: ubiquitin/proteasome ERAD(I) and autophagy/lysosome ERAD(II). Hum Mol Genet 16:618-629.

21. Ron, D., and P. Walter. 2007. Signal integration in the endoplasmic reticulum unfolded protein response. Nat Rev Mol Cell Biol 8:519-529.

22. Luo, B., and A. S. Lee. 2012. The critical roles of endoplasmic reticulum chaperones and unfolded protein response in tumorigenesis and anticancer therapies. Oncogene.

23. Schroder, M., and R. J. Kaufman. 2005. ER stress and the unfolded protein response. Mutat Res 569:29-63.

24. Hoyer-Hansen, M., and M. Jaattela. 2007. Connecting endoplasmic reticulum stress to autophagy by unfolded protein response and calcium. Cell Death Differ 14:1576-1582.

25. Fribley, A., K. Zhang, and R. J. Kaufman. 2009. Regulation of apoptosis by the unfolded protein response. Methods Mol Biol 559:191-204.

26. Yorimitsu, T., U. Nair, Z. Yang, and D. J. Klionsky. 2006. Endoplasmic reticulum stress triggers autophagy. J Biol Chem 281:30299-30304.

27. Bernales, S., K. L. McDonald, and P. Walter. 2006. Autophagy counterbalances endoplasmic reticulum expansion during the unfolded protein response. PLoS Biol 4:e423.

28. Ogata, M., S. Hino, A. Saito, K. Morikawa, S. Kondo, S. Kanemoto, T. Murakami, M. Taniguchi, I. Tanii, K. Yoshinaga, S. Shiosaka, J. A. Hammarback, F. Urano, and K. Imaizumi. 2006. Autophagy is activated for cell survival after endoplasmic reticulum stress. Mol Cell Biol 26:9220-9231.

29. Verfaillie, T., M. Salazar, G. Velasco, and P. Agostinis. 2010. Linking ER Stress to Autophagy: Potential Implications for Cancer Therapy. Int J Cell Biol 2010:930509.

30. Claerhout, S., B. Dutta, W. Bossuyt, F. Zhang, C. Nguyen-Charles, J. B. Dennison, Q. Yu, S. Yu, G. Balazsi, Y. Lu, and G. B. Mills. 2012. Abortive autophagy induces endoplasmic reticulum stress and cell death in cancer cells. PLoS One 7:e39400.

31. Criollo, A., J. M. Vicencio, E. Tasdemir, M. C. Maiuri, S. Lavandero, and G. Kroemer. 2007. The inositol trisphosphate receptor in the control of autophagy. Autophagy 3:350-353.

32. Li, X., K. Zhang, and Z. Li. 2011. Unfolded protein response in cancer: the physician's perspective. J Hematol Oncol 4:8.

33. Ding, W. X., H. M. Ni, W. Gao, X. Chen, J. H. Kang, D. B. Stolz, J. Liu, and X. M. Yin. 2009. Oncogenic transformation confers a selective susceptibility to the combined suppression of the proteasome and autophagy. Mol Cancer Ther 8:2036-2045.

34. Mizushima, N., B. Levine, A. M. Cuervo, and D. J. Klionsky. 2008. Autophagy fights disease through cellular self-digestion. Nature 451:1069-1075.

35. Levine, B., and G. Kroemer. 2008. Autophagy in the pathogenesis of disease. Cell 132:27-42.

36. Eskelinen, E. L. 2008. New insights into the mechanisms of macroautophagy in mammalian cells. Int Rev Cell Mol Biol 266:207-247.

37. Alexander, F., A. Mackie, N. Ghatge, and A. W. Waddell. 1958. Some observations on the fate of phenothiazine and oxidation products in rabbits and sheep. Arch Int Pharmacodyn Ther 113:254-260.

38. Klionsky, D. J., J. M. Cregg, W. A. Dunn, Jr., S. D. Emr, Y. Sakai, I. V. Sandoval, A. Sibirny, S. Subramani, M. Thumm, M. Veenhuis, and Y. Ohsumi. 2003. A unified nomenclature for yeast autophagy-related genes. Dev Cell 5:539-545.

39. Scott, S. V., A. Hefner-Gravink, K. A. Morano, T. Noda, Y. Ohsumi, and D. J. Klionsky. 1996. Cytoplasm-to-vacuole targeting and autophagy employ the same machinery to deliver proteins to the yeast vacuole. Proc Natl Acad Sci U S A 93:12304-12308.

40. Thumm, M. 2000. Structure and function of the yeast vacuole and its role in autophagy. Microsc Res Tech 51:563-572.

41. Klionsky, D. J., E. H. Baehrecke, J. H. Brumell, C. T. Chu, P. Codogno, A. M. Cuervo, J. Debnath, V. Deretic, Z. Elazar, E. L. Eskelinen, S. Finkbeiner, J. Fueyo-Margareto, D. Gewirtz, M. Jaattela, G. Kroemer, B. Levine, T. J. Melia, N. Mizushima, D. C. Rubinsztein, A. Simonsen, A. Thorburn, M.

Thumm, and S. A. Tooze. 2011. A comprehensive glossary of autophagy-related molecules and processes (2nd edition). Autophagy 7:1273-1294.

42. Funderburk, S. F., Q. J. Wang, and Z. Yue. 2010. The Beclin 1-VPS34 complex--at the crossroads of autophagy and beyond. Trends Cell Biol 20:355-362.

43. Takahashi, Y., D. Coppola, N. Matsushita, H. D. Cualing, M. Sun, Y. Sato, C. Liang, J. U. Jung, J. Q. Cheng, J. J. Mule, W. J. Pledger, and H. G. Wang. 2007. Bif-1 interacts with Beclin 1 through UVRAG and regulates autophagy and tumorigenesis. Nat Cell Biol 9:1142-1151.

44. Ohsumi, Y., and N. Mizushima. 2004. Two ubiquitin-like conjugation systems essential for autophagy. Semin Cell Dev Biol 15:231-236.

45. Mizushima, N., T. Noda, T. Yoshimori, Y. Tanaka, T. Ishii, M. D. George, D. J. Klionsky, M. Ohsumi, and Y. Ohsumi. 1998. A protein conjugation system essential for autophagy. Nature 395:395-398.

46. Kabeya, Y., N. Mizushima, T. Ueno, A. Yamamoto, T. Kirisako, T. Noda, E. Kominami, Y. Ohsumi, and T. Yoshimori. 2000. LC3, a mammalian homologue of yeast Apg8p, is localized in autophagosome membranes after processing. EMBO J 19:5720-5728.

47. Tanida, I. 2010. Autophagosome formation and molecular mechanism of autophagy. Antioxid Redox Signal 14:2201-2214.

48. Ohsumi, Y. 2001. Molecular dissection of autophagy: two ubiquitin-like systems. Nat Rev Mol Cell Biol 2:211-216.

49. Mann, S. S., and J. A. Hammarback. 1994. Molecular characterization of light chain 3. A microtubule binding subunit of MAP1A and MAP1B. J Biol Chem 269:11492-11497.

50. Tanida, I. 2010. Autophagy basics. Microbiol Immunol 55:1-11.

51. Ichimura, Y., T. Kirisako, T. Takao, Y. Satomi, Y. Shimonishi, N. Ishihara, N. Mizushima, I. Tanida, E. Kominami, M. Ohsumi, T. Noda, and Y. Ohsumi. 2000. A ubiquitin-like system mediates protein lipidation. Nature 408:488-492.

52. Codogno, P., E. Ogier-Denis, and J. J. Houri. 1997. Signal transduction pathways in macroautophagy. Cell Signal 9:125-130.

53. Kirisako, T., Y. Ichimura, H. Okada, Y. Kabeya, N. Mizushima, T. Yoshimori, M. Ohsumi, T. Takao, T. Noda, and Y. Ohsumi. 2000. The reversible modification regulates the membrane-binding state of Apg8/Aut7 essential for autophagy and the cytoplasm to vacuole targeting pathway. J Cell Biol 151:263-276.

54. Pattingre, S., L. Espert, M. Biard-Piechaczyk, and P. Codogno. 2008. Regulation of macroautophagy by mTOR and Beclin 1 complexes. Biochimie 90:313-323.

55. Mizushima, N. 2004. Methods for monitoring autophagy. Int J Biochem Cell Biol 36:2491-2502.

56. Kuma, A., M. Matsui, and N. Mizushima. 2007. LC3, an autophagosome marker, can be incorporated into protein aggregates independent of

autophagy: caution in the interpretation of LC3 localization. Autophagy 3:323-328.

57. Komatsu, M., and Y. Ichimura. 2010. Selective autophagy regulates various cellular functions. Genes Cells 15:923-933.

58. Pankiv, S., T. H. Clausen, T. Lamark, A. Brech, J. A. Bruun, H. Outzen, A. Overvatn, G. Bjorkoy, and T. Johansen. 2007. p62/SQSTM1 binds directly to Atg8/LC3 to facilitate degradation of ubiquitinated protein aggregates by autophagy. J Biol Chem 282:24131-24145.

59. Ichimura, Y., E. Kominami, K. Tanaka, and M. Komatsu. 2008. Selective turnover of p62/A170/SQSTM1 by autophagy. Autophagy 4:1063-1066.

60. Bjorkoy, G., T. Lamark, S. Pankiv, A. Overvatn, A. Brech, and T. Johansen. 2009. Monitoring autophagic degradation of p62/SQSTM1. Methods Enzymol 452:181-197.

61. Kimura, S., T. Noda, and T. Yoshimori. 2007. Dissection of the autophagosome maturation process by a novel reporter protein, tandem fluorescent-tagged LC3. Autophagy 3:452-460.

62. Kimmelman, A. C. 2011. The dynamic nature of autophagy in cancer. Genes Dev 25:1999-2010.

63. Mancias, J. D., and A. C. Kimmelman. 2011. Targeting autophagy addiction in cancer. Oncotarget 2:1302-1306.

64. Liang, X. H., S. Jackson, M. Seaman, K. Brown, B. Kempkes, H. Hibshoosh, and B. Levine. 1999. Induction of autophagy and inhibition of tumorigenesis by beclin 1. Nature 402:672-676.

65. Aita, V. M., X. H. Liang, V. V. Murty, D. L. Pincus, W. Yu, E. Cayanis, S. Kalachikov, T. C. Gilliam, and B. Levine. 1999. Cloning and genomic organization of beclin 1, a candidate tumor suppressor gene on chromosome 17q21. Genomics 59:59-65.

66. Miracco, C., E. Cosci, G. Oliveri, P. Luzi, L. Pacenti, I. Monciatti, S. Mannucci, M. C. De Nisi, M. Toscano, V. Malagnino, S. M. Falzarano, L. Pirtoli, and P. Tosi. 2007. Protein and mRNA expression of autophagy gene Beclin 1 in human brain tumours. Int J Oncol 30:429-436.

67. Furuya, N., J. Yu, M. Byfield, S. Pattingre, and B. Levine. 2005. The evolutionarily conserved domain of Beclin 1 is required for Vps34 binding, autophagy and tumor suppressor function. Autophagy 1:46-52.

68. Takamura, A., M. Komatsu, T. Hara, A. Sakamoto, C. Kishi, S. Waguri, Y. Eishi, O. Hino, K. Tanaka, and N. Mizushima. 2011. Autophagy-deficient mice develop multiple liver tumors. Genes Dev 25:795-800.

69. Marino, G., N. Salvador-Montoliu, A. Fueyo, E. Knecht, N. Mizushima, and C. Lopez-Otin. 2007. Tissue-specific autophagy alterations and increased tumorigenesis in mice deficient in Atg4C/autophagin-3. J Biol Chem 282:18573-18583.

70. Inami, Y., S. Waguri, A. Sakamoto, T. Kouno, K. Nakada, O. Hino, S. Watanabe, J. Ando, M. Iwadate, M. Yamamoto, M. S. Lee, K. Tanaka, and M. Komatsu. 2011. Persistent activation of Nrf2 through p62 in hepatocellular carcinoma cells. J Cell Biol 193:275-284.

71. Kung, C. P., A. Budina, G. Balaburski, M. K. Bergenstock, and M. Murphy. 2011. Autophagy in tumor suppression and cancer therapy. Crit Rev Eukaryot Gene Expr 21:71-100.

72. White, E. 2012Deconvoluting the context-dependent role for autophagy in cancer. Nat Rev Cancer.

73. Yao, F., G. Wang, W. Wei, Y. Tu, H. Tong, and S. Sun. 2011. An autophagy inhibitor enhances the inhibition of cell proliferation induced by a proteasome inhibitor in MCF-7 cells. Mol Med Report 5:84-88.

74. Abedin, M. J., D. Wang, M. A. McDonnell, U. Lehmann, and A. Kelekar. 2007. Autophagy delays apoptotic death in breast cancer cells following DNA damage. Cell Death Differ 14:500-510.

75. Tong, Y., Y. Y. Liu, L. S. You, and W. B. Qian. 2012. Perifosine induces protective autophagy and upregulation of ATG5 in human chronic myelogenous leukemia cells in vitro. Acta Pharmacol Sin 33:542-550.

76. Rossi, M., E. R. Munarriz, S. Bartesaghi, M. Milanese, D. Dinsdale, M. A. Guerra-Martin, E. T. Bampton, P. Glynn, G. Bonanno, R. A. Knight, P. Nicotera, and G. Melino. 2009. Desmethylclomipramine induces the accumulation of autophagy markers by blocking autophagic flux. J Cell Sci 122:3330-3339.

77. Guo, J. Y., H. Y. Chen, R. Mathew, J. Fan, A. M. Strohecker, G. Karsli-Uzunbas, J. J. Kamphorst, G. Chen, J. M. Lemons, V. Karantza, H. A. Coller, R. S. Dipaola, C. Gelinas, J. D. Rabinowitz, and E. White. 2011. Activated

Ras requires autophagy to maintain oxidative metabolism and tumorigenesis. Genes Dev 25:460-470.

78. Kim, M. J., S. J. Woo, C. H. Yoon, J. S. Lee, S. An, Y. H. Choi, S. G. Hwang, G. Yoon, and S. J. Lee. 2011. Involvement of autophagy in oncogenic K-Ras-induced malignant cell transformation. J Biol Chem 286:12924-12932.

79. Yang, S., X. Wang, G. Contino, M. Liesa, E. Sahin, H. Ying, A. Bause, Y. Li, J. M. Stommel, G. Dell'antonio, J. Mautner, G. Tonon, M. Haigis, O. S. Shirihai, C. Doglioni, N. Bardeesy, and A. C. Kimmelman. 2011. Pancreatic cancers require autophagy for tumor growth. Genes Dev 25:717-729.

80. Lock, R., S. Roy, C. M. Kenific, J. S. Su, E. Salas, S. M. Ronen, and J. Debnath. 2010. Autophagy facilitates glycolysis during Ras-mediated oncogenic transformation. Mol Biol Cell 22:165-178.

81. Zhang, H., P. Gao, R. Fukuda, G. Kumar, B. Krishnamachary, K. I. Zeller, C. V. Dang, and G. L. Semenza. 2007. HIF-1 inhibits mitochondrial biogenesis and cellular respiration in VHL-deficient renal cell carcinoma by repression of C-MYC activity. Cancer Cell 11:407-420.

82. Weinberg, F., R. Hamanaka, W. W. Wheaton, S. Weinberg, J. Joseph, M. Lopez, B. Kalyanaraman, G. M. Mutlu, G. R. Budinger, and N. S. Chandel. 2010. Mitochondrial metabolism and ROS generation are essential for Kras-mediated tumorigenicity. Proc Natl Acad Sci U S A 107:8788-8793.

83. Weinstein, J. N., and J. K. Buolamwini. 2000. Molecular targets in cancer drug discovery: cell-based profiling. Curr Pharm Des 6:473-483.

84. Ohlow, M. J., and B. Moosmann. 2011. Phenothiazine: the seven lives of pharmacology's first lead structure. Drug Discov Today 16:119-131.

85. Horn, A. S., and S. H. Snyder. 1971. Chlorpromazine and dopamine: conformational similarities that correlate with the antischizophrenic activity of phenothiazine drugs. Proc Natl Acad Sci U S A 68:2325-2328.

86. Feinberg, A. P., and S. H. Snyder. 1975. Phenothiazine drugs: structure-activity relationships explained by a conformation that mimics dopamine. Proc Natl Acad Sci U S A 72:1899-1903.

87. Seeman, P., and T. Lee. 1975. Antipsychotic drugs: direct correlation between clinical potency and presynaptic action on dopamine neurons. Science 188:1217-1219.

88. Julien, R. M. 2001. A primer of drug action : a concise, nontechnical guide to the actions, uses, and side effects of psychoactive drugs. W.H. Freeman and Co., New York.

89. Jaszczyszyn, A., K. Gasiorowski, P. Swiatek, W. Malinka, K. Cieslik-Boczula, J. Petrus, and B. Czarnik-Matusewicz. 2012. Chemical structure of phenothiazines and their biological activity. Pharmacol Rep 64:16-23.

90. Mitchell, S. C. 2006. Phenothiazine: the parent molecule. Curr Drug Targets 7:1181-1189.

91. Motohashi, N., S. R. Gollapudi, J. Emrani, and K. R. Bhattiprolu. 1991. Antitumor properties of phenothiazines. Cancer Invest 9:305-319.

92. Morak-Mlodawska, B., M. Jelen, and K. Pluta. 2009. [New derivatives of phenothiazines with anticancer activities]. Pol Merkur Lekarski 26:671-675.

93. Sudeshna, G., and K. Parimal. 2010. Multiple non-psychiatric effects of phenothiazines: a review. Eur J Pharmacol 648:6-14.

94. Missale, C., S. R. Nash, S. W. Robinson, M. Jaber, and M. G. Caron. 1998. Dopamine receptors: from structure to function. Physiol Rev 78:189-225.

95. Pivonello, R., D. Ferone, G. Lombardi, A. Colao, S. W. Lamberts, and L. J. Hofland. 2007. Novel insights in dopamine receptor physiology. Eur J Endocrinol 156 Suppl 1:S13-21.

96. Scemama, J. L., C. Ruellan, P. Clerc, F. Clemente, and A. Ribet. 1984. Dopamine receptors in a human colonic cancer cell line (HT29). Some receptor-related biological effects of dopamine. Int J Cancer 34:675-679.

97. Arvigo, M., F. Gatto, M. Ruscica, P. Ameri, E. Dozio, M. Albertelli, M. D. Culler, M. Motta, F. Minuto, P. Magni, and D. Ferone. 2010. Somatostatin and dopamine receptor interaction in prostate and lung cancer cell lines. J Endocrinol 207:309-317.

98. Sokoloff, P., J. F. Riou, M. P. Martres, and J. C. Schwartz. 1989. Presence of dopamine D-2 receptors in human tumoral cell lines. Biochem Biophys Res Commun 162:575-582.

99. Morgan, R. J., Jr., T. Synold, B. I. Carr, J. H. Doroshow, E. P. Womack, S. Shibata, G. Somlo, J. Raschko, L. Leong, M. McNamara, W. Chow, M. Tetef, K. Margolin, S. Akman, and J. Longmate. 2001. Continuous infusion prochlorperazine: pharmacokinetics, antiemetic efficacy, and feasibility of high-dose therapy. Cancer Chemother Pharmacol 47:327-332.

100. Skinner, J., and A. Skinner. 1999. Levomepromazine for nausea and vomiting in advanced cancer. Hosp Med 60:568-570.

101. Fortner, C. L., R. S. Finley, and W. R. Grove. 1985. Combination antiemetic therapy in the control of chemotherapy-induced emesis. Drug Intell Clin Pharm 19:21-24.

102. Ikediobi, O. N., M. Reimers, S. Durinck, P. E. Blower, A. P. Futreal, M. R. Stratton, and J. N. Weinstein. 2008. In vitro differential sensitivity of melanomas to phenothiazines is based on the presence of codon 600 BRAF mutation. Mol Cancer Ther 7:1337-1346.

103. Nordenberg, J., E. Fenig, M. Landau, R. Weizman, and A. Weizman. 1999. Effects of psychotropic drugs on cell proliferation and differentiation. Biochem Pharmacol 58:1229-1236.

104. Argyriou, A. A., A. Antonacopoulou, G. Iconomou, and H. P. Kalofonos. 2009. Treatment options for malignant gliomas, emphasizing towards new molecularly targeted therapies. Crit Rev Oncol Hematol 69:199-210.

105. Lialiaris, T. S., F. Papachristou, C. Mourelatos, and M. Simopoulou. 2009. Antineoplastic and cytogenetic effects of chlorpromazine on human lymphocytes in vitro and on Ehrlich ascites tumor cells in vivo. Anticancer Drugs 20:746-751.

106. Lee, M. S., L. Johansen, Y. Zhang, A. Wilson, M. Keegan, W. Avery, P. Elliott, A. A. Borisy, and C. T. Keith. 2007. The novel combination of chlorpromazine and pentamidine exerts synergistic antiproliferative effects through dual mitotic action. Cancer Res 67:11359-11367.

107. Kuzma-Richeret, A., J. Saczko, A. Choromanska, M. Dumanska, M. Drag-Zalesinska, T. Wysocka, A. Chwilkowska, A. Pola, D. Mosiadz, A. Marcinkowska, and J. Kulbacka. 2011. The influence of phenothiazine derivatives on Doxorubicin treatment in sensitive and resistant human breast adenocarcinoma cells. Folia Biol (Praha) 57:261-267.

108. Yde, C. W., M. P. Clausen, M. V. Bennetzen, A. E. Lykkesfeldt, O. G. Mouritsen, and B. Guerra. 2009. The antipsychotic drug chlorpromazine enhances the cytotoxic effect of tamoxifen in tamoxifen-sensitive and tamoxifen-resistant human breast cancer cells. Anticancer Drugs 20:723-735.

109. Hait, W. N., and D. T. Aftab. 1992. Rational design and pre-clinical pharmacology of drugs for reversing multidrug resistance. Biochem Pharmacol 43:103-107.

110. Keohavong, P., D. Zhu, T. L. Whiteside, P. Swalsky, A. Bakker, E. M. Elder, J. M. Siegfried, S. Srivastava, and S. D. Finkelstein. 1997. Detection of infrequent and multiple K-ras mutations in human tumors and tumor-adjacent tissues. Anal Biochem 247:394-403.

111. Kast, R. E., and E. L. Altschuler. 2007. Consideration of use of phenothiazines in particular trifluorperazine for epidermal growth factor receptor associated cancers. Med Hypotheses 69:1074-1075.

112. DiPaola, M., C. H. Keith, D. Feldman, B. Tycko, and F. R. Maxfield. 1984. Loss of alpha 2-macroglobulin and epidermal growth factor surface binding

induced by phenothiazines and naphthalene sulfonamides. J Cell Physiol 118:193-202.

113. Ross, A. H., C. Damsky, P. D. Phillips, F. Hwang, and P. Vance. 1985. Inhibition of epidermal growth factor-induced phosphorylation by trifluoperazine. J Cell Physiol 124:499-506.

114. Motohashi, N. 1991. Phenothiazines and calmodulin (review). Anticancer Res 11:1125-1164.

115. Hait, W. N., L. Grais, C. Benz, and E. C. Cadman. 1985. Inhibition of growth of leukemic cells by inhibitors of calmodulin: phenothiazines and melittin. Cancer Chemother Pharmacol 14:202-205.

116. Benaim, G., and A. Villalobo. 2002. Phosphorylation of calmodulin. Functional implications. Eur J Biochem 269:3619-3631.

117. Shenoy, M. A., J. E. Biaglow, M. E. Varnes, and J. W. Daniel. 1982. A biochemical basis for the radiosensitizing and cytotoxic effects of chlorpromazine hydrochloride in vitro and in vivo. Int J Radiat Oncol Biol Phys 8:725-728.

118. Shenoy, M. A., and B. B. Singh. 1980. Cytotoxic & radiosensitizing effects of chlorpromazine hydrochloride in sarcoma 180A. Indian J Exp Biol 18:791-795.

119. Zhang, L., J. Yu, H. Pan, P. Hu, Y. Hao, W. Cai, H. Zhu, A. D. Yu, X. Xie, D. Ma, and J. Yuan. 2007. Small molecule regulators of autophagy identified by an image-based high-throughput screen. Proc Natl Acad Sci U S A 104:19023-19028.

120. Hundeshagen, P., A. Hamacher-Brady, R. Eils, and N. R. Brady. 2011. Concurrent detection of autolysosome formation and lysosomal degradation by flow cytometry in a high-content screen for inducers of autophagy. BMC Biol 9:38.

121. Tibes, R., Y. Qiu, Y. Lu, B. Hennessy, M. Andreeff, G. B. Mills, and S. M. Kornblau. 2006. Reverse phase protein array: validation of a novel proteomic technology and utility for analysis of primary leukemia specimens and hematopoietic stem cells. Mol Cancer Ther 5:2512-2521.

122. Liang, J., S. H. Shao, Z. X. Xu, B. Hennessy, Z. Ding, M. Larrea, S. Kondo, D. J. Dumont, J. U. Gutterman, C. L. Walker, J. M. Slingerland, and G. B. Mills. 2007. The energy sensing LKB1-AMPK pathway regulates p27(kip1) phosphorylation mediating the decision to enter autophagy or apoptosis. Nat Cell Biol 9:218-224.

123. Wasko, B. M., A. Dudakovic, and R. J. Hohl. Bisphosphonates induce autophagy by depleting geranylgeranyl diphosphate. J Pharmacol Exp Ther 337:540-546.

124. Tasdemir, E., L. Galluzzi, M. C. Maiuri, A. Criollo, I. Vitale, E. Hangen, N. Modjtahedi, and G. Kroemer. 2008. Methods for assessing autophagy and autophagic cell death. Methods Mol Biol 445:29-76.

125. Ertmer, A., V. Huber, S. Gilch, T. Yoshimori, V. Erfle, J. Duyster, H. P. Elsasser, and H. M. Schatzl. 2007. The anticancer drug imatinib induces cellular autophagy. Leukemia 21:936-942.

126. Ben Sahra, I., J. F. Tanti, and F. Bost. 2010. The combination of metformin and 2 deoxyglucose inhibits autophagy and induces AMPK-dependent apoptosis in prostate cancer cells. Autophagy 6.

127. Kanzawa, T., I. M. Germano, T. Komata, H. Ito, Y. Kondo, and S. Kondo. 2004. Role of autophagy in temozolomide-induced cytotoxicity for malignant glioma cells. Cell Death Differ 11:448-457.

128. Cutler, N. S., J. Heitman, and M. E. Cardenas. 1999. TOR kinase homologs function in a signal transduction pathway that is conserved from yeast to mammals. Mol Cell Endocrinol 155:135-142.

129. Nadanaciva, S., S. Lu, D. F. Gebhard, B. A. Jessen, W. D. Pennie, and Y. Will. 2010. A high content screening assay for identifying lysosomotropic compounds. Toxicol In Vitro 25:715-723.

130. Zhelev, Z., H. Ohba, R. Bakalova, V. Hadjimitova, M. Ishikawa, Y. Shinohara, and Y. Baba. 2004. Phenothiazines suppress proliferation and induce apoptosis in cultured leukemic cells without any influence on the viability of normal lymphocytes. Phenothiazines and leukemia. Cancer Chemother Pharmacol 53:267-275.

131. Jones, G. R. 1985. Cancer therapy: phenothiazines in an unexpected role. Tumori 71:563-569.

132. Dalton, S. O., L. Mellemkjaer, L. Thomassen, P. B. Mortensen, and C. Johansen. 2005. Risk for cancer in a cohort of patients hospitalized for schizophrenia in Denmark, 1969-1993. Schizophr Res 75:315-324.

133. Levin, R. M., and B. Weiss. 1977. Binding of trifluoperazine to the calcium-dependent activator of cyclic nucleotide phosphodiesterase. Mol Pharmacol 13:690-697.

134. Bianchi, N. O., M. S. Bianchi, and S. M. Richard. 2001. Mitochondrial genome instability in human cancers. Mutat Res 488:9-23.

135. Gil-Ad, I., B. Shtaif, Y. Levkovitz, J. Nordenberg, M. Taler, I. Korov, and A. Weizman. 2006. Phenothiazines induce apoptosis in a B16 mouse melanoma cell line and attenuate in vivo melanoma tumor growth. Oncol Rep 15:107-112.

136. Choi, J. H., Y. R. Yang, S. K. Lee, S. H. Kim, Y. H. Kim, J. Y. Cha, S. W. Oh, J. R. Ha, S. H. Ryu, and P. G. Suh. 2008. Potential inhibition of PDK1/Akt signaling by phenothiazines suppresses cancer cell proliferation and survival. Ann N Y Acad Sci 1138:393-403.

137. Motohashi, N., M. Kawase, S. Saito, and H. Sakagami. 2000. Antitumor potential and possible targets of phenothiazine-related compounds. Curr Drug Targets 1:237-245.

138. Kapur, S., S. C. Barsoum, and P. Seeman. 2000. Dopamine D(2) receptor blockade by haloperidol. (3)H-raclopride reveals much higher occupancy than EEDQ. Neuropsychopharmacology 23:595-598.

139. Fox, C. A., A. Mansour, and S. J. Watson, Jr. 1994. The effects of haloperidol on dopamine receptor gene expression. Exp Neurol 130:288-303.

140. Rupinder, S. K., A. K. Gurpreet, and S. Manjeet. 2007. Cell suicide and caspases. Vascul Pharmacol 46:383-393.

141. De Duve, C., and R. Wattiaux. 1966. Functions of lysosomes. Annu Rev Physiol 28:435-492.

142. Eskelinen, E. L., F. Reggiori, M. Baba, A. L. Kovacs, and P. O. Seglen. 2011. Seeing is believing: the impact of electron microscopy on autophagy research. Autophagy 7:935-956.

143. Swanlund, J. M., K. C. Kregel, and T. D. Oberley. 2010. Investigating autophagy: quantitative morphometric analysis using electron microscopy. Autophagy 6:270-277.

144. Dent, R., M. Trudeau, K. I. Pritchard, W. M. Hanna, H. K. Kahn, C. A. Sawka, L. A. Lickley, E. Rawlinson, P. Sun, and S. A. Narod. 2007. Triple-negative breast cancer: clinical features and patterns of recurrence. Clin Cancer Res 13:4429-4434.

145. Sachlos, E., R. M. Risueno, S. Laronde, Z. Shapovalova, J. H. Lee, J. Russell, M. Malig, J. D. McNicol, A. Fiebig-Comyn, M. Graham, M. Levadoux-Martin, J. B. Lee, A. O. Giacomelli, J. A. Hassell, D. Fischer-Russell, M. R. Trus, R. Foley, B. Leber, A. Xenocostas, E. D. Brown, T. J. Collins, and M. Bhatia. 2012. Identification of Drugs Including a Dopamine Receptor Antagonist that Selectively Target Cancer Stem Cells. Cell 149:1284-1297.

146. Ruben, L., and H. Rasmussen. 1981. Phenothiazines and related compounds disrupt mitochondrial energy production by a calmodulin-independent reaction. Biochim Biophys Acta 637:415-422.

147. Martin, D. S., and G. K. Schwartz. 1997. Chemotherapeutically induced DNA damage, ATP depletion, and the apoptotic biochemical cascade. Oncol Res 9:1-5.

148. Albini, A., and R. Benelli. 2007. The chemoinvasion assay: a method to assess tumor and endothelial cell invasion and its modulation. Nat Protoc 2:504-511.

149. Kleinman, H. K., and G. R. Martin. 2005. Matrigel: basement membrane matrix with biological activity. Semin Cancer Biol 15:378-386.

150. Puck, T. T., P. I. Marcus, and S. J. Cieciura. 1956. Clonal growth of mammalian cells in vitro; growth characteristics of colonies from single HeLa cells with and without a feeder layer. J Exp Med 103:273-283.

151. Franken, N. A., H. M. Rodermond, J. Stap, J. Haveman, and C. van Bree. 2006. Clonogenic assay of cells in vitro. Nat Protoc 1:2315-2319.

152. Kanzawa, F., A. Hoshi, and K. Kuretani. 1970. Relationship between antitumor activity and chemical structure in psychotropic agents. Gann 61:529-534.

153. Holmsen, H., and T. Rygh. 1990. Chlorpromazine makes the platelet plasma membrane permeable for low-molecular weight substances and reduces ATP production. Biochem Pharmacol 40:373-376.

154. Huang, C. L., and A. A. Kurland. 1964. Perphenazine (Trilafon) Metabolism in Psychotic Patients. Arch Gen Psychiatry 10:639-646.

155. Malheiros, S. V., E. de Paula, and N. C. Meirelles. 1998. Contribution of trifluoperazine/lipid ratio and drug ionization to hemolysis. Biochim Biophys Acta 1373:332-340.

156. Klionsky, D. J., and S. D. Emr. 2000. Autophagy as a regulated pathway of cellular degradation. Science 290:1717-1721.

157. Bjorkoy, G., T. Lamark, A. Brech, H. Outzen, M. Perander, A. Overvatn, H. Stenmark, and T. Johansen. 2005. p62/SQSTM1 forms protein aggregates degraded by autophagy and has a protective effect on huntingtin-induced cell death. J Cell Biol 171:603-614.

158. Zeng, X., J. H. Overmeyer, and W. A. Maltese. 2006. Functional specificity of the mammalian Beclin-Vps34 PI 3-kinase complex in macroautophagy versus endocytosis and lysosomal enzyme trafficking. J Cell Sci 119:259-270.

159. Mizushima, N., T. Noda, and Y. Ohsumi. 1999. Apg16p is required for the function of the Apg12p-Apg5p conjugate in the yeast autophagy pathway. EMBO J 18:3888-3896.

160. Hendil, K. B., A. M. Lauridsen, and P. O. Seglen. 1990. Both endocytic and endogenous protein degradation in fibroblasts is stimulated by serum/amino acid deprivation and inhibited by 3-methyladenine. Biochem J 272:577-581.

161. Yamamoto, A., Y. Tagawa, T. Yoshimori, Y. Moriyama, R. Masaki, and Y. Tashiro. 1998. Bafilomycin A1 prevents maturation of autophagic vacuoles by inhibiting fusion between autophagosomes and lysosomes in rat hepatoma cell line, H-4-II-E cells. Cell Struct Funct 23:33-42.

162. Tanida, I., N. Minematsu-Ikeguchi, T. Ueno, and E. Kominami. 2005. Lysosomal turnover, but not a cellular level, of endogenous LC3 is a marker for autophagy. Autophagy 1:84-91.

163. Tanida, I., and S. Waguri. 2010. Measurement of autophagy in cells and tissues. Methods Mol Biol 648:193-214.

164. Juenemann, K., and E. A. Reits. 2012. Alternative macroautophagic pathways. Int J Cell Biol 2012:189794.

165. Klionsky, D. J., A. M. Cuervo, and P. O. Seglen. 2007. Methods for monitoring autophagy from yeast to human. Autophagy 3:181-206.

166. Nishida, Y., S. Arakawa, K. Fujitani, H. Yamaguchi, T. Mizuta, T. Kanaseki, M. Komatsu, K. Otsu, Y. Tsujimoto, and S. Shimizu. 2009. Discovery of Atg5/Atg7-independent alternative macroautophagy. Nature 461:654-658.

167. Zong, D., P. Haag, I. Yakymovych, R. Lewensohn, and K. Viktorsson. 2011. Chemosensitization by phenothiazines in human lung cancer cells: impaired resolution of gammaH2AX and increased oxidative stress elicit apoptosis associated with lysosomal expansion and intense vacuolation. Cell Death Dis 2:e181.

168. Funk, R. S., and J. P. Krise. 2012. Cationic amphiphilic drugs cause a marked expansion of apparent lysosomal volume: implications for an intracellular distribution-based drug interaction. Mol Pharm 9:1384-1395.

169. Yang, W. C., F. F. Strasser, and C. M. Pomerat. 1965. Mechanism of Drug-Induced Vacuolization in Tissue Culture. Exp Cell Res 38:495-506.

170. Scarlatti, F., R. Maffei, I. Beau, P. Codogno, and R. Ghidoni. 2008. Role of non-canonical Beclin 1-independent autophagy in cell death induced by resveratrol in human breast cancer cells. Cell Death Differ 15:1318-1329.

171. Luzio, J. P., P. R. Pryor, and N. A. Bright. 2007. Lysosomes: fusion and function. Nat Rev Mol Cell Biol 8:622-632.

172. de Duve, C., T. de Barsy, B. Poole, A. Trouet, P. Tulkens, and F. Van Hoof. 1974. Commentary. Lysosomotropic agents. Biochem Pharmacol 23:2495-2531.

173. Ohkuma, S., and B. Poole. 1981. Cytoplasmic vacuolation of mouse peritoneal macrophages and the uptake into lysosomes of weakly basic substances. J Cell Biol 90:656-664.

174. Goldman, S. D., R. S. Funk, R. A. Rajewski, and J. P. Krise. 2009. Mechanisms of amine accumulation in, and egress from, lysosomes. Bioanalysis 1:1445-1459.

175. Ishizaki, J., K. Yokogawa, F. Ichimura, and S. Ohkuma. 2000. Uptake of imipramine in rat liver lysosomes in vitro and its inhibition by basic drugs. J Pharmacol Exp Ther 294:1088-1098.

176. Kaufmann, A. M., and J. P. Krise. 2007. Lysosomal sequestration of amine-containing drugs: analysis and therapeutic implications. J Pharm Sci 96:729-746.

177. Poole, B., and S. Ohkuma. 1981. Effect of weak bases on the intralysosomal pH in mouse peritoneal macrophages. J Cell Biol 90:665-669.

178. Yokogawa, K., J. Ishizaki, S. Ohkuma, and K. Miyamoto. 2002. Influence of lipophilicity and lysosomal accumulation on tissue distribution kinetics of basic drugs: a physiologically based pharmacokinetic model. Methods Find Exp Clin Pharmacol 24:81-93.

179. Namazi, M. R. 2009. The potential negative impact of proton pump inhibitors on the immunopharmacologic effects of chloroquine and hydroxychloroquine. Lupus 18:104-105.

180. Yoon, Y. H., K. S. Cho, J. J. Hwang, S. J. Lee, J. A. Choi, and J. Y. Koh. 2010. Induction of lysosomal dilatation, arrested autophagy, and cell death by chloroquine in cultured ARPE-19 cells. Invest Ophthalmol Vis Sci 51:6030-6037.

181. Butler, D., Q. B. Brown, D. J. Chin, L. Batey, S. Karim, M. S. Mutneja, D. A. Karanian, and B. A. Bahr. 2005. Cellular responses to protein accumulation involve autophagy and lysosomal enzyme activation. Rejuvenation Res 8:227-237.

182. Sundelin, S. P., and A. Terman. 2002. Different effects of chloroquine and hydroxychloroquine on lysosomal function in cultured retinal pigment epithelial cells. APMIS 110:481-489.

183. Daniel, W. A. 2003. Mechanisms of cellular distribution of psychotropic drugs. Significance for drug action and interactions. Prog Neuropsychopharmacol Biol Psychiatry 27:65-73.

184. Daniel, W. A., and J. Wojcikowski. 1999. Lysosomal trapping as an important mechanism involved in the cellular distribution of perazine and in

pharmacokinetic interaction with antidepressants. Eur Neuropsychopharmacol 9:483-491.

185. Daniel, W. A., M. H. Bickel, and U. E. Honegger. 1995. The contribution of lysosomal trapping in the uptake of desipramine and chloroquine by different tissues. Pharmacol Toxicol 77:402-406.

186. Marceau, F., M. T. Bawolak, J. Bouthillier, and G. Morissette. 2009. Vacuolar ATPase-mediated cellular concentration and retention of quinacrine: a model for the distribution of lipophilic cationic drugs to autophagic vacuoles. Drug Metab Dispos 37:2271-2274.

187. Domanska, U., A. Pelczarska, and A. Pobudkowska. 2011. Solubility and pKa determination of six structurally related phenothiazines. Int J Pharm 421:135-144.

188. Morissette, G., E. Moreau, C. G. R, and F. Marceau. 2004. Massive cell vacuolization induced by organic amines such as procainamide. J Pharmacol Exp Ther 310:395-406.

189. Peterson, J. K., and P. J. Houghton. 2004. Integrating pharmacology and in vivo cancer models in preclinical and clinical drug development. Eur J Cancer 40:837-844.

190. Creighton, C. J., K. E. Cordero, J. M. Larios, R. S. Miller, M. D. Johnson, A. M. Chinnaiyan, M. E. Lippman, and J. M. Rae. 2006. Genes regulated by estrogen in breast tumor cells in vitro are similarly regulated in vivo in tumor xenografts and human breast tumors. Genome Biol 7:R28.

191. Boelens, J., S. Lust, F. Offner, M. E. Bracke, and B. W. Vanhoecke. 2007. Review. The endoplasmic reticulum: a target for new anticancer drugs. In Vivo 21:215-226.

192. Lazo, J. S., W. N. Hait, K. A. Kennedy, I. D. Braun, and B. Meandzija. 1985. Enhanced bleomycin-induced DNA damage and cytotoxicity with calmodulin antagonists. Mol Pharmacol 27:387-393.

193. Wu, J., and R. J. Kaufman. 2006. From acute ER stress to physiological roles of the Unfolded Protein Response. Cell Death Differ 13:374-384.

194. Janicke, R. U., M. L. Sprengart, M. R. Wati, and A. G. Porter. 1998. Caspase-3 is required for DNA fragmentation and morphological changes associated with apoptosis. J Biol Chem 273:9357-9360.

195. Scott, R. C., O. Schuldiner, and T. P. Neufeld. 2004. Role and regulation of starvation-induced autophagy in the Drosophila fat body. Dev Cell 7:167-178.

196. Zeng, X., and T. J. Kinsella. 2008. Mammalian target of rapamycin and S6 kinase 1 positively regulate 6-thioguanine-induced autophagy. Cancer Res 68:2384-2390.

197. Wu, W. K., S. B. Coffelt, C. H. Cho, X. J. Wang, C. W. Lee, F. K. Chan, J. Yu, and J. J. Sung. 2011. The autophagic paradox in cancer therapy. Oncogene 31:939-953.

198. Lee, J. T., L. Li, P. A. Brafford, M. van den Eijnden, M. B. Halloran, K. Sproesser, N. K. Haass, K. S. Smalley, J. Tsai, G. Bollag, and M. Herlyn. 2010. PLX4032, a potent inhibitor of the B-Raf V600E oncogene, selectively

inhibits V600E-positive melanomas. Pigment Cell Melanoma Res 23:820-827.

199. Long, B. H., and C. R. Fairchild. 1994. Paclitaxel inhibits progression of mitotic cells to G1 phase by interference with spindle formation without affecting other microtubule functions during anaphase and telephase. Cancer Res 54:4355-4361.

200. Rowinsky, E. K. 1997. The development and clinical utility of the taxane class of antimicrotubule chemotherapy agents. Annu Rev Med 48:353-374.

201. Burkhart, C. A., M. Kavallaris, and S. Band Horwitz. 2001. The role of beta-tubulin isotypes in resistance to antimitotic drugs. Biochim Biophys Acta 1471:O1-9.

202. Giannakakou, P., D. L. Sackett, Y. K. Kang, Z. Zhan, J. T. Buters, T. Fojo, and M. S. Poruchynsky. 1997. Paclitaxel-resistant human ovarian cancer cells have mutant beta-tubulins that exhibit impaired paclitaxel-driven polymerization. J Biol Chem 272:17118-17125.

203. Nagy, S., G. Argyelan, J. Molnar, M. Kawase, and N. Motohashi. 1996. Antitumor activity of phenothiazine-related compounds. Anticancer Res 16:1915-1918.

204. Ahn, J. H., and M. Lee. 2011. Suppression of autophagy sensitizes multidrug resistant cells towards Src tyrosine kinase specific inhibitor PP2. Cancer Lett 310:188-197.

205. Bauvy, C., P. Gane, S. Arico, P. Codogno, and E. Ogier-Denis. 2001. Autophagy delays sulindac sulfide-induced apoptosis in the human intestinal colon cancer cell line HT-29. Exp Cell Res 268:139-149.

206. Ito, H., S. Daido, T. Kanzawa, S. Kondo, and Y. Kondo. 2005. Radiation-induced autophagy is associated with LC3 and its inhibition sensitizes malignant glioma cells. Int J Oncol 26:1401-1410.

207. Gonzalez-Polo, R. A., M. Niso-Santano, M. A. Ortiz-Ortiz, A. Gomez-Martin, J. M. Moran, L. Garcia-Rubio, J. Francisco-Morcillo, C. Zaragoza, G. Soler, and J. M. Fuentes. 2007. Inhibition of paraquat-induced autophagy accelerates the apoptotic cell death in neuroblastoma SH-SY5Y cells. Toxicol Sci 97:448-458.

208. Lambert, L. A., N. Qiao, K. K. Hunt, D. H. Lambert, G. B. Mills, L. Meijer, and K. Keyomarsi. 2008. Autophagy: a novel mechanism of synergistic cytotoxicity between doxorubicin and roscovitine in a sarcoma model. Cancer Res 68:7966-7974.

209. Qadir, M. A., B. Kwok, W. H. Dragowska, K. H. To, D. Le, M. B. Bally, and S. M. Gorski. 2008. Macroautophagy inhibition sensitizes tamoxifen-resistant breast cancer cells and enhances mitochondrial depolarization. Breast Cancer Res Treat 112:389-403.

210. Cook, K. L., A. N. Shajahan, and R. Clarke. 2011. Autophagy and endocrine resistance in breast cancer. Expert Rev Anticancer Ther 11:1283-1294.

211. Shin, J. H., S. J. Park, Y. K. Jo, E. S. Kim, H. Kang, J. H. Park, E. H. Lee, and D. H. Cho. 2012. Suppression of autophagy exacerbates Mefloquine-mediated cell death. Neurosci Lett 515:162-167.

212. Bae, H., and J. L. Guan. 2011. Suppression of autophagy by FIP200 deletion impairs DNA damage repair and increases cell death upon treatments with anticancer agents. Mol Cancer Res 9:1232-1241.

213. Amrein, L., D. Soulieres, J. B. Johnston, and R. Aloyz. 2010. p53 and autophagy contribute to dasatinib resistance in primary CLL lymphocytes. Leuk Res 35:99-102.

214. Maycotte, P., and A. Thorburn. 2011. Autophagy and cancer therapy. Cancer Biol Ther 11:127-137.

215. Cesen, M. H., K. Pegan, A. Spes, and B. Turk. 2012. Lysosomal pathways to cell death and their therapeutic applications. Exp Cell Res 318:1245-1251.

VITA

Publications:

Claerhout S, Dutta B, Bossuyt B, Zhang F, **Nguyen-Charles C**, Dennison JB, Yu Q, Yu S, Balázsi G, Lu Y, Mills GB. *Abortive autophagy induces endoplasmic reticulum stress and cell death in cancer cells.* PLoS ONE 7(6): **2012**.

Cheong,JH, ParkES, Liang J, Dennison JB, Tsavachidou D**, Nguyen-Charles C**,Wa Cheng K,Hall H,Zhang D, Lu Y,Ravoori M, Kundra V, Ajani J, Lee JS, Ki Hong W, Mills GB*. Dual inhibition of tumor energy pathway by 2-deoxyglucose and metformin is effective against a broad spectrum of preclinical cancer models.* Mol Cancer Ther. **2011**.

PMCID: 21992792

Siwak DR, Carey M, Hennessy BT, **Nguyen CT**, McGahren Murray MJ, Nolden L, Mills GB. Targeting the epidermal growth factor receptor in epithelial ovarian cancer: current knowledge and future challenges. J Oncol. **2010**

PMCID: PMC2796463

Anbanandam A, Albarado DC, **Nguyen CT**,Halder G,Gao X,Veeraraghavan, S. Insights into transcription enhancer factor 1 (TEF-1) activity from the solution structure of the TEA domain. Proc Natl Acad Sci USA. **2006.**

Awards

Keck Pharmacoinformatics training grant fellowship **4/2008 to 4/2010**

Posters & Presentations

Identification of Compounds that Perturb Autophagy in Cancer Cells using High-Throughput Small Molecule Imaged Based Screen

Charles C, Maxwell D, Bornmann W, Lu Y, and Mills GB

Poster

Keck Annual Symposium

October 2008 – Houston, Tx

An Example of a Small Molecule Screen

Nguyen C, Lu Y, and Mills GB

Presented talk

Workshop on High Throughput / High Content Screening and its Application to Target Based Drug Discovery Research

John S. Dunn GCC Chemical Genomics Research Consortium:

November 2007 – Houston, Tx